DIFFERENTITAION OF PAPER TYPES USING ELEMENT PROFILES GENERATED USING INDUCTIVELY COUPLED PLASMA-OPTICAL EMISSION SPECTROSCOPY AND INDUCTIVELY COUPLED PLASMA-MASS SPECTROMETRY

By

Emily Riddell

A THESIS

Submitted to
Michigan State University
in partial fulfillment of the requirements
for the degree of

Forensic Science- Master of Science

2013

ABSTRACT

DIFFERENTITAION OF PAPER TYPES USING ELEMENT PROFILES GENERATED USING INDUCTIVELY COUPLED PLASMA-OPTICAL EMISSION SPECTROSCOPY AND INDUCTIVELY COUPLED PLASMA-MASS SPECTROMETRY

By

Emily Riddell

The analysis of questioned documents in a forensic laboratory traditionally focuses on the visual examination of the physical properties of the paper such as brightness and thickness. Improvements in the paper making process have made visual differentiation of different types of paper difficult which has increased the research in the elemental analysis of paper. Inductively coupled plasma- mass spectrometry (ICP-MS) has been used to generate element profiles for paper samples; however, this technique is expensive and not widely available for forensic laboratories.

For this project, inductively coupled plasma-optical emission spectroscopy (ICP-OES) was investigated as alternative to ICP-MS analysis of paper sample. Four types of paper from the same manufacturer were microwave digested and analyzed by both ICP-OES and ICP-MS. Analysis of variance (ANOVA) and Tukey's honestly significant difference (HSD) test were used to determine if there were differences in element concentration within a paper type and among the four paper types. This had to be done separately for each element and each paper type so multivariate statistical procedures were used to compare the full element profile of all paper types simultaneously. Principal components analysis (PCA) and hierarchical cluster analysis (HCA) were used to assess the association among sheets of the same paper type and the differentiation among paper types.

ACKNOWLEDGEMENTS

I would like to thank all the people who provided help and support during my time in graduate school and in preparing this thesis. First, Dr. Ruth Smith who introduced me to research as an undergraduate and provided encouragement as my advisor during my time as a graduate student.

Next, I would like to acknowledge Matt Parsons and Justin Zyskowski for their assistance in the analysis by ICP-MS. Thank you for taking the time to run my samples over and over again.

I would also like to thank my fellow graduate students in the Forensic Chemistry program who were there for both the good and the frustrating times. Thank you John McIlroy, Kaitlin Prather, Monica Bugeja, Karlie McManaman, Suzanne Towner, Christy Hay, Drew DeJarnette Seth Hogg, Melissa Bodnar Willard , Jordyn Geiger, and Johanna Smeekens. This process would not have been nearly as fun without you.

I would like to thank my committee members Dr. Kathryn Severin and Dr. April Zeoli for their input for my thesis. A special thank you to Dr. Severin for her assistance with and access to the ICP-OES.

Finally, I would like to thank all my family and friends for their continued support throughout these last few years. Thank you for being there when I was frustrated and for acting interested in my research even when you really were not. I could not have done this without your love and support.

TABLE OF CONTENTS

LIST OF TABLES

LIST OF FIGURES

Chapter 1: Introduction

1.1 Questioned Documents in Forensic Science

The analysis of questioned documents in forensic laboratories has become more important in the past fifty years with most aspects of daily life requiring a written or typed document. This can include a lease for an apartment, a marriage license, or a will. Crimes occur daily that involve the use of documents. Examples of these crimes are embezzlement, forged or altered wills, and welfare fraud[1]. Such crimes account for $140 billion in damages for the United States economy, which is greater than the cost associated with violent crimes[2]. As there are many ways in which a document can be altered (*e.g.*, altering the writing or replacing a page of the document), there are many aspects of a document that can be examined.

1.2 Questioned Document Analysis

When a document is submitted to a forensic laboratory, most of the analysis focuses on what is written, typed, or printed on the paper. This includes analysis of handwriting, ink or toner, as well as any impressions left on the paper. Samples of handwriting from the document can be compared to known samples from the author or to samples from a suspect to determine if the signature on a document is an original or a forgery. Ink and toner can be analyzed using a variety of techniques such as thin layer chromatography, gas chromatography-mass spectrometry, and x-ray fluorescence [3-7]. By characterizing the chemical composition of the ink,

information can be obtained about the manufacturer and age of the ink. Chemical analysis of the toner can also provide information about the type and age, as well as the type of printer used to create the document. Electrostatic detection apparatus is used to determine impressions or indentations on paper. This is especially useful in multi-page documents to determine if writing was added at a later time.

In cases where analysis of handwriting, ink and toner, or impressions does not lead to any valuable conclusions, the paper itself may be analyzed. This typically involves physical characterization of the paper, as well as a microscopic examination of the fibers. More recently, chemical characterization of paper has been used to compare paper samples in cases where microscopic examination cannot distinguish between papers. All of these features can be used to differentiate papers from different sources due to differences in the raw materials, chemicals, and additives used to make paper.

1.3 Paper-making Process

Approximately 90% of the raw materials used for paper production are hard- or soft-wood. In the first step of the paper-making process (Figure 1.1), the wood is debarked and chipped. The woodchips are then pulped to remove most of the lignin, which acts as the glue that holds together the fibers of the wood and is responsible for the yellowing of papers over time[8]. Although there are many pulping processes available, the two most common are mechanical and chemical pulping. Mechanical pulping involves grinding the wood chips between stone plates in water. An advantage of mechanical pulping is that approximately 80-95% of the raw material is used compared to only about 45-55% of the raw material used in chemical pulping. However, in

mechanical pulping, lignin remains in the pulp which weakens the paper fibers. In 2010, mechanical pulping accounted for only 10% of the pulp used to make paper[9].

The two most common methods of chemical pulping are the sulfite and the sulfate processes. The sulfite process uses sodium dioxide and lime to remove lignin from the fibers. The sulfate process, which is also known as the Kraft process, uses sodium hydroxide and sodium sulfate to remove lignin from the fiber. The Kraft process is the more commonly used chemical pulping method because it produces a better quality paper with improved smoothness and printability[8].

The next stage in the process is washing (Figure 1.1) in which bleaching agents and other chemical additives are added to the pulp to improve the quality of the final paper. Bleaching agents, such as caustic soda (NaOH), sodium hypochlorite (NaClO), and chlorine dioxide (ClO_2), are added to increase the whiteness of the paper. Examples of other additives include fillers (*e.g.*, calcium carbonate ($CaCO_3$) and titanium dioxide (TiO_2)) which are added to increase the smoothness of the paper, coating pigments (*e.g.*, kaolin clay ($Al_2O_3.2SiO_2.2H_2O$) ground calcium carbonate ($CaCO_3$,$MgCO_3$), precipitated calcium carbonate ($CaCO_3$)) which increase the brightness and opacity, and sizing agents (*e.g.*, alkyl ketene dimer ($C_{34}H_{70}O_2$) and paper maker's alum ($Al_2(SO_4)_3.14H_2O$)) which make the paper water resistant.

At this stage, the pulp solution, which contains 99% water and 1% pulp material, is moved into the headbox[8]. The solution is then fed onto a moving wire mesh belt called a fourdrinier which shakes in order to interlace the fibers. The paper is moved onto dandy rolls

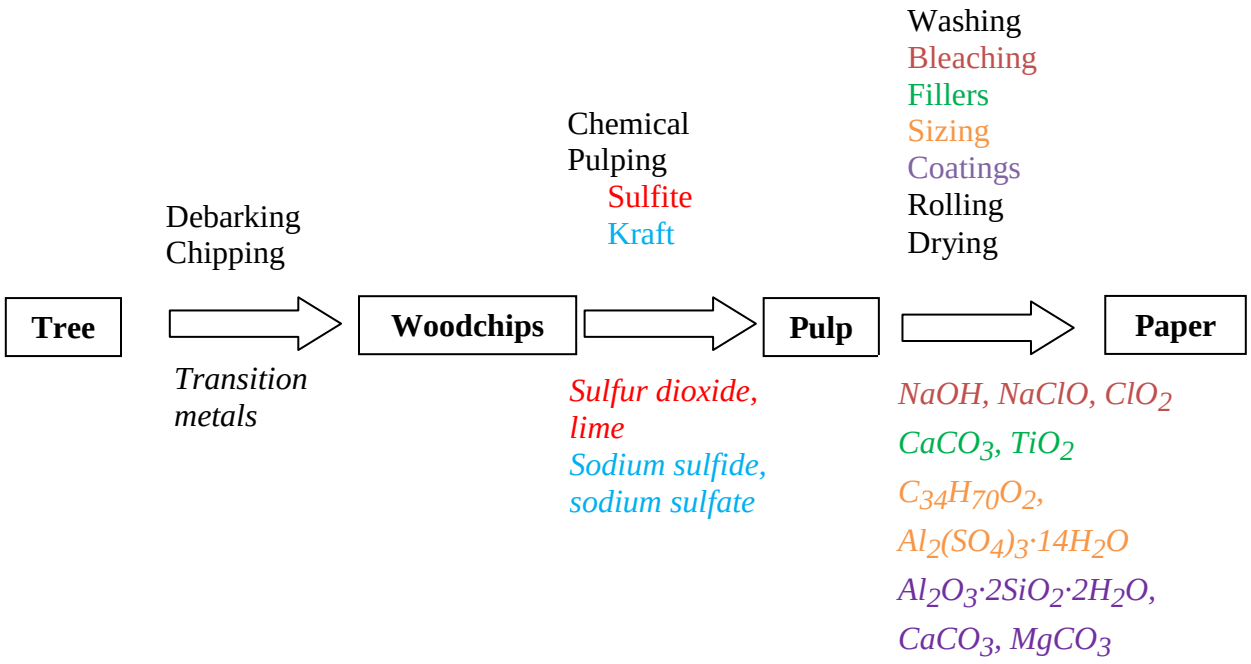

Figure 1.1 Overview of paper making with the process and chemicals added at that stage in the same color. For interpretation of the references to color in this and all other figures, the reader is referred to the electronic version of this thesis.

which apply pressure to further remove water and to smooth the paper. Watermarks, via mechanical means such as a stamp, can be added to the wet product at this point by displacing the fibers. Most of the remaining water is removed from the paper so the final product contains about 5% water. If all the water was removed from the paper, it would be brittle and break[8]. Watermarks using chemical means can be added to the dry product to make the paper more transparent.

The final steps of the paper-making process involve applying an additional coating followed by calendaring. The coating is applied to both sides of the paper. The coating composition can vary according to the grade of the paper and sizing rosins may also be added during this process. Calendaring involves passing the paper between stacked iron rollers to improve the smoothness. The paper is then cut into sheets of the required size, and packaged into reams. Up to ten different rolls of paper can feed into the same ream, meaning that sheets of paper within the same ream can originate from different rolls[10]. As a result, some sheets will be from the same original roll and therefore should be similar in chemical composition; however, some sheets will originate from different rolls and hence, could have slight differences in chemical composition.

1.4 Literature Review of Paper Analysis

1.4.1 Physical Characteristics of Paper

Several physical characteristics of paper can be used for comparison, such as the thickness, presence of watermarks, whiteness, weight, and fiber content[1]. Microscopic

examination of the fibers in the paper can also be used for comparison of two or more papers[11,12]. Differences in the physical appearance of the pulp can provide information about the type of wood used, as well as the pulping method[1]. More recently, differentiation of paper based only on the physical characteristics has become more difficult due to improvements in the paper-making process. However, as various chemicals are used during the paper-making process, papers can be compared based on the elemental composition (Figure 1.1).

1.4.2 Elemental Analysis of Paper

Elemental analysis of paper has been reported in the literature, using a variety of different analytical techniques, such as neutron activation analysis (NAA) [13], atomic absorption spectroscopy (AAS) [14, 15], x-ray fluorescence (XRF) [16-18], and inductively coupled plasma-mass spectrometry (ICP-MS) [18-20].

Schlesinger and Settle were the first to use NAA for the elemental analysis of paper [13]. Papers from nine different manufacturers were analyzed and element profiles were generated using concentrations of the following elements: Ti, Al, Ca, Mn, Na, Cl, Ta, Zn, Sb, Sc, Au, and La. The elements that were present in all of the samples were Al, Mn, and Na while the elements that were present in the highest concentrations were Ti, Al, and Ca. Of the 120 paper samples analyzed, 102 could be grouped into pairs that came from the same production batch, with one sample coming from the beginning and the other coming from the end of the batch which was confirmed by the manufacturers[13]. The relative standard deviation (RSD) among all pairs was calculated and ranged from 45% for Ta to 12% for Al, Ca, and Na.

Since Ti, Al, and Ca are intentionally added by the manufacturers during the paper making process, it was assumed by the authors of this paper that the concentration would not vary as much within paper types. To test this, the RSDs of Al and Ti were calculated in the ten pairs that had the highest concentration. The resulting RSDs were 3.7% for Al and 7.7% for Ti indicating that the concentrations within a paper type were more similar within a paper type than among all paper types. An advantage of NAA is that there is minimal sample preparation while a disadvantage is that the samples remain radioactive after analysis and a nuclear reactor is required.

Langmyhr *et al.* used a graphite furnace AAS to generate element profiles for one pulp sample and four different paper types[14]. The pulp sample came from photographic paper and the paper types analyzed were letterhead paper, chromatographic paper, filter paper, and grease-proof paper. Pulp was analyzed because trace metals are present in the raw materials and the different paper types were analyzed because other chemicals are added during the paper-making process. Each pulp sample and the paper samples were analyzed to determine the concentration of Cu, Pb, Cd, and Mn present.

Copper was present in the highest concentration in grease-proof paper which was over 100 times the concentration detected in pulp. The other elements were present in the highest concentration in letterhead paper indicating differences in element concentrations among paper types. While AAS is beneficial because it allows detection of trace elements in paper, only a few elements can be analyzed at a time, which would be time consuming if many elements were to be used.

Simon *et al*. used graphite furnace AAS to generate element profiles for 19 reams of 11 paper types from seven different manufacturers[15]. Four consecutive sheets were taken from each ream and from each sheet, 150 samples were cut using a hole-punch. The elements that were used for the profile were Cu, Pb, Mn, Sb, Cr, Co, Cd, Fe, Mg, and Ag.

The concentrations of Fe and Mg in the samples varied greatly within a sheet and were not included in further statistical analysis of the data. The RSDs for Mn and Sb were high within a paper type; however, when calculated for alternating sheets, the RSDs were less than 5%, indicating an interweaving of sheets during the packaging process. Hierarchical cluster analysis (HCA) was performed and differentiation of 12 of the 19 reams was possible based on differences in the concentrations of Co, Cr, Cu, Mn, and Sb. These five elements were used because they were present in all paper types and 0did not vary greatly within a ream. HCA was performed again using the five elements and the density of the paper. When these six characteristics were considered, differentiation of 16 of the 19 paper types was possible. The three reams that could not be differentiated were different batches of the same paper type.

Manso *et al.* investigated differences in element concentrations in papers collected from different time periods[16, 17]. Samples of papyrus paper from 1000 and 2005, parchment paper from 1630 and 2005, and newspaper from 1919, 1941, and 2005 were analyzed by XRF to determine the element profile[16]. The elements present in the highest concentration in papyrus paper were Cl, K, and Ca. The elements present in highest concentration in parchment paper were Ca, Fe, and K. Calcium and Fe were present in the parchment paper from 2005 while K was below detection limits. For newspaper, there were 14 elements present in the paper from 1919 and only six elements present in the paper from 2005. Sulfur, Ba, and Ca were present in

the highest concentration in the newspaper from 1919 while Ca was present in the highest concentration in the paper from 2005. Calcium is used as a brightener in paper and in recent years, calcium carbonate ($CaCO_3$) has replaced kaolin ($Al_2O_3.2SiO_2.2H_2O$) as the most common brightener added for paper making[9]. For all paper types, the number of elements present and the concentration of these elements was lower in the paper from 2005 compared to the older paper samples.

In a subsequent study, Manso *et al.* used XRF to generate element profiles of 12 different types of paper collected between 1555 and 2005[17]. It was again observed that the fewest number of elements was detected in the paper from 2005; however, Ca, Cu, Fe, Sr, and Zn were present in all papers analyzed. Hierarchical cluster analysis (HCA), using Euclidean distance, was performed using all elements to cluster the samples based on element concentrations. The greatest difference in distance was calculated between samples from 1919 and 2005. All samples produced in 1919 and earlier were more chemically similar indicating a change in the paper-making process between 1919 and 2005. Using the element profile of each paper sample in addition to the dendrogram, the paper samples could be grouped into ten different paper types.

Differentiation based on paper type, as opposed to age, was also investigated using XRF. Van Es *et al.* analyzed one sheet from each of twenty-five different paper types from sixteen different manufacturers[18]. A total of 56 elements were detected in the samples and 13 of these elements were used for further analysis based on the detection limits of the instrument and precision in replicate measurements. When HCA was performed, 22 of the 25 paper types could be differentiated. Of the three reams that could not be differentiated, two were the same type of

paper, all three were from different manufacturers however; using discriminant analysis (DA), all paper samples were correctly differentiated.

Additional research on the elemental analysis of paper has focused on using ICP-MS to generate element profiles[19, 20]. Advantages of ICP-MS over the other analytical techniques used previously are that it allows for rapid multi-element analysis of samples, with low detection limits. Spence *et al.* compared reams of 17 different brands of paper from ten different countries[19]. For each ream of paper, five samples were taken from the same sheet, prepared by microwave digestion using nitric acid and hydrogen peroxide, and analyzed by ICP-MS[19]. A total of 23 elements were measured and the elements selected for discrimination were Na, Mg, Al, Sr, Y, Ba, La, and Ce. These were chosen because they were present in concentrations higher than the limit of detection, did not vary within a sheet, and were not affected by spectral interferences. Ternary plots were used to show the differences in the concentration ratio of the three elements (Mn, Sr, and Al,) that varied the most among the samples. The ternary plots showed that all but two clusters, each cluster containing two paper types, could be differentiated based on the concentration ratio of the three elements. One cluster contained a paper from the United States and Japan and these papers could be differentiated using the actual concentration of Al in the samples. The other cluster, two papers from Finland, could be differentiated using the concentration of Mg. All paper types could be differentiation if more elements were used.

The student's t-test, at a 99% confidence level, was then used to make pair-wise comparisons of the Mn concentrations among all paper types. Manganese concentrations were compared first and if differentiation was not possible, then Sr concentrations were compared. There were four pairs of paper types that could not be differentiated based on Mn concentration;

however, when the student's t-test was then performed using Sr concentrations, all paper types could be differentiated.

An additional study was performed to compare element concentrations in rolls of paper produced at the same mill over a four-month period. The concentrations of Zr, Mn, and Al could be used, at a 99% confidence level, to differentiate rolls produced in consecutive months. However, a limit to using t-tests for comparisons is that only one pair of samples can be compared at a time and, in this case, the comparisons have to be performed for each element individually, which is time consuming.

McGaw *et al.* also used ICP-MS to generate element profiles for paper samples from five reams from two manufacturers[20]. From each ream, three sheets were selected for analysis and five samples were taken from each sheet. Fourteen elements were measured in the analysis. The concentrations of the elements in the samples compared to the concentration in procedural blanks as well as the variation of element concentration within a sheet were used to determine which elements could be used for differentiation. The elements that could be used were Mg, Al, Mn, Fe, Sr, Y, Ba, Ce, and Nd. Analysis of variance (ANOVA) and Tukey's honestly significant difference (HSD) test were used to determine if there were statistical differences in element concentrations within reams produced by the same manufacturer, as well as between manufacturers. Differentiation among the five reams from one manufacturer was possible at the 95% confidence level using the concentrations of Al and Ba. Differentiation among reams from the second manufacturer was possible at the 95% confidence level using the concentrations of Mg, Mn, and Sr. Differentiation among samples from the two manufacturers was possible using the concentrations of Ba and Nd.

Paper samples have also been analyzed using laser ablation (LA)-ICP-MS in which the solid sample is analyzed directly[4, 18]. This procedure reduces the possibility of contamination from the reagents used for microwave digestion. Trejos *et al.* compared 17 different paper types from seven different brands that were manufactured at ten different plants in the United States[4]. There were 39 elements used in the original analysis; however, only Na, Al, Zn, Mg, Sr, Fe, Mn, Cu, Ti, Ba, and Zr were used for differentiation because they were present at levels greater than the limit of detection and had high precision among replicates. The element concentrations of the 17 samples were then compared using ANOVA and Tukey's (HSD) test at the 95% confidence level to determine if the samples were significantly different. A total of 171 different pairs were compared using the eleven elements previously mentioned and 99.4% of the samples could be differentiated. The pair of paper samples that was not differentiated was reams of the same brand manufactured in the same plant.

Van Es *et al.* also used LA-ICP-MS to analyze 25 types of paper from 16 manufacturers, analyzing three samples per paper type[18]. A total of 51 elements were analyzed and all elements were used for subsequent statistical analysis. Principal components analysis (PCA) was performed; however 10 principal components were needed to describe the majority of the variance and therefore the results were not further investigated. The authors do not provide any additional information about using PCA for this data set. When HCA was performed, the three samples per sheet were clustered for 23 of the 25 paper types. The samples that could not be differentiated were the same type of paper but from different manufacturers. Using LA-ICP-MS allowed for more differentiation than observed when the same samples were also analyzed by XRF.

1.4.3 Comparison of ICP-OES and ICP-MS Analysis

ICP-MS has been demonstrated to be a powerful technique for the generation of element profiles for paper samples. Of the techniques previously used for element analysis of paper, ICP-MS has the lowest detection limits for most elements, which is beneficial due to the trace element concentrations in paper samples. Unfortunately, ICP-MS is not widely available in forensic laboratories and has high operating costs associated with sample analysis. An alternative method, inductively coupled plasma-optical emission spectroscopy (ICP-OES) is more widely available and has lower operating costs. However, this technique has higher detection limits (µg /L range) for most elements compared to ICP-MS (pg/L range). Despite this, the applicability of ICP-OES for the elemental analysis of various food products including honey, instant soup, and wine has been demonstrated[21-25].

Mendes *et al.* used ICP-OES to analyze the element concentrations in 81 honey samples from nine different countries[21]. The elements that were analyzed were Ca, K, Mg, Na, Cd, Co, Cu, Fe, Mn, Ni, Pb, and Zn. The accuracy and precision of the analysis was evaluated by calculating the percent recovery when a known concentration of each element was added to honey samples. For most samples, the percent recovery was between 90-110% and the RSD for each element was less than 10%. ICP-OES was also used by Krejcova *et al.* to analyze the element concentrations in instant soup samples[22]. The elements that were measured were Na, Mg, P, Cd, Cr, Cu, Fe, Mn, Ni, Pb, and Zn. The limits of detection ranged from 0.129 mg/kg for Mg to 12.2 mg/kg for K with the RSDs for all elements less than 9%. Thus, both of these studies demonstrated that ICP-OES was sensitive enough for elemental analysis with acceptable precision.

There has also been work performed on the elemental analysis of wine samples using ICP-OES[23-25]. Gonzalvez *et al*. used the technique to generate element profiles for 67 wine samples from seven different regions of Spain[23]. There were 41 elements analyzed in the samples but only 38 were found to be greater than the limits of detection for the instrument. All 38 elements were used for statistical analysis by PCA, classification and regression trees (CART), HCA, and DA. Using HCA and PCA, samples from the Valencia and Yecla regions could not be differentiated; however, wines from the other regions could be differentiated. Only using discriminant analysis were all samples correctly classified by region of origin. The authors did not mention which of the 38 elements were used for differentiation.

Another study by Gonzalvez *et al.* directly compared the results of analysis of wine samples using both ICP-OES and ICP-MS[24]. It was determined that 17 elements could be measured by ICP-MS while only 15 elements were accurately measured by ICP-OES. This was because of higher sensitivity and lower limits of detection for ICP-MS. All element concentrations from both instruments were plotted against each other on a single graph and a linear least squares regression was fit to the data. The slope and intercept of the line were approximately 1 and 0, respectively, which indicated that there was not a statistical difference in the results obtained by the two instruments. Thus, both instruments could be used to accurately measure the trace element concentrations in wine samples.

Bentlin *et al.* used both ICP-MS and ICP-OES to analyze 53 red wine samples to determine if ICP-OES was a viable alternative to ICP-MS due to complications associated with ICP-MS analysis[25]. Wine samples were spiked with Sr, Fe, Al, Ba, Mn, Rd, Zn, and Ti and analyzed by both techniques to determine the percent recoveries. The concentrations were

compared using the Student's t-test at the 95% confidence level. For each element, there was no statistical difference in the concentration determined by the two techniques, indicating that both were comparable in the ability to accurately quantify trace element concentrations in a sample with a complex matrix.

ICP-OES has also been used in forensic applications, particularly for the analysis of glass and soil. Schnek and Almirall designed a study to determine if LA-ICP-OES was as sensitive as LA-ICP-MS for the differentiation of 41 samples of windshield glass[26]. The LA-ICP-OES data was analyzed in two ways: first using the full element profile (Al, Ba, Ca, Fe, Li, Mg, Sr, Ti, and Zr) and then using only the elements which varied the most (Sr, Al, Mg, Ba, and Zr). These elements were selected so that the number of factors used for statistical analysis was the same for both techniques. There were only four indistinguishable pairs determined using LA-ICP-OES at the 95% confidence level using either the selected elements or the full profile. For analysis by LA-ICP-MS data, five pairs of samples were indistinguishable at the 95% confidence level using only the selected element profiles. Two of the indistinguishable pairs could not be differentiated by either instrument and all pairs of indistinguishable samples were from the same source. This study showed that ICP-OES was sufficiently sensitive to determine differences in element concentrations for differentiation of glass samples; however, the applicability for the analysis of other forensic evidence, such as paper samples, has not been previously investigated.

1.5 Research Objectives

The objective of this research is to determine if ICP-OES is sufficiently sensitive for the differentiation of paper types based on the element profiles generated. Elemental analysis of papers and the differentiation of these papers have been successful using ICP-MS; however, this technique is not widely available in forensic laboratories and the instrument has high operating costs. Although ICP-OES has higher detection limits for most elements than ICP-MS, it is more widely available and has lower operating costs.

In order to accomplish the objective of this research, several goals had to be met. The first was to generate element profiles for four different types of paper using both ICP-OES and ICP-MS. To do this, paper samples were digested using microwave digestion and the same digest was analyzed using both techniques. The second goal was to determine the variation of element concentrations within and among paper types. To do this, element concentrations within a ream and within reams of the same paper type were statistically compared using ANOVA and Tukey's HSD test. The same statistical procedures were used to determine if there was variation in element concentrations among the four different paper types.

The third goal was to use multivariate statistical procedures to determine if sheets of the same paper type could be associated while there was differentiation among the paper types. To do this, PCA and HCA were both used as these procedures had been successful in other studies to correctly cluster paper samples. Finally, the association and discrimination of the papers based on the ICP-OES element profiles were compared to the association and discrimination obtained based on the ICP-MS element profiles. This was done to determine if ICP-OES was sufficiently sensitive, compared to ICP-MS, to differentiate the different paper types.

REFERENCES

REFERENCES

1. Brunelle RL. In *Forensic Science Handbook*, 2nd ed.; Saferstein, R., Ed.; Prentice Hall: Upper Saddle River, New Jersey, 2002; Vol. I, pp 697-744.

2. Bryan E. Questioned document examination. 2010. <http://www.evidencemagazine.com/index.php?option=com_content&task=view&id=267>.

3. Zlotnick JA, Smit, FP. Chromatographic and electrophoretic approaches in ink analysis. *J Chromatogr B* 1999; 733: 265-272.

4. Trejos T, Flore, A, Almirall JR. Micro-spectrochemical analysis of document paper and gel inks by laser ablation inductively coupled plasma mass spectrometry and laser induced breakdown spectroscopy. *Spectrochim Acta B* 2010; 65: 884-895.

5. Djozan D, Baheri T, Karimian G, Shahidi, M. Forensic discrimination of blue ballpoint pen inks based on thin layer chromatography and image analysis. *Forensic Sci Int* 2008: 179: 199-205.

6. Szynkowska MI, Czerski K, Paryjczak T, Parczewski, A. Ablative analysis of black and colored toners using LA-ICP-TOF-MS for the forensic discrimination of photocopy and printer toners. *Surf. Interface Anal* 2010; 42: 429-437.

7. Siegel J, Allison J, Mohr D, Dunn J. The use of laser desorption/ionization mass spectrometry in the analysis of inks in questioned documents. *Talanta* 2005; 67: 425-429.

8. Saltman D. Paper Basics: Forestry, Manufacture, Selection, Mathematics, and Metrics, Recycling. Litton Educational Publishing, Inc 1978 New York, NY

9. Holik H. Ed. Handbook of Paper and Board. 2006. Wiley-VCH Verlag GmbH & Co. Weinheim, Germany.

10. Hilton O. Pitfalls in the use of ultraviolet Examinations to Differentiate between writing papers. *J Crim Law Crim* 1949; 40: 519-522

11. Williams GJ, Drummond JG, Cisneros HA. A microscopical approach for examining fibre and paper structures. *J Pulp Pap Sci* 1994; 20: 110-114.

12. Kettunen H, Yu Y, Niskanen K. Microscopic Damage in paper. Part II: Effect of fibre properties. *J Pulp Pap Sci* 2000; 26: 260-265.

13. Schlesinger HL, Settle DM. A large-scale study of paper by neutron activation analysis. *J Forensic Sci* 1971; 16: 309-330.

14. Langmyhr FJ, Thomassen Y, Massoumi A. Atomic-absorption spectrometric determination of copper, lead, cadmium and manganese in pulp and paper by the direct-atomization technique. *Anal Chim Acta* 1974; 68: 305-309.

15. Simon PJ, Glessen BC, Copeland TR. Categorization of papers by trace metal content using atomic absorption spectrometric and pattern recognition techniques. *Anal Chem* 1977; 49: 2285-2288.

16. Manso M, Costa M, Carvalho ML. From papyrus to paper: Elemental characterization by x-ray fluorescence spectrometry. *Nucl Instrum and Meth A* 2007; 580: 732-734

17. Manso M, Costa M, Carvalho ML. Comparison of elemental content on modern and ancient papers by EDXRF. *Appl. Phys. A* 2008; 90: 43-48.

18. Van Es A, de Koeijer J, van der Peijl G. Discrimination of document paper by XRF, LA-ICP-MS and IRMS using multivariate statistical techniques. *Sci Justice* 2009; 49: 120-126.

19. Spence LD, Baker AT, Byrne JP. Characterization of document paper using elemental compositions determined by inductively coupled plasma mass spectrometry. *J. Anal. Atom Spectrom* 2000; 15: 813-819.

20. McGaw EA, Symanski DW, Smith RW. Determination of trace elemental concentrations in document papers for forensic comparison using inductively coupled plasma-mass spectrometry. *J. Forensic Sci* 2009; 54: 1163-1170.

21. Mendes TMFF, Baccan SN, Cadore S. Samples treatment procedures for the determination of mineral constituents in honey by inductively coupled plasma optical emission spectrometry. *J. Brazil Chem. Soc* 2006; 17: 168-176.

22. Krejčová A, Černohorský T, Meixner D. Elemental analysis of instant soups and seasoning mixtures by ICP-OES. *Food Chemistry* 2007; 105: 242-247.

23. Gonzálvez A, Llorens A, Cervera ML, Armenta A, de la Guardia M. Elemental fingerprint of wines from the protected designation of origin Valencia. *Food Chem* 2009; 112: 26-34.

24. Gonzálvez A, Armenta S, Pastor A, de la Guardia M. Searching the most appropriate sample pretreatment for the elemental analysis of wines by inductively coupled plasma-based techniques. *J. Agri. Food Chem* 2008; 56: 4943-4954.

25. Bentlin FRS, Pulgati FH, Dressler VL, Pozebon D. Elemental analysis of wines from South America and their classification according to country. *J. Brazil Chem. Soc* 2011; 22: 327-336.

26. Schnek ER, Almirall JR. Elemental analysis of glass by laser ablation inductively coupled plasma optical emission spectrometry (LA-ICP-OES). *Forensic Sci In* 2010; 217: 222-228.

Chapter 2: Theory

2.1 Microwave-assisted Digestion

Microwave-assisted digestion is a technique used to convert solid samples into liquid samples for trace element analysis by spectroscopic techniques, including inductively coupled plasma-mass spectrometry (ICP-MS), inductively coupled plasma-optical emission spectroscopy (ICP-OES), atomic absorption spectroscopy, and flame atomic absorption[1]. Microwave-assisted digestion converts microwave energy to heat using an electromagnetic field in order to obtain a homogenous solution of the sample for further analysis[2].

The main components of a microwave system are the magnetron, waveguide, mode stirrer, microwave cavity, and rotator plate (Figure 2.1). The magnetron is composed of a cathode surrounded by an anode containing an even number of resonant cavities[3]. Resonant cavities are hollow tubes that are coated in a material that is made to reflect a certain frequency[4]. As the cathode is heated, electrons are released and attracted to the anode. A magnet positioned between the cathode and anode creates a magnetic field which causes, the electrons move in a circular path around the cathode[4]. As the electrons pass by the cavities of the anode, the cavities resonate to generate microwaves. The microwaves are directed into the microwave cavity by the waveguide which is a reflective channel made of sheet metal.

Microwaves are homogenized by a mode stirrer in the microwave cavity and the plate that holds the samples are rotated so that all samples experience the same effect from the

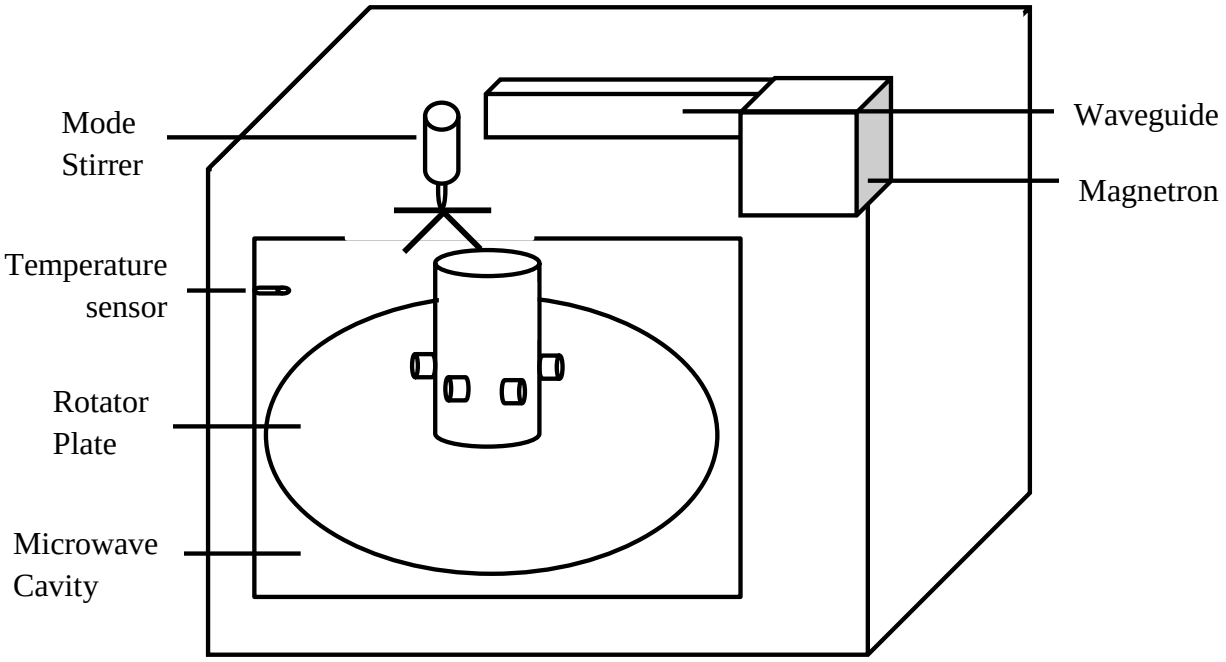

Figure 2.1. Diagram of a microwave-assisted digestion system.

microwaves. The inner walls of the microwave cavity are also made of a reflective material to increase the heating capacity of the microwave, as well as to prevent leakage of microwaves. A fiber-optic temperature probe is inserted in the reference vessel to monitor the temperature and pressure during the digestion. The temperature and pressure used for digestion depend on the composition of the actual sample; however, temperatures between 170-200 °C and pressures between 8-10 atm are common for microwave digestion[3].

For digestion, the solid sample is placed in an appropriate solution, such as a mineral acid, in a quartz vessel which is then placed in a Teflon® holder. Quartz and Teflon® can withstand the high temperatures and pressures used for digestion. Additionally, quartz does not leach elements into the sample and the microwave energy can pass through Teflon® to heat the sample[5]. Nitric acid is commonly used for digestion as it efficiently converts microwave energy to heat and, as this acid is a strong oxidizing agent, it can digest most elements in the periodic table. The oxidation potential of nitric acid is enhanced by increasing the temperature, increasing the pressure, and/or adding other reagents [5,6]. A common reagent that is used in addition to nitric acid is hydrogen peroxide. If used alone, hydrogen peroxide can react violently; however, when used in the presence of acid, it increases the oxidizing potential[5].

The Teflon® holder is placed into a sample holder which is sealed tightly and then placed on the rotator plate in the microwave. A four-step process is involved in heating the solution to the desired temperature. In the first step, microwave energy is used to heat the acid. This heating occurs by dielectric polarization and ionic conduction. Dielectric polarization is the alignment

and random reorientation of polar molecules, which creates friction from the forced movement due to oscillation. Ionic conduction is the attraction of free ions by the opposite charge of the electromagnetic field. There is resistance to the flow of the ions which also creates friction to heat the solution[5].

In the second step of the heating process, the solution is heated above its boiling point and vapors are formed. These vapors cannot absorb microwave energy so as they come in contact with the walls of the quartz vessel, the vapor condenses and releases energy to the vessel. In the third step, the energy released from the vapor to the wall is used to heat the vessel. In the final step, the temperature is maintained because the energy absorbed by the acid is the same as the energy released by the vessel as the vapor cools[5]. After digestion, samples are cooled to room temperature before removing them from the microwave to prevent the loss of trace metals present in the vapor.

An advantage of microwave digestion is the ability to use high temperatures for digestion while maintaining low pressures. The high temperatures are beneficial because a more complete digestion of the sample is possible in a short time period. Microwave digestion also allows for complete digestion of a sample in minutes while traditional digestion processes that use a hot plate could take 8 hours or more[6]. This is beneficial because more samples can be digested and analyzed compared to other methods in a given amount of time. However, in microwave-assisted digestion, the sample size is limited by the maximum volume that can be contained by the quartz vessel. As with other digestion techniques, there are also some elements that cannot be digested by microwave digestion, such as tungsten and zirconium.

2.2 Inductively Coupled Plasma

Inductively coupled plasma (ICP) is one type of plasma that can be used to atomize, ionize, and excite elements in a sample to allow for elemental analysis when coupled to a detector. A plasma is an electrically neutral medium that consists of atoms, ions, and free electrons[7]. While different gases such as argon, helium, and nitrogen can be used to create the plasma, argon is preferred because it is has a high gas kinetic temperature and a high electron number density compared to the other gases[8]. The importance of these characteristics to the ionization potential of a gas will be discussed later in this section.

The main components of an ICP are a torch, which consists of three concentric quartz tubes, a copper load coil, which is wrapped around the torch, and the plasma (Figure 2.2). Liquid samples are introduced into the plasma through the centermost quartz tube in a flow of Ar (1 L/min). A second stream of Ar, flowing through the middle tube at flow rates of approximately 0.5-2 L/min, is used to create the plasma[7,9]. To do this, a spark from a Tesla coil is used to seed the argon gas, resulting in loss of electrons and subsequent ionization of the gas. The plasma is sustained by the continuous collisions between the Ar ions and the electrons under the influence of the RF current applied to the coil. A third stream of Ar (15 L/min) is introduced tangentially to the flow of gas in the center tube to create a circular flow. This stream of Ar is used to lift the plasma clear of the quartz tubes and therefore prevent damage due to the high temperatures used.

The sample introduced to the plasma is desolvated, atomized, excited and ionized. Each of these processes occurs at different regions of the plasma over a range of temperatures

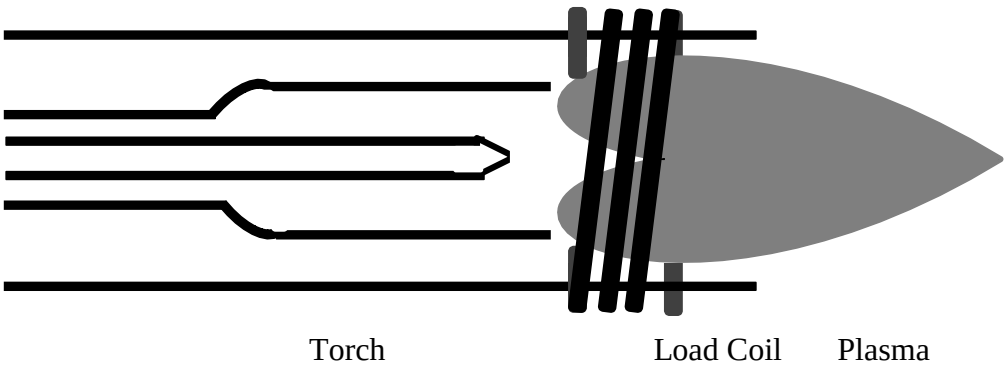

Figure 2.2. Schematic of an ICP showing the torch, the load coil, and the plasma

(Figure 2.3). Region A, the pre-heating area, has a temperature of approximately 8,000 K and is where desolvation of the samples occurs [7,10]. Region B is the initial heating area in which the temperature is approximately 6,500 K. In this region, atomization of the sample occurs. Region C is the normal analytical zone in which the temperature is approximately 6,000 K. In this region, ionization and excitation of the sample occurs. All of these processes occur rapidly, with the sample only spending approximately 2 ms in the plasma [10,11].

An important characteristic of elements analyzed by ICP is the degree of ionization which refers to the ratio of neutral atoms to ions in the plasma. The degree of ionization of an element depends on the electron number density, the temperature of the plasma, and the ionization energy of the element of interest which can be represented by the Saha equation

$$\frac{n_i n_e}{n_a} = \frac{2Z_i}{Z_a}\left(2\pi mk\frac{T}{h^2}\right)^{\frac{3}{2}} e^{-E_i/kT} \qquad \text{Equation 2.1}$$

where n_i, n_e, and n_a are the number densities of the ions, electrons, and atoms respectively (cm^{-3}), Z_i is the ionic partition function, Z_a is that atomic partition function, m is the mass of an electron ($9.11x10^{-31}$ kg), k is Boltzman's constant ($1.38x10^{-23}$ J/K), T is temperature of the plasma (K), h is Planck's constant ($6.63x10^{-34}$ Js), and E_i is the first ionization energy of the element (eV)[13]. The processes that occur in the ICP are not in true equilibrium because there are many different temperature zones in the plasma; however, the Saha equation can be used to approximate the degree of ionization [7]. When estimates of the degree of ionization for selected elements are calculated, the same temperature and electron density are used for all elements[7,13].

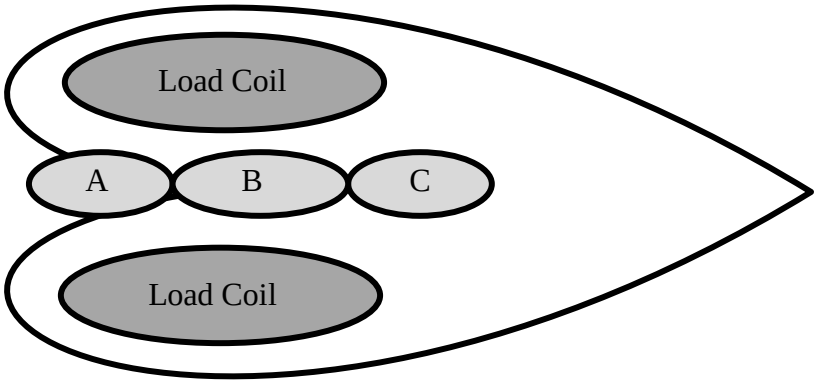

Figure 2.3. Temperature regions within the plasma of an ICP with A representing the preheating area, B representing the initial heating zone, and C representing the normal analytical zone[7]

As previously discussed, there are advantages to using Ar to generate the plasma. The first ionization energy of Ar is 15.76 eV so only elements that have first ionization potentials less than this will be ionized using an Ar plasma[7]. Over 80% of the elements in the periodic table have first ionization potentials less than 16 eV and therefore can be ionized using an Ar plasma[13]. Advantages of ionization using ICP are that there are few interferences, the ionization occurs using an inert gas, and the high temperatures allow for complete ionization compared to other types of plasma[10,11]. There are minimal interferences due to the constant presence of electrons generated by the plasma which ensures there are constant collisions and rearrangements between the free electrons and ions produced[10]. The sample is atomized and ionized by the plasma but never comes in direct contact with the plasma. This results in minimal interferences and carryover in the ionization and excitation processes.

2.3 Inductively Coupled Plasma-Optical Emission Spectrometry

Inductively coupled plasma optical emission spectroscopy (ICP-OES) is an atomic spectrometry technique used to quantify elements in a sample. In this technique, the ICP is used to atomize and excite elements in the sample while the OES is used as the detector. As the excited elements generated in the ICP relax to the ground state, energy is released in the form of light. Each element emits a set of characteristic wavelengths that correspond to changes in energy levels. The light is dispersed by the use of both a diffraction grating and a prism and detected by the OES where each wavelength is used to detect a different element and therefore detection of the elements present in the sample is possible.

The major components of an ICP-OES are shown in Figure 2.4. The sample is atomized and excited in the ICP (A). The light emitted as the sample relaxes to the ground state is focused using a lens (B) and directed into the spectrometer through the entrance slit (C). The light reaches the collimating mirror (D) which reflects the light so that the rays are parallel to each other. The light then reaches the echelle grating (E) where light rays of different wavelengths are diffracted at different angles. Constructive interference occurs when the difference in path lengths travelled by the light rays differ by an integer value[12]. The relationship for constructive interference is diffracted is described by

$$d(\sin i - \sin r) = m\lambda \qquad \text{Equation 2.2}$$

where d is the distance between the grooves of the grating, i is the angle of incidence, r is the diffraction angle, m is the integer diffraction order, and λ is the wavelength [10]. As seen from Equation 2.2, the intensity of light at a given diffraction angle may be the result of light rays of multiple wavelengths. For example, first order light (m=1) with a wavelength of 200 nm and second order (n=2) light with a wavelength of 100 nm would be diffracted at the same angle. The light is further separated by a prism (F) so that the different diffraction orders can be separated.

Finally, the light is reflected by a plane mirror (G) into an aperture plate (H) where the individual wavelengths are detected. The detector used with the ICP-OES system in this research was a charge-coupled device (CCD), which is a two-dimensional array of photosensitive elements that measures light intensity radiation[10]. The output of ICP-OES analysis is an emission spectrum in which the intensity is plotted on the y-axis and the wavelength is plotted on the x-axis. Each element has many characteristic emission lines so one of these lines, usually

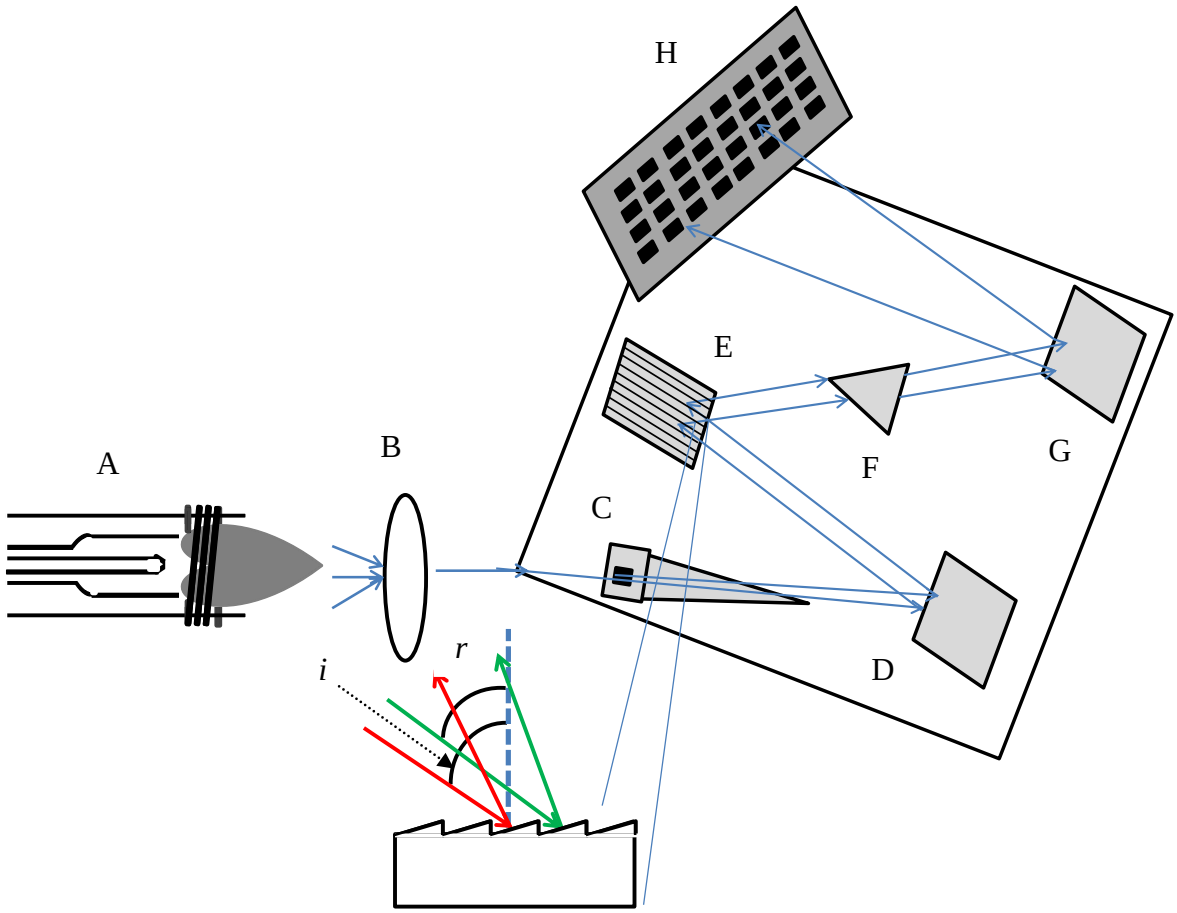

Figure 2.4 Schematic representation of an inductively coupled plasma optical emission spectrometer (ICP-OES) showing the ICP (A), focusing lens (B), entrance slit (C), collimating mirror (D), echelle grating (E), prism (F), plane mirror (G), and aperture plate (H) with the inset showing the echelle grating. The dashed line represents the normal to the plane, i is the angle of incident, r and is the angle of refraction.

with the highest intensity, is used for analysis. The intensity at that wavelength is proportional to the concentration of that element in the sample.

2.4 Inductively Coupled Plasma-Mass Spectrometry

Inductively coupled plasma mass spectrometry (ICP-MS) is a multi-elemental technique that is also used to detect and quantify elements in a sample. In ICP-MS, the ICP is used to ionize elements in the sample and the mass spectrometer is used as the detector. In the mass spectrometer, the ions generated in the ICP are separated by their mass-to-charge (m/z) ratio and the number of ions at each m/z is measured.

The samples are ionized at atmospheric pressure in the ICP; however, the mass spectrometer operates under vacuum. Therefore, the ions generated in the ICP (A) pass through an interface consisting of a sampler cone (B) and a skimmer cone (C) to enter the mass spectrometer (Figure 2.5). The sampler cone is positioned at the end of the normal analytical zone in the plasma and the ions are focused through a small orifice (~1 mm) in the cone to form an ion beam in a region of 2.5 torr of pressure[7]. This reduction in pressure occurs using a mechanical vacuum pump. The skimmer cone is positioned a few millimeters behind the sampler cone and has an orifice of less than 0.5 mm. The purpose of this cone is to limit the ions that are directed into the mass spectrometer. The pressure is reduced in the area behind the skimmer cone using an oil diffusion or turbomolecular pump[7].

When the ions leave the skimmer cone, a photon stop (D) is used to filter out the photons and neutral species still present in the plasma cloud. The photons need to be removed because

they can increase the background signal if the reach the detector[7]. An ion lens (E) is then used to further focus the ion beam. Before entering the mass analyzer, the ion beam passes through a collision cell (F) which is used to minimize the presence of molecular ions in the mass spectrometer. This is done to reduce interference between ions and elements at certain *m/z* values. The collision cell uses a fill gas fragment with the molecular ions[14]. Polyatomic ions may enter the collision cell with the same mass as an atomic ion but will have a different radius. The collision gas is used to remove the larger ion from the ion stream so only the ions of interest are detected. The gases, or scan modes, that can be used are hydrogen, helium, or no gas. Helium is used to reduce the energy spread of ions as they enter the mass analyzer and hydrogen is used to reduce the interference of argon-based molecules[14].

The most common mass analyzer used in ICP-MS analysis is a quadrupole mass analyzer. A quadrupole consists of four identical parallel cylindrical rods (Figure 2.6). A direct current (DC) potential is applied to the rods so that opposite pairs have the same potential and the potential alternates between positive and negative on the pairs. A radio-frequency (RF) alternating current is also applied to the rods. For each DC:RF ratio, only ions within a narrow range of m/z pass through the cavity between the rods and reach the detector. All other ions hit the rods, are neutralized, and pumped away by the vacuum system. By maintaining the DC:RF ratio but increasing the values used, the range of m/z values can be scanned to cover a wide range, such as 50-500 m/z. Most instruments are capable of scanning up to 3000 atomic mass units (amu) per second. This allows for rapid multi-element analysis of most elements in the periodic table.

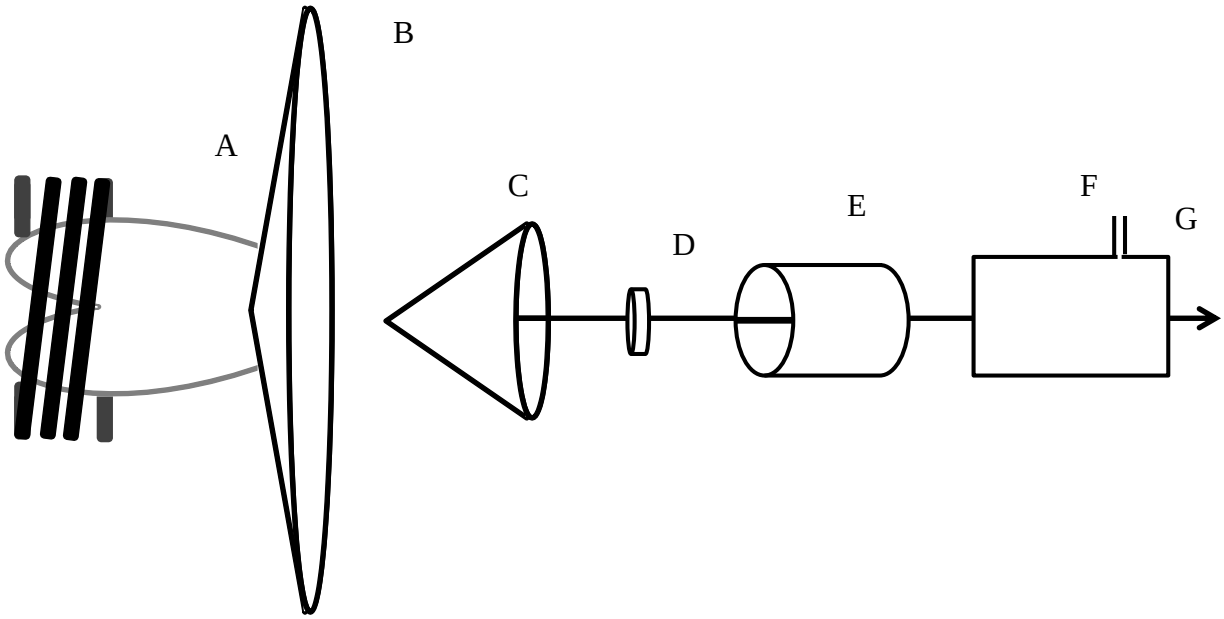

Figure 2.5. Interface between the ICP and MS showing the plasma (A), sampler cone (B), skimmer cone (C), photon stop (D), ion lens (E), and collision cell (F) with the ion beam (G) being directed into the mass spectrometer

After the ions are separated in the mass analyzer, they reach a detector. The detector used with most ICP-MS instruments is a continuous dynode electron multiplier. This consists of a curved, glass tube that narrows at the bottom. The top end of the multiplier, where ions enter, is held at high, negative potential (*e.g.*, -1 to -3 kV), while the bottom end is referenced to ground. The surface of the multiplier is coated with a substance that readily emits secondary electrons (*e.g.*, lead oxide). When a positively-charged ion from the mass analyzer strikes the surface of the tube, an average of two secondary electrons are emitted. The two electrons are attracted further into the tube by the increasing positive potential and undergo further collision with the surface of the tube. With each collision, more secondary electrons are released, increasing the original signal. In general, the total signal magnification is on the order of 2^n, where n is the number of collisions with the multiplier surface. In most multipliers, there are 18-20 collisions, resulting in a 10^5 to 10^6 increase in signal.

The output of analysis by ICP-MS is a mass spectrum, in which the signal intensity is plotted on the y-axis and the m/z is plotted on the x-axis. The m/z can be used to identify the element and the intensity is directly related to the concentration of the isotope in the sample.

2.5 Statistical Procedures

2.5.1 Grubbs' Test

Grubbs' test is used to determine if there are statistical outliers within a data set. The Grubbs's test is recommended in place of Dixon's test to determine if there are outliers when the data set consists of more than seven data points[15]. For this research, Grubbs' test was performed on the element concentrations within a ream of paper if the relative standard deviation of that

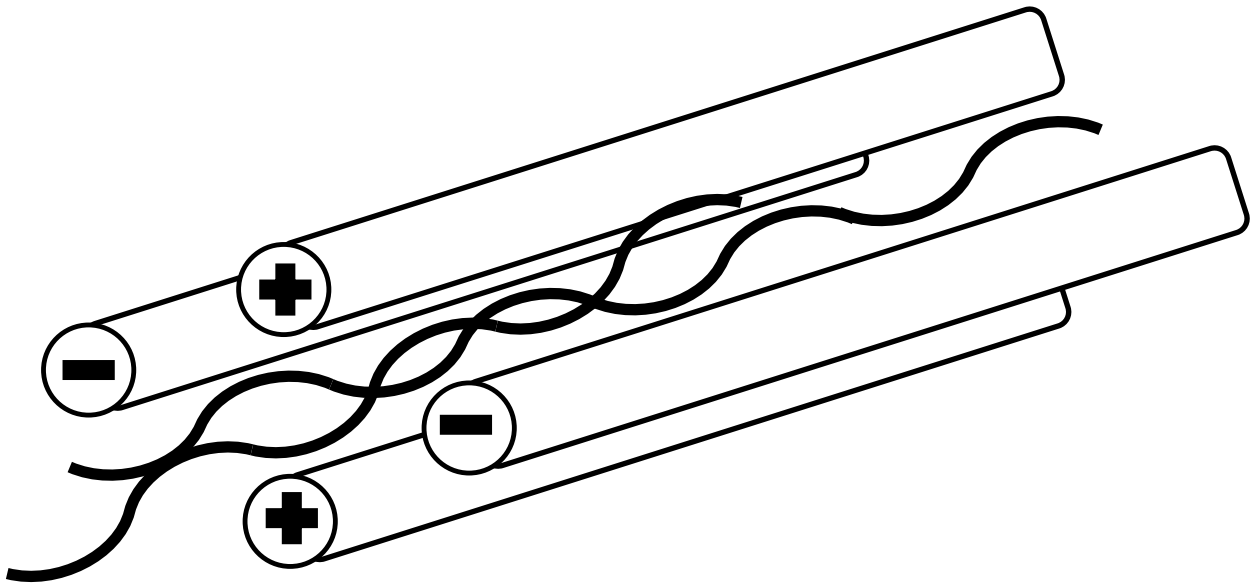

Figure 2.6. Schematic of a quadrupole mass analyzer indicating the opposite potentials on pairs of roads and the path of an ion

ream was greater than 15% for ICP-OES and greater than 25% for ICP-MS. Grubbs' test is performed by

$$G = \frac{|questioned\ concentration - \bar{x}|}{s} \qquad \text{Equation 2.3}$$

where, in this research, $\bar{x}$ is the mean element concentration of the ream and s is the standard deviation of the element concentration in the ream[15].

The calculated G-value is then compared to critical G-values to determine if the deviation between the questioned concentration and the mean of the ream is greater than the deviation within the ream. The critical G-value is based on the number of samples and the confidence level. If the calculated G-value is greater than the critical G-value, the sample is a statistical outlier and is rejected from the data set.

2.5.2 Analysis of Variance

Analysis of variance (ANOVA) is a statistical procedure that tests the null hypothesis (H_0) that there is not a statistical difference among the means of at least three groups within a data set. For this research, when the concentrations are compared within a paper type, each ream represents a group and the null hypothesis tested is that the mean element concentrations of the reams within a paper type are not statistically different. To test the null hypothesis, variation due to the two sources of error inherent in any experimental design are compared. The first source is the random error and refers to the error in the measurement[15]. The second source of error is the fixed-effect error and refers to the changing variable in the data set.

For this research, the random error is the error of the concentration within a single ream and the fixed-effect error is the error that exists among the different reams. One-way ANOVA was performed for this research because only one factor, the element concentration, was being compared within and among reams. ANOVA was first performed within a paper type to determine if there was variation in element concentration among reams of the same paper type. ANOVA was then performed to determine if there were statistical differences in average element concentration among the paper types.

There are three calculations required to perform ANOVA. In this research, each calculations is performed within a ream, between reams, and for each paper type. These calculations are shown in Table 2.1 only using two reams for simplicity[16]. The number of calculations does not change if more reams are compared; however, the number of terms used within the calculation would increase. The first calculation is the sum of squares (SS), which is the measure of the variability of the data set and can be calculated within a ream, between reams, or for the whole data set. For the total SS and among ream SS, there is a correction to the mean that has to be calculated. This correction, C, is calculated by:

$$C = \frac{\left(\sum T_{ij}\right)^2}{N} \qquad \text{Equation 2.4}$$

where Y represents all the data points and N is the total number of samples in the data set. The correction factor is used in the calculation of the among reams SS and the total SS because the variance is due to both the random error and the fixed-effect error[17].

The second calculation is the degrees of freedom (DF) within a group, between groups, and for the paper type. The DF represents how many values were used to perform a specific

Table 2.1. Calculations needed for one-way analysis of variance

Source of variance	Sum of squares	Degrees of freedom	Mean square
Between reams	$\sum_{i=1}^{k} \frac{T_i^2}{n_i} - C$	k-1	$\frac{between\ ream\ SS}{k-1}$
Within ream	$SS_{Total} - SS_{Between\ reams}$	N-k	$\frac{within\ ream\ SS}{N-k}$
Total	$\sum (T_{ij})^2 - C$	N-1	

T_{ij}= individual concentration, T_i=sum of measurements in ream n=number of replicates per ream, k=number of reams, N=total number of samples, C=correction to mean

calculation[16]. The final calculation is to determine the mean square (MS), or variance, among the groups and within a group. This value could also be found for all samples in the paper type; however, this calculation is not needed to perform ANOVA[16].

In order to determine if there is a statistical difference among mean element concentrations of the reams of a paper type, either the calculated F-value or the p-value can be used. The F-value is calculated by

$$F = \frac{among\ ream\ MS}{within\ ream\ MS} \qquad \text{Equation 2.5}$$

The F-value is compared to a critical F-value obtained from statistical tables, which depends on the number of samples, degrees of freedom, and confidence level of interest. If the calculated F-value is greater than the critical F-value, there is a statistical difference among the means in the data set.

If ANOVA is performed using a software program, such as Microsoft Excel, a p-value is calculated in addition to an F-value. A p-value is used in a hypothesis test to determine the probability of a measurement falling in the range where the null hypothesis is true. A p-value of 0.05 indicates that a measurement lies within the 5% of all possible measurements that make the null hypothesis true. In this research, ANOVA was performed at the 95% confidence level, such that a p-value less than 0.05 indicated a statistical difference among the means of the reams.

2.5.3 Tukey's Honestly Significant Difference Test

Tukey's honestly significant difference (HSD) test is a pair-wise comparison which calculates a q-value to determine if the difference between the means of two groups within a data set is statistically significant[16]. Tukey's test is typically performed after ANOVA has shown that the means in a data set are statistically different. For this research, Tukey's HSD test was used to determine which ream was significantly different in concentration for each paper type. The q-value is calculated by

$$q = \frac{\bar{X}_B - \bar{X}_A}{SE} \qquad \text{Equation 2.6}$$

where $\bar{X}_B$ is the mean of ream B, $\bar{X}_A$ is the mean of ream A, and SE is the standard error, which is calculated by

$$SE = \sqrt{\frac{s^2}{n}} \qquad \text{Equation 2.7}$$

where s^2 is the within ream mean square calculated during ANOVA and n is the number of samples in a ream[16]. If there are a different number of samples in each ream, the standard error is calculated by

$$SE = \sqrt{\frac{s^2}{2}\left(\frac{1}{n_A} + \frac{1}{n_B}\right)} \qquad \text{Equation 2.8}$$

where n_A is the number of measurements in ream A and n_B is the number of measurements in ream B. The calculated q-value is compared to a critical q-value obtained from statistical tables. The critical q-value depends on the confidence level, the number of samples, and the degrees of

freedom of the data set. If the calculated q-value is less than the critical q, there is a statistical difference between the two means and the null hypothesis is rejected.

2.5.4 Principal Components Analysis

Principal components analysis (PCA) is an unsupervised multivariate statistical procedure that reduces the dimensionality of a data set while still retaining all the information in the original data set. This is done by reducing the number of variables of the data set to only those that contribute most to the variance. The variables can be continuous, such as in a chromatogram, or discrete, such as the element concentrations used in this research. An n-dimensional scores plot is generated from PCA which is used to visually assess the association of chemically similar samples and the discrimination of chemically different samples. The scores plot is usually plotted in two dimensions to simplify visual assessment of the positioning of the samples. A loadings plot is also generated which shows the variables or, as in this research, the elements, that contribute to the variance and can be used to explain the positioning of the samples on a scores plot.

The first step in PCA is to mean center the data so that the mean of each variable is set to zero. This is done to ensure that the first principal component accounts for the most variance among samples[18]. The mean of each variable is calculated and subtracted from the value of each individual sample. In this research, the mean concentration of each element among all samples was calculated and then subtracted from the element concentration of each sample to generate the mean-centered data.

After the data are mean centered, the covariance matrix is calculated. Covariance is a measure of how far an individual concentration is from the mean in two dimensions and can be calculated for all dimensions of the data. If the data are plotted on xy-coordinates, the covariance between variables X and Y is calculated by the equation:

$$\text{cov}\,(X,Y) = \frac{\sum_{i=1}^{n}(X_i-\overline{X})(Y_i-\overline{Y})}{n-1} \qquad \text{Equation 2.9}$$

where n is the number of dimensions in the data set, X_i is the x-coordinate of data point *i*, $\overline{X}$ is the mean concentration in the x-dimension, Y_i is the y-coordinate of data point *i*, $\overline{Y}$ is the mean value in the y-dimension. This calculation is done for all variables, in each dimension, for all dimensions of the data. For example, if there are 3 dimensions (x, y, and z), the covariance is summarized in a 3 x 3 covariance matrix, as shown below:

$$C = \begin{pmatrix} cov(x,x) & cov(x,y) & cov(x,z) \\ cov(y,x) & cov(y,y) & cov(y,z) \\ cov(z,x) & cov(z,y) & cov(z,z) \end{pmatrix} \qquad \text{Equation 2.10}$$

In this matrix, the covariance along the diagonal is equivalent to the variance of x, y, and z and the matrix is symmetric around the diagonal as cov(x,y)=cov(y,x)[18].

Using the covariance matrix, the eigenvectors and eigenvalues can be calculated. An eigenvector is a unit vector that is multiplied by the data matrix to produce a vector that is a multiple of the unit vector. Eigenvectors can only be found for a square matrix so if the original matrix is not square, zeros are added to make it square. For an n x n matrix, there are *n* eigenvectors, all of which are orthogonal to each other. The eigenvectors represent the reduced set of variables for the data and are called principal components (PCs). The eigenvalue is the

integer that the unit vector is multiplied by to produce the eigenvector. The largest eigenvalue is associated with PC1 and accounts for the most variance among the samples. The amount of variance that an eigenvalue accounts for is calculated by the ratio of that eigenvalue to the sum of all eigenvalues and is normally represented as a percentage. Ideally, the first two or three PCs should account for more than ~95% of the variance in the data set [19].

There are two plots that can be generated from the output of PCA. The first is a scores plot which allows for visual assessment of the similarities and differences among the samples. The score of a sample on a particular PC is calculated by multiplying the eigenvector of that PC by the mean-centered data for the sample and summing. While this could be done for all PCs, the scores are usually only calculated for the first few PCs which account for most of the variance in the data set.

The second plot is a loadings plot that shows which variables contribute most to the variance among the samples. The loadings plot is generated by plotting the eigenvectors of at least two PCs. The loadings plot can be used to explain the positioning of samples on the scores plot. The further a variable is from the origin of the loadings plot, the more influence it has on the positioning of the samples on the scores plot. For this research, the further an element is from the origin, there is more variation in concentration of that element among samples.

Once a scores plot is generated, additional samples can be projected onto it. For this research, the element concentrations in the sheets of reams A and B were used to create the scores plot and then the scores for the sheets in ream N were calculated and projected onto the scores plot. To calculate scores, the element concentrations in ream N were mean centered using the average concentration for that element in corresponding reams A and B. The mean-centered data for each sample were multiplied by the eigenvector for PC1 and summed to calculate the

score for the sample on PC1. This process was repeated to calculate scores for each sample on PC2. The calculated scores were then projected onto the original scores plot to determine if there was association among the three reams of a paper type.

2.5.5 Hierarchical Cluster Analysis

Hierarchical cluster analysis (HCA) is another unsupervised statistical procedure used to form groups within a data set. While PCA identifies differences among samples, HCA uses similarities among the samples in a data set to form these groups. The data are plotted on a coordinate plane with n dimensions and the distance between samples is measured[15]. There are many methods used to calculate the distance between two points but the most common is Euclidean distance which is calculated by

$$d = \mathrm{sqrt}[(X_1-Y_1)^2 + (X_2-Y_2)^2+\ldots+(X_n-Y_n)^2] \qquad \text{Equation 2.11}$$

where X and Y are the two samples, n is the number of dimensions in the data set, and the subscripts represent the dimension being compared. In agglomerative HCA, which was used in this research, each sample begins as its own group. The two samples that have the shortest Euclidean distance between them form a cluster and the process repeats, calculating Euclidean distances. The distance between clusters can be calculated using many different linkage methods but the most common are single linkage and complete linkage (Figure 2.7). In the complete linkage method, the Euclidean distance is calculated between the two furthest apart data points in the two clusters being considered. In the single linkage method, the Euclidean distance is calculated between the two nearest data points in the two clusters being considered.

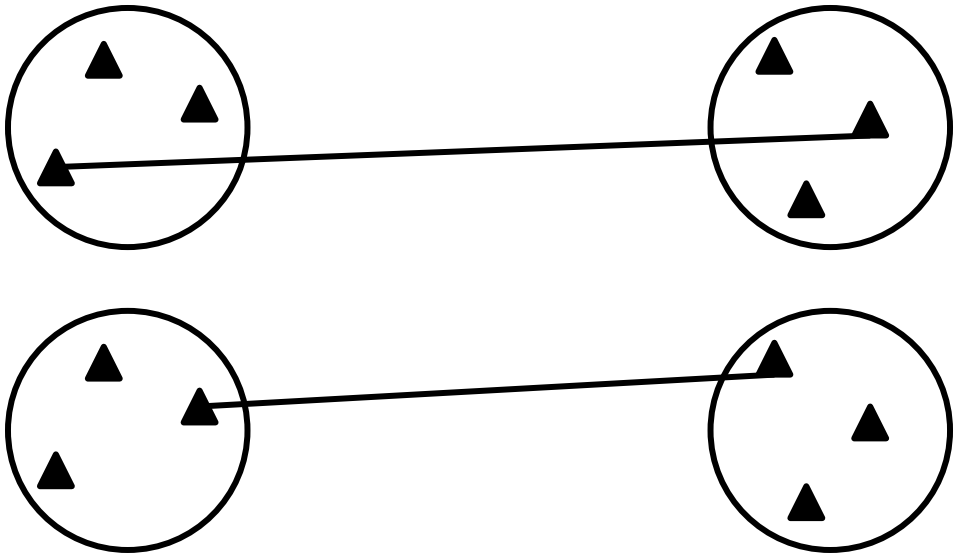

Figure 2.7 Diagram of the linkage methods that can be used for HCA

The process of calculating distances and linking clusters continues iteratively until all samples are clustered in one group. The output of HCA is a dendrogram which shows how the clusters form and the level of similarity among clusters. The similarity (s_{ij}) between two clusters is calculated by

$$s_{ij}=100\left(1-d_{ij}/d_{max}\right) \qquad \text{Equation 2.12}$$

where d_{ij} is the Euclidean distance between two clusters, i and j represent two different clusters and d_{max} is the greatest distance between any two samples in the data set[15]. Chemically similar samples will be clustered together at higher similarity levels while chemically different samples will be clustered at lower similarity levels.

REFERENCES

REFERENCES

1. Bizzi CA, Flores EMM, Barin JS, Garcia EE, Nóbrega JA. Understanding the process of microwave-assisted digestion combining diluted nitric acid and oxygen as auxiliary reagent. *Microchem J* 2011; 99: 193-196.

2. Kingston HM, Walter PJ. The art and science of microwave sample preparation for trace and ultratrace elemental analysis. In: Montaser A, editor. Inductively coupled plasma mass spectrometry. New York, NY: Wiley-VCH, 1998; 33-81.

3. Mingos DMP, Baghurst DR. Applications of microwave dielectric heating effects to synthetic problems in chemistry. In: Kingston HM, Haswell SJ, editors. Microwave-enhanced chemistry fundamentals, sample preparation, and applications. Washington, DC: American Chemical Society, 1997; 3-53.

4. Surducan V, Surducan E, Ciupa R. Variable power, short microwave pulses generation using a CW magnetron. *Advs Electrochl El Eng* 2011; 11: 49-54

5. Kingston HM, Walter PJ, Chalk S, Lorentzen E, Link D. Environmental microwave sample preparation: Fundamental, methods and applications. In: Kingston HM, Haswell SJ, editors. Microwave-enhanced chemistry fundamentals, sample preparation, and applications. Washington, DC: American Chemical Society, 1997; 223-349.

6. Walter PJ, Chalk S, Kingston HM. Overview of microwave-assisted sample preparation. In Kingston HM, Haswell SJ, editors Microwave-enhanced chemistry fundamentals, sample preparation, and applications. Washington, DC: American Chemical Society, 1997; 55-222.

7. Taylor HE. Inductively Coupled Plasma-Mass Spectrometry Practices and Techniques. San Diego, CA: Academic Press, 2001.

8. Montaser A, Zhang H. Mass spectrometry with mixed-gas and helium ICPs. In: Montaser A editor. Inductively coupled plasma mass spectrometry. Wiley-VCH: New York, NY, 1998; 809-890.

9. Hill, SJ, Fisher, A, Foules, M. Basic concepts and instrumentation for plasma spectrometry. In Hill, SJ, editor. Inductively coupled plasma spectrometry and its applications. Oxford, England: Blackwell Publishing Ltd, 2007;61-97.

10. Skoog DA, Holler FJ, Crouch SR. Principles of instrumental analysis. 6th ed. Belmont, CA: Thomson, 2007.

11. Lajunen LHJ, Perämäki P. Spectrochemical analysis by atomic absorption and emission. 2nd ed. Cambridge, England: The Royal Society of Chemistry, 2004.

12. Harris, DC. Exploring chemical analysis. 4th ed. New York, NY: W.H. Freeman, 2009.

13. O'Connor G, Evans EH. Fundamental aspects of inductively coupled plasma-mass spectrometry (ICP-MS). In: In Hill SJ, editor. Inductively coupled plasma spectrometry and its applications. Oxford, England: Blackwell Publishing Ltd, 2007;134-159.

14. Turner PJ, Mills DJ, Schröder E, Lapitajs G, Jung G, Iacone LA, Hayday DA, Montaser A. Instrumentation for low- and high-resolution ICPMS. In: Montaser A editor. Inductively coupled plasma mass spectrometry. New York, NY: Wiley-VCH, 1998; pp 421-501.

15. Miller JN, Miller JC. Statistics and chemometrics for analytical chemistry. 4th ed. Harlow, England: Pearson Education Limited, 2000.

16. Zar JH. Biostatistical Analysis. 4th ed. Upper Saddle River, NJ: Prentice Hill, 1999.

17. Fryer HC. Concepts of Methods of Experimental Statistics. Boston, MA: Allyn and Bacon, Inc, 1966.

18. Smith LI, A tutorial on principal components analysis. 2002. <www.cs.otago.ac.nt/ cosc453/student-tutorials/principal-components>

19. Brereton RG. Applied chemometrics for scientists. Hoboken, NJ: John Wiley & Sons, Ltd, 2007.

Chapter 3 Materials and Methods

3.1 Sample Collection and Preparation

Two reams (labeled A and B) of four different types of document paper (color inkjet, laserjet, multipurpose, and office paper) from one manufacturer (Hewlett-Packard) were purchased in October 2010. Laserjet, multipurpose, and office paper were purchased from online suppliers, while color inkjet paper was purchased from a local office supply store in Okemos, MI. In November 2011, one additional ream (labeled N) of each paper type was purchased from office supply stores in Okemos. The physical characteristics of each paper type are summarized in Table 3.1.

Samples of paper for analysis were taken from two sheets within each ream: one sheet was selected from the top third of the ream and the other sheet was selected from the bottom third of the ream. All sheets were 8.5 in x 11 in and five samples, approximately 2 cm x 3 cm, were cut from each sheet using plastic scissors. Samples numbered 1–5 were cut from the sheet from the top third of the ream and samples numbered 6–10 were cut from the sheet from the bottom third of the ream as shown in Figure 3.1.

Samples were placed individually into separate plastic bead bags (Hobby Lobby Stores®, Oklahoma City, OK) that were previously weighed. The bag was re-weighed to determine the mass of the paper sample (average mass = 0.078 ± 0.005 g) and the samples were stored in the bag until digestion.

Table 3.1. Physical characteristics of each paper type

Paper Type	Purchased From	Ream	Purchase Date	Bright-ness	# sheets/ ream	Weight (lbs)	Barcode Number	Identification Number
Color Inkjet	Meijer, Okemos, MI	A	October 2010	96	500	24	764025-202008	C-C720101 1010013/2B
Color Inkjet	Meijer, Okemos, MI	B	October 2010	96	500	24	764025-202008	C-C720101 1010013/2B
Color Inkjet	Meijer, Okemos, MI	N	November 2011	96	500	24	764025-202008	C-C7201102 280005/1C
Laserjet	www.officemax.com	A	October 2010	97	500	24	764025-931007	TI 10 132123 AC 010 05 05:19
Laserjet	www.officemax.com	B	October 2010	97	500	24	764025-931007	TI 10 132123 AC 010 05:21
Laserjet	Office Max, Okemos MI	N	November 2011	97	500	24	764025-931007	TI 10 299 23 AC 015 04:18
Multipurpose	www.officemax.com	A	October 2010	96	500	20	764025-930000	C-C920100 9050016/1D
Multipurpose	www.officemax.com	B	October 2010	96	500	20	764025-930000	C-C920100 9050016/1D
Multipurpose	Office Max, Okemos MI	N	November 2011	96	500	20	764025-930000	C-C920110 1290017/2C
Office	www.officemax.com	A	October 2010	92	500	20	764205-932493	C-C720091 0060005/1A
Office	www.officemax.com	B	October 2010	92	500	20	764205-932493	C-C720091 0060005/1A
Office	Target, Okemos, MI	N	November 2011	92	500	20	764205-932493	C-C720110 7080004/2A

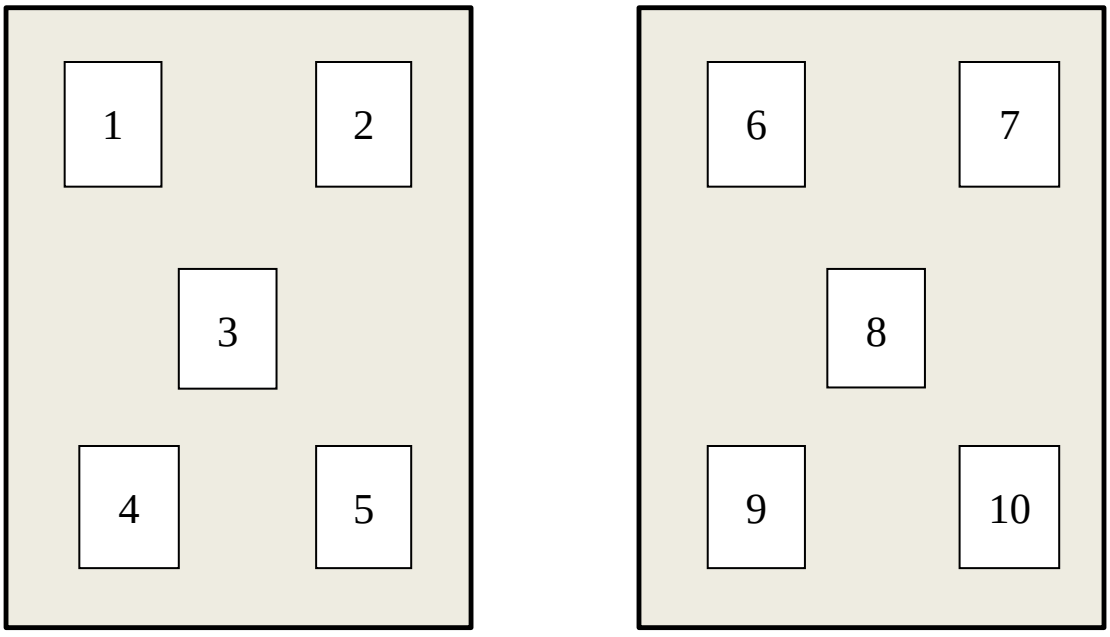

Figure 3.1. Diagram of samples from a single sheet with Sheet 1 denoting the sheet from the top third and Sheet 2 denoting the sheet from the bottom third of the ream and the numbers representing the samples analyzed. This figure is not to scale.

3.2 Microwave-assisted Digestion

All microwave digestions were performed in an Ethos EX Microwave Solvent Extraction Labstation (Milestone Inc., Shelton, CT). Prior to digestion, all glassware used was acid washed according to the standard operating procedures of the laboratory. Samples of paper were placed into separate quartz digestion vessels (Milestone Inc.), 1.5 mL 70% nitric acid (Fisher Scientific, Pittsburg, PA), and 0.75 mL 30% hydrogen peroxide (J.T. Baker, Center Valley, PA) were added to the vessel. Each quartz vessel was then capped and placed into a separate Teflon® liner (Milestone Inc.) that contained 1.0 mL 30% hydrogen peroxide (J.T. Baker) and 11 mL distilled water, which was available in the laboratory. The Teflon® liners were sealed and secured following the manufacturer's recommendations. Figure 3.2 shows a diagram of the sample holder system prior to digestion.

The sealed Teflon® liners were placed on the rotator plate that was inside the microwave. A total of eight paper samples were digested at a time and the ninth vessel contained a procedural blank, which was prepared in the same way as previously described, except omitting the paper sample. The temperature probe was inserted into the vessel containing the procedural blank and the samples were digested using the following program: 15 min ramp to 210 °C, 10 min hold at 210 °C[2]. The maximum allowed wattage, based on the number of samples being digested and the temperature program used, was set to 1000 W[1].

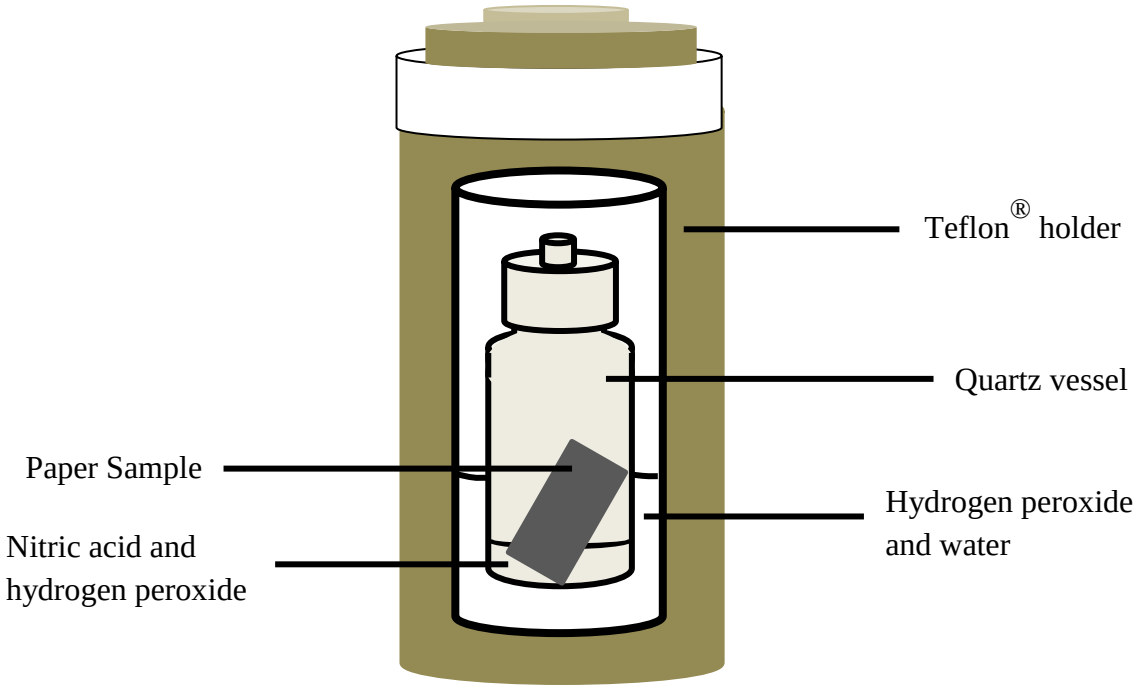

Figure 3.2. Diagram of the digestion vessel with a paper sample

After digestion, the vessels were cooled to below 60 °C before being opened to prevent vapor loss. Each quartz vessel was removed from the Teflon® liner and dried slightly on a paper towel so the water solution would not mix with the digest. The digest was then poured into a 15 mL centrifuge tube (Corning Inc., Corning, NY) and stored in a refrigerator until analysis. After each digestion, the quartz vessels were cleaned. The same procedure was used to clean the vessels as was used for digestion, except the paper samples were omitted when the vessels were cleaned.

The same digest was used for analysis by both inductively coupled plasma-optical emission spectroscopy (ICP-OES) and inductively coupled plasma-mass spectrometry (ICP-MS); however separate aliquots of the digest were used for each instrument. Prior to elemental analysis, the digests were diluted so that the nitric acid concentration was compatible with the instrumental technique. Following the microwave digestion, each digest contained approximately 46% nitric acid, which was diluted to a final concentration of 2% nitric acid. To do this, 430 µL of digest were transferred into a new centrifuge tube (Corning Inc.) and 10 mL HPLC-grade water (J.T. Baker) were added.

For ICP-OES analysis, 520 µL of the internal standard solution, which contained 200 mg/L germanium (Ge) and 20 mg/L indium (In) and bismuth (Bi) (Specpure®, Alfa Aesar, Ward Hill, MA) were added to the 10.43 mL of the diluted digest to give a final concentration of 9.49 mg/L of Ge and 0.9491 mg/L of In. For ICP-MS analysis, 200 µL of the diluted digest were added to 5 mL of the internal standard solution which contained 0.8 mg/L Ge, 0.8 mg/L scandium (Sc), 0.08 mg/L In, and 0.08 mg/L Bi (GFS Chemicals, Columbus, OH) to give a final concentration of 0.769 mg/L Ge and Sc, and 0.0769 mg/L In and Bi. The concentration of the

internal standard was prepared so that the signal intensity was similar to the signal intensity in the samples as observed in preliminary work.

3.3 Standard Preparation

Element standards were prepared to calibrate both the ICP-MS and ICP-OES instruments. The elements used for analysis were selected based on preliminary experiments in the forensic chemistry laboratory at Michigan State University, in addition to elements previously reported in the literature and were as follows: aluminum (Al), antimony (Sb), barium (Ba), cadmium (Cd), cobalt (Co), chromium (Cr), copper (Cu), iron (Fe), magnesium (Mg), manganese (Mn), nickel (Ni), lead (Pb), vanadium (V), and zinc (Zn) (Specpure®, Alfa Aesar, Ward Hill, MA)[2,3]. The concentration of the stock solutions of the Cu, Fe, and Mg standards was 10,000 mg/L in nitric acid, while the concentration of the stock solutions of the remaining elements was 1,000 mg/L in nitric acid.

The same elements were used for both instruments; however, the concentration range of the standards was different. All standards were prepared in 2% nitric acid, which was diluted from high-purity nitric acid (Fisher Scientific) using HPLC-grade water (J.T. Baker). Seven multi-element standards were prepared with the element concentrations shown in Tables 3.2 and 3.3 for ICP-OES and ICP-MS, respectively.

For ICP-OES, Ge, In, and Bi were used as internal standards and these elements were added to each standard to a final concentration of 10 mg /L Ge and 1 mg /L In and Bi. For ICP-MS, 200 µL of each calibration standard were added to 5 mL of the internal standard solution,

Table 3.2. Concentration of elements in each standard (µg/L) used for ICP-OES calibration

Standard	1	2	3	4	5	6	7
Al, Fe, and Mg	25.0	50.0	100	250	500	1000	2000
Ba, Mn, Pb, Sb, and Zn	0.0500	0.100	1.00	3.00	5.00	10.0	25.0
Cd, Co, Cr, Cu, Ni, and V	0.0500	0.100	0.500	0.750	1.00	3.00	5.00

Table 3.3. Concentration of elements in each standard (µg/L) used for ICP-MS calibration

Standard	1	2	3	4	5	6	7
Al, Fe, and Mg	0.962	1.923	3.846	9.615	19.231	38.462	76.923
Ba, Mn, Pb, Sb, and Zn	0.00192	0.00385	0.0385	0.115	0.192	0.385	0.962
Cd, Co, Cr, Cu, Ni, and V	0.00192	0.00385	0.0192	0.0288	0.0385	0.115	0.192

containing Ge, Sc, In and Bi, so that the final internal standard concentration was 0.769 mg /L for Ge and Sc and 0.0769 mg/L for In and Bi.

3.4 Sample and Standard Analysis

Prior to analysis by either instrument, all samples and standards were vortexed to ensure uniform concentration throughout the sample. In preliminary studies, the concentration of the internal standard was similar in all standards and samples only when the samples were vortexed prior to analysis. For the first set of calibration samples analyzed each day, a 0 μg/L standard (nitric acid only) was analyzed first, followed by the seven standards, which were analyzed in a random order. For all additional calibration sets analyzed on that day, the eight standards were placed in the autosampler in random order. A total of thirty paper samples and procedural blanks were analyzed between each set of calibration standards.

The ICP-OES used was a Varian 710-ES Axial ICP-OES (Agilent Technologies Inc., Santa Clara, CA) with Lytron Modular Cooling System (Lytron® Total Thermal Solutions, Woburn, MA) and a Varian SPS3 sample preparation system (Agilent Technologies Inc.). The ICP-MS used was an Agilent 7500ce ICP-MS (Agilent Technologies Inc.) with an ASX-520 Autoampler (CETAC, Omaha, NE). The operating parameters for each instrument are listed in Table 3.4.

For ICP-OES, the wavelength emission line used for each element was selected based on its intensity and distance from the wavelength of other elements of interest. Emission lines used for the elements of interest are shown in Table 3.5. For ICP-MS, the most common isotope for each element was used along with the recommended scan mode for each element (Table 3.5).

Table 3.4 Instrument parameters used for ICP-OES and ICP-MS analysis

Parameter	ICP-OES	ICP-MS
RF power (W)	1000	1500
Plasma gas flow (L/min)	15	8
Auxiliary gas flow (L/min)	1	0.82
Nebulizer pump (rps)	0.25	0.22
Replicate read time (s)	5	280
Uptake delay (s)	30	30
MS Resolution	n/a	Unit mass
Quadrupole Bias (V)	n/a	-3

Table 3.5 List of the elements used with the emission line used for ICP-OES analysis and the mass and scan mode used for ICP-MS analysis and the internal standard used for normalization

Element	Emission Line (nm)	Internal Standard Used with ICP-OES	Mass (m/z)	Scan Mode	Internal Standard Used with ICP-MS
Al	396.120	In	27	3	Ge
Ba	455.400	In	137	3	In
Bi	190.171	Bi	209	3	Bi
Cd	214.439	Ge	111	3	Ge
Co	231.160	Ge	59	2	Ge
Cr	267.716	Ge	53	2	Ge
Cu	327.395	Ge	65	2	Ge
Fe	238.204	Ge	56	1	Ge
Ge	206.866	Ge	72	1,2,3	Ge
In	410.176	In	115	1,2,3	In
Mg	279.553	Ge	24	2	Ge
Mn	257.610	Ge	55	3	Ge
Ni	231.604	Ge	60	2	Ge
Pb	220.353	In	206	3	Bi
Pb	220.353	In	207	3	Bi
Pb	220.353	In	208	3	Bi
Sb	187.052	Bi	121	3	In
Sc	n/a	Sc	45	1,2,3	Sc
V	292.401	Ge	51	2	Ge
Zn	213.857	Ge	66	1,2,3	Ge

The scan mode describes the gas used in the collision cell for the mass spectrometer. In scan mode 1, hydrogen is used, in scan mode 2, helium is used, and in scan mode 3, no gas is used. The internal standards (Ge, In, and Sc) were analyzed using the three scan modes because for normalization, the intensities of the element of interest and the internal standards had to be compared using the same scan mode. For both ICP-OES and ICP-MS, standards and samples were analyzed in triplicate and the average intensity, or counts, of the triplicates was used for calibration and all additional statistical analyses of the samples.

The signal of each element in the sample was normalized to the appropriate internal standard. For ICP-OES, the internal standard was the element with the emission line closest to that of the element of interest. For ICP-MS, the internal standard was the element with the mass closest to the element of interest, analyzed using the same scan mode. Calibration curves were plotted for each element using the normalized instrument responses for the standards analyzed immediately before and immediately after the samples to be quantified. This was done to account for instrument drift occurring during the analytical run. A linear regression line was fit to the calibration curve for each element. The regression equation was used to quantify the concentration of each element in the samples.

Prior to any statistical analysis, the concentration of each sample was blank corrected using the procedural blank that was microwave digested in the same digestion. Then, the concentration was corrected for the dilution factor and the mass of paper initially digested so the concentration of the samples was expressed as microgram of element per gram of paper (µg/g).

3.5. Analytical Figures of Merit

Analytical figures of merit for each instrument were determined for all elements using the calibration curves for each element. Separate calibration curves were made for each paper type to represent the operation of the instrument. Each calibration curve consisted of the set of standard analyzed directly before and after the paper samples. The coefficient of determination, r^2, was used to determine the linearity of the calibration line using the eight points. The relative standard deviation (RSD) of the normalized signal at each concentration was used to assess instrument precision. The relative standard deviation is found by dividing the standard deviation by the mean and is a measure of the variation among samples with respect to the mean.

For these elements, the limit of detection (LOD) and limit of quantitation (LOQ) were determined. The LOD was calculated as the signal of the nitric acid blank plus three times the standard deviation of the blank and the LOQ was calculated as the signal of the nitric acid blank plus ten times the standard deviation of the signal of the blank[4].

3.6. Data Analysis

The homogeneity of element concentration within a ream was determined by calculating the RSD for each element concentration per ream, per paper type. For any element concentration in which the RSD was greater than 15%, the Grubbs' test was used to determine if any of the samples were statistical outliers within the ream[5]. Any outliers were removed and the RSD was

recalculated. If the recalculated RSD was still greater than 15%, the Grubbs' test was performed again.

3.6.1. Analysis of Variance

Concentrations of each element within a paper type and between paper types were compared using analysis of variance (ANOVA) and Tukey's honestly significant difference (HSD) test. ANOVA was performed using the data analysis add-on in Microsoft Excel (version 12.0.6661.5000, Microsoft Corp., Redmond, WA) and Tukey's HSD test was performed in Microsoft Excel (Microsoft Corp.). All statistical tests were performed at the 95% confidence level.

First, the element concentrations within a paper type were assessed for statistically significant differences. To do this, one-way ANOVA was performed for one element at a time, based on the ten concentrations (five samples per sheet, two sheets per ream) in each of the three reams for each paper type[6]. If there was a statistically significant difference in element concentration, Tukey's honestly significant difference (HSD) test was performed to determine which of the three reams was statistically different [6].

Next, element concentrations among the paper types were compared for statistically significant differences using ANOVA. To do this, the average element concentration in reams A and B of each paper type were compared, one element at a time. Again, Tukey's HSD test was performed if there was a difference to determine which paper types were statistically different.

3.6.2. Principal Components Analysis

Principal components analysis (PCA) was performed in MatLab (version 7.7.0.471, The Mathworks, Natick, MA) using the average concentration of each element per sheet in reams A and B for all paper types (n=4). The resulting eigenvalues, eigenvectors, and scores for each sheet were then used to generate the scores and loadings plots in Microsoft Excel (Microsoft Corp.). The scores for the sheets of ream N (n=2) for each paper type were calculated and projected onto the original scores plot. The first step was to mean center the element concentrations in ream N. To do this, the average concentration of each element in reams A and B of all paper types was calculated and subtracted from the corresponding element concentration in each sheet of ream N. The resulting mean-centered data for each sheet of ream N was then multiplied by the eigenvector for PC1. The product was summed to generate the score for each sheet on PC1. This was repeated using the mean-centered data and the eigenvector for PC2 to determine the score on PC2. The sheets of ream N were then projected on the scores plot for ream A and B using the calculated scores.

The association of chemically similar sheets from the same paper type and the discrimination of chemically different paper types were investigated based on visual assessment of the positioning of the sheets on the scores plot. The positioning of the sheets on the scores plot was explained by positioning of the elements in the loadings plot.

3.6.3. Hierarchical Cluster Analysis

Hierarchical cluster analysis (HCA) was performed in Pirouette (version 4.5, Informetrix, Bothell, WA) on the average concentration of each element per sheet for all three reams using Euclidean distance and complete linkage methods. The resulting dendrogram was assessed at

different levels of similarity to investigate the clustering of the paper types. The clustering of the sheets from ream N to the corresponding reams of the same paper type was also investigated.

REFERENCES

REFERENCES

1. Borowski K Ph.D. An Operations Overview& Practical Guide. Milestone Inc 2003.

2. McGaw EA, Symanski DW, Smith RW. Determination of trace elemental concentrations in document papers for forensic comparison using inductively coupled plasma-mass spectrometry. *J. Forensic Sci* 2009; 54: 1163-1170.

3. Spence LD, Baker AT, Byrne JP. Characterization of document paper using elemental compositions determined by inductively coupled plasma mass spectrometry. *J. Anal. At. Spectrom* 2000; 15: 813-819.

4. Skoog DA, Holler FJ, Crouch SR. Principles of instrumental analysis. 6th ed. Belmont, CA: Thomson, 2007.

5. Miller JN, Miller JC. Statistics and chemometrics for analytical chemistry. 4th ed. Harlow, England: Pearson Education Limited, 2000.

6. Zar JH. Biostatistical Analysis. 4th ed. Upper Saddle River, NJ: Prentice Hall, 1998.

Chapter 4 Discrimination of Paper Type Based on Element Profiles Obtained Using Inductively Coupled Plasma-Optical Emission Spectroscopy

In this chapter, the potential of differentiating paper types based on element profiles generated using inductively coupled plasma-optical emission spectroscopy (ICP-OES) was investigated. The analytical figures of merit for the ICP-OES instrument were determined for various elements. Then, samples of four different paper types produced by the same manufacturer were microwave digested, analyzed by ICP-OES, and the element concentrations in each paper sample were determined. Multivariate statistical procedures were used to investigate association of samples of the same type and distinction of the different paper types based on differences in element concentration.

4.1. Analytical Figures of Merit for Inductively Coupled Plasma-Optical Emission Spectroscopy

Standard solutions for 14 elements (aluminum (Al), barium (Ba), cadmium (Cd), cobalt (Co), chromium (Cr), copper (Cu), iron (Fe), nickel (Ni), magnesium (Mg), manganese (Mn), lead (Pb), antimony (Sb), vanadium (V), and zinc (Zn)) for a range of concentrations were prepared and analyzed to determine the analytical figures of merit for the ICP-OES instrument. For each element, the signal at each concentration was normalized to the signal of the internal standard (germanium (Ge), indium (In), or bismuth (Bi)) that had the most similar wavelength. Calibration curves were made per paper type for each of the fourteen elements. The calibration curves consisted of the standards analyzed directly before and after the samples for each paper type.

The coefficient of determination, r^2, was used to assess the linearity of the calibration curve over the concentration range of the standards for each element. Ideally, r^2 should be at least 0.999; however, since two sets of standards were used to make the calibration curves, r^2 of at least 0.990 was considered acceptable. Of the 14 elements, Cd, Co, Cr, Cu, Ni, Pb, Sb, V, and Zn were found to have poor linearity ($r^2 < 0.98$) and were therefore discounted. For the remaining elements, the limit of detection (LOD), the limit of quantitation (LOQ), and the relative standard deviation (RSD) of the normalized signal at each concentration were calculated (Table 4.1). This table represents the average value for all of the paper types and the figures of merit for the calibration curve of each paper type can be found in Appendix A.

For the remaining elements, the LOD was calculated as the signal of the nitric acid blank plus three times the standard deviation of the blank and represents the lowest concentration that can be differentiated from the blank[1]. The LOQ is the lowest concentration that can be accurately quantified and was calculated by the signal of the nitric acid blank plus ten times the standard deviation of the blank[1]. The calculated LODs for Al, Ba, and Fe were negative and the calculated concentration for the LOQ for Al was negative because the y-intercept of the calibration curve determined from regression analysis was slightly higher than the signal in the nitric acid blanks[2]. Despite this, the entire range of standards could still be used for quantification because the signal of the procedural blanks was greater than the signal of the nitric acid blanks. A difference of 18 µg/g in calculated Al concentration was not significant due to the high concentration of Al present in the paper samples.

Table 4.1. Summary of the average analytical figures of merit for selected elements in ICP-OES analysis

	Al	Ba	Fe	Mg	Mn
r^2	0.999	0.997	0.999	0.999	0.999
Limit of Detection (µg/L)	-23.2	-0.0501	-0.748	12.5	0.553
Limit of Quantitation (µg/L)	-17.7	0.272	4.53	13.3	0.271
Highest RSD of normalized signal (%)*	2.34	10.4	4.07	2.26	36.4
Working Range** (µg/L)	0-2000	0.277-25	4.53-2000	13.3-2000	0.271-25

* The RSD was calculated at each concentration for each calibration used. The highest RSD among the days of analysis was chosen to emphasize the precision of the instrument.

** Working range based only on the concentrations investigated. 2000 µg/L was the highest concentration used for Al, Fe, and Mg while 25 µg/L was the highest for Ba and Mn.

Finally, the RSD of the normalized signal at each concentration above the LOQ was used as a measure of the instrument precision for that element. A RSD of less than 10% indicated precision in the measurement of a signal at a given concentration. Only for Mn was the RSD higher than 10% and this was for the lowest calibration standard. This concentration was close to the LOD and therefore slight differences in the normalized signal resulted in a high RSD for the low concentrations. The elements that could be used for the element profiles were Al, Ba, Fe, Mg, and Mn.

4.2. Variation of Element Concentration Within Paper Type

In a forensic investigation, it would be most important to relate a sample back to a ream in order to determine paper type and manufacturer. The variation of element concentration within a ream of paper was determined by calculating the RSD of the ten paper samples within the ream. If the RSD was greater than 15% for any element in a ream, the Grubb's test was used to determine if there was a statistical outlier among the ten samples[3]. Any outlier was removed and the RSD was recalculated for the nine remaining samples. This was repeated if the RSD was still greater than 15%. Analysis of variance (ANOVA) was then performed at the 95% confidence level to determine if there was a statistical difference in element concentration among reams of the same paper type. This was done using the concentration of the ten samples per element per ream for the three reams of each paper type. If there was a statistical difference in concentration among the reams, Tukey's honestly significant difference (HSD) test was used to determine between which reams the difference occurred[4].

The RSDs for each element in the three reams of each paper type are shown along with a summary of the ANOVA and Tukey's HSD test results (Tables 4.2-4.5). In color inkjet paper (Table 4.2), the RSDs of all elements were less than 15%, after removing a statistical outlier in Mn, indicating there was little variation in element concentration within a ream. There was not a statistically significant difference in Fe or Mg concentration among the three reams; however, there was a statistically significant difference in the concentration of Al, Ba, and Mn among the reams A, B and N. For these elements, the concentration of ream N was statistically different from the concentration in reams A and B.

In laserjet paper, RSDs for all elements in all reams were less than 15% indicating little variation in element concentration within a ream (Table 4.3). There was a statistical difference in the concentration of all elements among the three reams and as before, the element concentrations in ream N only were statistically different from the corresponding concentrations in reams A and B.

In multipurpose paper, the RSDs for all elements in all reams were less than 15%, indicating little variation in element concentration within a ream (Table 4.4). Similar to color inkjet paper, the concentrations of Ba and Fe were not statistically different among the three reams; however, concentrations of Al, Mg, and Mn were statistically different among reams. As before, concentrations of these elements in ream N were statistically different from the corresponding concentrations in reams A and B.

In office paper, the RSDs for all elements in all reams were less than 15%, indicating little variation in element concentration within a ream (Table 4.5). For this paper type, there was not a statistical difference in the concentration of Al and Mn among the three reams; however, the concentrations of Ba, Fe, and Mg were statistically different among the reams. As before,

Table 4.2. Average element concentration (µg/g) and relative standard deviation (%) for color inkjet paper

Color Inkjet	Ream A		Ream B		Ream N		Significant difference at 95% confidence	Statistically different ream
	Avg. Conc. N=10 (µg/g)	RSD (%)	Avg. Conc. N=10 (µg/g)	RSD (%)	Avg. Conc. N=10 (µg/g)	RSD (%)		
Al	484	8.2	491	7.0	611	7.1	Yes	Ream N
Ba	9.95	7.3	10.2	7.4	21.4	5.6	Yes	Ream N
Fe	73.8	6.9	77.1	6.7	73.8	6.0	No	None
Mg	937	6.7	920	5.7	977	5.0	No	None
Mn	4.64	6.9	5.04#	9.9#	5.77	5.6	Yes	Ream N

# indicates average concentration and RSD calculated using n=9

Table 4.3. Average element concentration (µg/g) and relative standard deviation (%) for laserjet paper

LaserJet	Ream A		Ream B		Ream N		Significant difference at 95% confidence	Statistically different ream
	Avg. Conc. N=10 (µg/g)	RSD (%)	Avg. Conc. N=10 (µg/g)	RSD (%)	Avg. Conc. N=10 (µg/g)	RSD (%)		
Al	61.3	15	56.1	8.9	218	6.1	Yes	Ream N
Ba	0.941	10	0.837	5.5	2.72	6.4	Yes	Ream N
Fe	142	10	140	6.1	120	6.4	Yes	Ream N
Mg	362	9.7	356	6.2	611	5.3	Yes	Ream N
Mn	5.53	10	5.48	6.4	6.75	6.0	Yes	Ream N

Table 4.4. Average element concentration (µg/g) and relative standard deviation (%) for multipurpose paper

Multi-purpose	Ream A		Ream B		Ream N		Significant difference at 95% confidence	Statistically different ream
	Avg. Conc. N=10 (µg/g)	RSD (%)	Avg. Conc. N=10 (µg/g)	RSD (%)	Avg. Conc. N=10 (µg/g)	RSD (%)		
Al	602	15	591	7.66	804	8.6	Yes	Ream N
Ba	12.7	13	11.6	6.19	12.5	8.7	No	None
Fe	76.9	13	73.5	4.76	78.2	9.5	No	None
Mg	1010	12	962	4.60	1170	9.1	Yes	Ream N
Mn	5.85	13	5.67	5.33	4.98	8.0	Yes	Ream N

Table 4.5. Average element concentration (µg/g) and relative standard deviation (%) for office paper

Office	Ream A		Ream B		Ream N		Significant difference at 95% confidence	Statistically different ream
	Avg. Conc. N=10 (µg/g)	RSD (%)	Avg. Conc. N=10 (µg/g)	RSD (%)	Avg. Conc. N=10 (µg/g)	RSD (%)		
Al	920	7.1	885	9.7	919	11	No	None
Ba	12.2	7.0	11.8	6.9	10.8	8.9	Yes	Ream N
Fe	77.8	6.9	73.6	6.3	91.5	8.9	Yes	Ream N
Mg	925	7.0	896	5.3	1020	8.1	Yes	Ream N
Mn	5.84	7.3	5.63	6.2	5.64	8.1	No	None

concentrations of these elements in ream N were statistically different from the corresponding concentrations in reams A and B.

Since there was not a statistical difference in the concentration of reams A and B for most elements, the average concentration for the reams of papers purchased at the same time could be represented by the average concentration of reams A and B for all elements. All additional statistical comparisons was performed using the average concentration per paper type.

4.3. Variation in Element Concentration Among Paper Types

To investigate variation in element concentration among the four paper types, ANOVA and Tukey's HSD test were performed at the 95% confidence level, using the average concentration of each element in reams A and B of each paper type. The results are summarized in Table 4.6.

At the 95% confidence level, there was a significant difference in Al concentration among all paper types, with the concentrations ranging from 58.7 µg/g to 903 µg/g. Compounds containing Al are added at many stages of the paper-making process. For example, kaolin hydrous is added as filler to ensure smoothness and aluminum trihydrate is added as both a filler and as a coating pigment to increase the brightness of the sheet[5]. Office paper had the highest concentration of Al but the lowest brightness (92) of all paper types while laserjet paper had the lowest Al concentration but the highest brightness (97) rating of all paper types. This indicated that the Al in the samples was likely from the paper-making process and not from the brightening process. Based on the significant differences in concentration, all four paper types could be differentiated from each other based on Al concentration.

Table 4.6. Average element concentration in reams A and B for each paper type

	Average Element Concentration (µg/g)				
	Al	Ba	Fe	Mg	Mn
Color Inkjet	487	10.1	75.5	929	4.95
LaserJet	58.7	0.889	141	359	5.51
Multi-purpose	596	12.1	75.2	984	5.75
Office	903	12.0	77.8	925	5.74
Statistical difference at 95% confidence level	Yes	Yes	Yes	Yes	Yes
Statistically different paper type	All*	Laserjet** Color inkjet**	Laserjet	Laserjet	Color inkjet***

* Al could be used to differentiate all paper types from each other

** Ba could be used to differentiate laserjet from the other three and color inkjet from the other three paper types

***Mn could be used to differentiated color inkjet paper from multipurpose and office paper only

The concentration of Ba ranged from 0.889 µg/g in laserjet paper to 12.1 µg/g in office paper. Barium sulfate is used as a filler which is added to the paper pulp[6]. Ba could be used to differentiate laserjet paper from the other paper types and to differentiate color inkjet paper from the other three types. Multipurpose and office paper had similar concentrations of Ba and could not be differentiated.

The concentration of Mg ranged from 359 to 984 µg/g among the paper types. Magnesium-containing compounds are also used as fillers and magnesium carbonate is found in ground calcium carbonate which is used as brightening agent[5]. Magnesium could only be used to differentiate laserjet paper from the other three paper types. Iron could also be used to differentiate laserjet paper from the other three types. Iron oxide is used to make bauxite, a precursor for aluminum trihydrate, which is used as a filler[5]. Since the iron oxide is not used directly, it was likely that the Fe present in the paper comes from a different source such as in the raw materials used to make paper. Laserjet paper was the only paper made specifically for laserjet printers which use heat to bond toner to the paper. The ability to differentiate this paper from the other three types was most likely due to differences in the surface treatment of laserjet paper.

The concentration of Mn in the papers was the lowest of all elements. Mn is not added during the paper making process; however, it is present in the raw materials used to make the paper. Mn could be used to differentiate color inkjet paper from multipurpose and office paper but differentiation from laserjet paper was not possible. The difference in concentration was only about 1 µg/g among all paper types. This indicated that Mn may not be as useful as other

elements in differentiating paper types because the concentrations did not vary greatly among all paper types.

In summary, all paper types were differentiated from each other based on the concentration of Al. In addition, laserjet paper was differentiated from the other three paper types based on differences in concentration of Ba, Fe, and Mg. Color inkjet paper was differentiated from the other three paper types based on differences in concentration of Ba and from office and multipurpose paper based on Mn concentration. This showed that differentiation of paper types produced at the same time was possible. While differentiation of the paper types was possible using ANOVA, this procedure was time consuming since only one element could be compared at a time and it had to be done for all paper types individually.

4.4. Differentiation of Paper Types Using Principal Components Analysis

Because of the limitations of ANOVA described above, principal components analysis (PCA) was used to investigate differentiation of the four paper types using all five elements simultaneously. The average element concentrations were calculated per sheet of paper using the five samples analyzed per sheet and PCA was performed on the sheets in reams A and B of all paper types.

In the resulting PCA scores plot (Figure 4.1), principal component 1 (PC1) and principal component 2 (PC2) accounted for 99.98% of the variance among the paper types. The four sheets from the same paper type (two sheets from ream A and two sheets from ream B) were generally positioned closely. Differentiation was possible for laserjet and office paper, both from each other and from the other two paper types; however, differentiation between color inkjet and

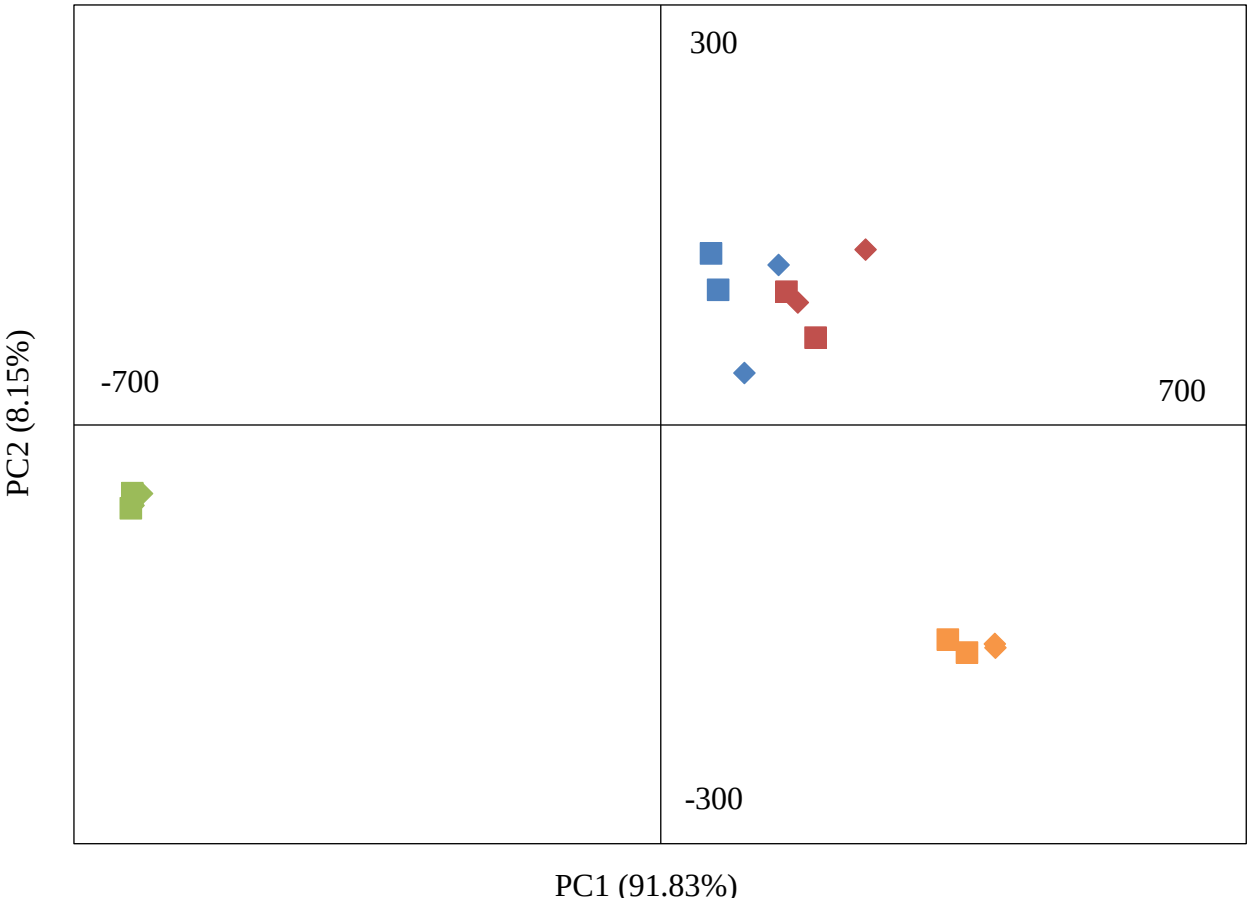

Figure 4.1. Scores plot of PC1 and PC2 based on element concentrations in Reams A (◆) and B (■) of four different paper types. Paper types are as follows: Laserjet (▲), Color Inkjet (▲), Multipurpose (▲), and Office Paper (▲)

multipurpose paper was not possible. Laserjet paper was positioned negatively on both PC1 and PC2. Color inkjet and multipurpose papers were positioned positively on both PC1 and PC2. Office paper was positioned positively on PC1 and negatively on PC2.

The positioning of the samples on the scores plot could be explained by the positioning of the elements on the loadings plot (Figure 4.2). Al was weighted most positively on PC1 and most negatively on PC2. Mg had the next highest positive weighting on PC1 and had the most positive weighting on PC2. Fe was weighted slightly negatively on both PC1 and PC2. Ba and Mn were positioned near the origin and hence, did not contribute to the positioning of the papers on the scores plot. There was less variation in concentration among paper types for Ba and Mn compared to the variation in the other elements, which is why these two elements did not contribute to the positioning on the scores plot.

In order to explain the positioning of sheets on the scores plot, the concentration of each element in the paper type and the weighting of the element on the loadings plot have to be considered. The first step of PCA is to mean center the data. This is done by determining the average concentration of each element for all paper types and subtracting this value from the average element concentration of each sheet. The mean-centered concentration for each element is multiplied by the PC1 eigenvector for that element. This is done for all elements and the score on PC1 is the sum of all elements. This is repeated to determine the score of the sheet on PC2. As Al and Mg were furthest from the origin in the loadings plot, they had the most influence on the positioning of the samples on the scores plot. The mean-centered data of Fe will only be discussed for laserjet paper because the three other types of paper had similar concentration of Fe which were much lower than the concentration of Al and Mg.

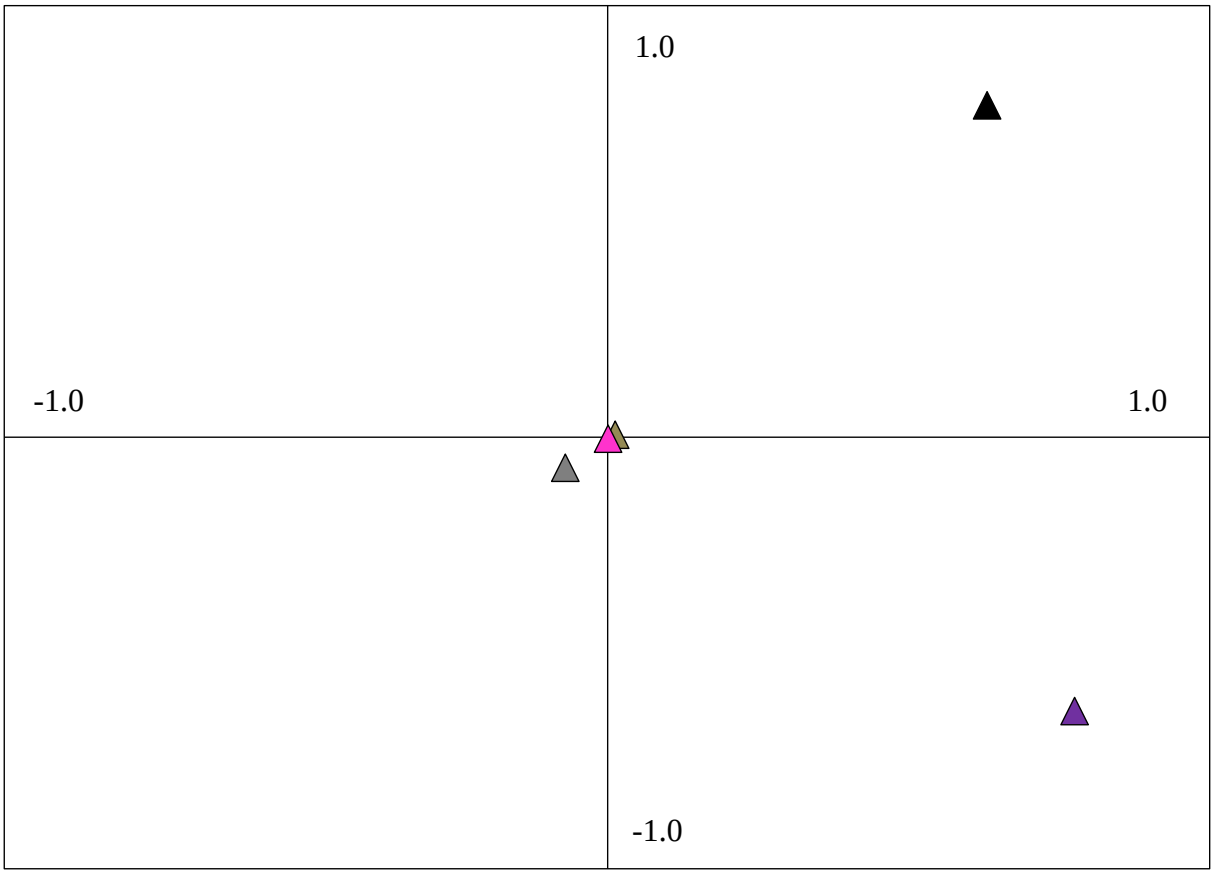

Figure 4.2. Loadings plot of PC1 and PC2 based on element concentrations in two reams of four different paper types. Elements are as follows: Al (▲), Ba (▲), Fe (▲), Mg (▲), and Mn (▲)

Laserjet paper was positioned negatively on both PC1 and PC2 in the scores plot. The mean-centered data for Fe in this paper type was positive and Fe was weighted negatively on both PC1 and PC2 in the loadings plot. When the negative weighting of Fe on the loadings plot was multiplied by the negative mean-centered data, the resulting contribution from Fe was positive on PC1 and PC2. The mean-centered data for both Al and Mg was negative indicating that the concentration of these elements was less than the average for the data set. Both of these elements were weighted positively on PC1 so when this weighting was multiplied by the mean-centered data, the contribution was negative for both elements on PC1. The weighting of Al, Mg, and Fe were summed and the resulting score on PC1 was negative for this paper type.

This was repeated to determine the score on PC2. The weighting of Al was negative on PC2 and the weighting of Mg was positive on PC2. When the weightings were multiplied by the negative mean-centered data, the contribution from Al was positive and from Mg was negative. The mean-centered concentrations were similar for the two elements; however, the weighting of Mg on PC2 was greater than the loading for Al and therefore the sheets were positioned negatively on PC2.

Office paper was positioned positively on PC1 and negatively on PC2 in the scores plot. Office paper had the highest concentration of Al among all the paper types. The mean-centered data for Al and Mg were positive and, when these concentrations were multiplied by the positive weightings of Al and Mg on PC1, the resulting score on PC1 was positive. The negative positioning on PC2 was due to the high mean-centered concentration of Al, which is weighted negatively on PC2.

The sheets of color inkjet and multipurpose paper were positioned similarly on both PC1 and PC2 and could not be differentiated from each other. The concentrations of Al and Mg were

slightly higher in multipurpose paper than in color inkjet paper which contributes to the slightly more positive positioning of multipurpose paper on PC1.

Multipurpose paper was positioned positively on PC1 and PC2 because it had the highest Mg concentration among the four types of paper which resulted in positive mean-centered data for Mg. This element was weighted positively on both PC1 and PC2 and had the largest contribution to the weighting for this paper type. Multipurpose paper had the second highest concentration of Al among the four types and this element also contributes positively to the positioning on PC1. The high concentration of Mg can also be used to explain the positive positioning on PC2.

Color inkjet paper was positioned positively on PC1 and PC2. The mean-centered data for Al in color inkjet paper was negative and when multiplied by the positive weighting of Al on PC1 resulted in a negative contribution to the score on PC1. The mean-centered data for Mg was positive and when multiplied by the positive weighting on PC1 resulted in positive contribution on PC1. When the contributions from Al and Mg we added together, the resulting score on PC1 was only slightly positive. The sheets of color inkjet paper are positioned more positively on PC2 than the sheets of multipurpose paper due to the negative mean-centered data of Al which is weighted negatively on PC2 and therefore results in more positive positioning on PC2.

Scores for the two sheets from ream N of each paper type were calculated and projected onto the scores plot (Figure 4.3). For each paper type, the two sheets from ream N were positioned closely together. Based on visual assessment of the scores plot, the sheets from ream N could be associated back to reams A and B of the same paper type for office paper and laserjet paper only. The sheets in ream N of color inkjet paper were similar to reams A and B for this

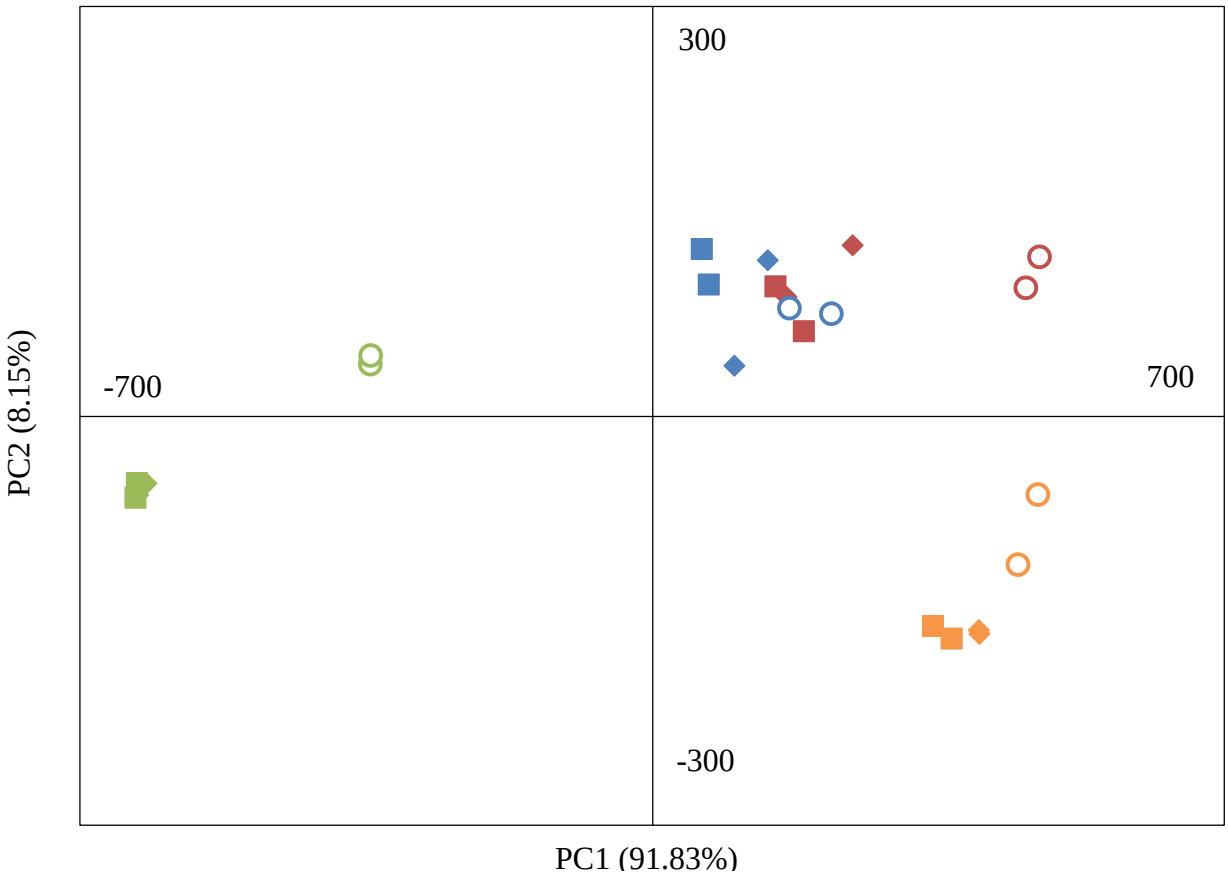

Figure 4.3. Scores Plot Showing the Scores for the New Reams (○) Projected onto the Scores Plot for the Reams A (◆) and B (■) of Laserjet (▲), Color Inkjet (▲), Multipurpose (▲), and Office Paper (▲)

paper type; however, they could not be differentiated from sheets in reams A and B of multipurpose paper.

For laserjet paper, the sheets from ream N were positioned more positively on both PC1 and PC2 compared to the sheets from reams A and B. The concentration of Fe in ream N was similar to reams A and B; however, the concentrations of Al and Mg were greater in ream N. Both Al and Mg were weighted positively on PC1 which explains the more positive positioning of ream N on PC1. The concentration of Mg in ream N was almost double the Mg concentration in ream A and B and, since this element was weighted positively on PC2, sheets from ream N were positioned more positive on PC2.

The sheets from ream N of color inkjet paper were positioned close together and were similar in positioning to the corresponding sheets from reams A and B; however, the sheets in ream N were more closely associated with the sheets in reams A and B of multipurpose paper. Sheets from ream N were positioned slightly more positively on PC1 than reams A and B because the concentration of both Al and Mg slightly increased (Table 4.2) and both these elements were weighted positively on PC1 in the loadings plot. These sheets were most similar in positioning to the sheets in reams A and B of multipurpose paper due to similar concentrations of Al and Mg among the sheets.

Ream N of multipurpose paper was positioned more positively on both PC1 and PC2 on the scores plot than reams A and B. This was due to an increase in the Al and Mg concentrations in ream N. Both Al and Mg were weighted positively on PC1 in the loadings plot so the higher concentrations in ream N resulted in more positive positioning on PC1 in the scores plot. The sheets in ream N had a higher concentration of Mg than the sheets in reams A and B which

resulted in the more positive positioning of ream N on PC2 because Mg was weighted positively on PC2.

The sheets from ream N of office paper were positioned more positively on PC1 because there was an increase in the Al and Mg concentrations compared to reams A and B and the elements were weighted positively on PC1. The sheets of ream N were positioned more positively on PC2 than reams A and B because there was an increase in Mg concentration which was positioned positively on PC2. The concentration of Al was still the highest in this paper type which resulted in overall negative positioning on PC2.

It was interesting to note that sheets of ream N for both office and multipurpose paper were positioned similarly on PC1. This was due to concentrations of Al and Mg in these samples being very similar (Tables 4.4 and 4.5). Both elements were weighted positively on PC1 and, due to the similar concentrations of Al and Mg in office and multipurpose paper, the scores were similar on PC1. Despite this, the two paper types were still differentiated on PC2. Multipurpose paper had a higher Mg concentration and was therefore positioned positively on PC2 while office paper had a higher concentration of Al and was positioned negatively on PC2.

In summary, using PCA, sheets of each paper type were generally positioned closely. It was possible to differentiate laser jet and office paper from each other and from the other paper types. However, differentiation between color inkjet and multipurpose paper was not possible. Al, Fe, and Mg contributed to the positioning of the samples on the scores plot because there was greatest variation in the concentration of these elements among the paper types. The concentration of Ba and Mn did not greatly vary among the four paper types and therefore these elements did not contribute to positioning on the scores plot. When scores for sheets from ream N were projected onto the scores plot, the sheets could be associated back to reams A and B for

laserjet and office paper only. The sheets of ream N of color inkjet paper were associated with sheets of reams A and B of multipurpose paper. The sheets in ream N of multipurpose paper were more positive on PC1 than the sheets in reams A and B of this paper type. The differences in positioning between reams A, B and N could be explained by differences in the concentration of Al, Fe, and Mg in the sheets. Since differentiation of two of the paper types was possible, PCA may be useful in forensic laboratories in identifying the paper type of an unknown sample.

4.5. Clustering of Paper Types Using Hierarchical Cluster Analysis

Hierarchical cluster analysis (HCA) was performed using the average element concentrations per sheet for the paper types. The sheets in reams A, B, and N were compared at the same time. The sheets of ream N, for most paper types, were clustered to the corresponding sheet from the same ream at at least 94.9% similarity before being clustered to a sheet in a different ream for each paper type (Figure 4.4). This was not observed for the sheets of ream N for color inkjet paper where the sheets were clustered to two different sheets of multipurpose paper. This was similar to the ANOVA results in which element concentrations in ream N were statistically different from corresponding concentrations in reams A and B for all paper types. The sheets of reams A and B for laserjet, office, and color inkjet papers were clustered at at least a 93.9% similarity before being clustered to another type of paper. For laserjet and office paper, all sheets in reams A, B and N clustered together before being clustered to sheets of a different paper type.

Office paper was the only paper type in which the two sheets in a ream were clustered together first before being clustered to another ream of the same paper type. For office paper,

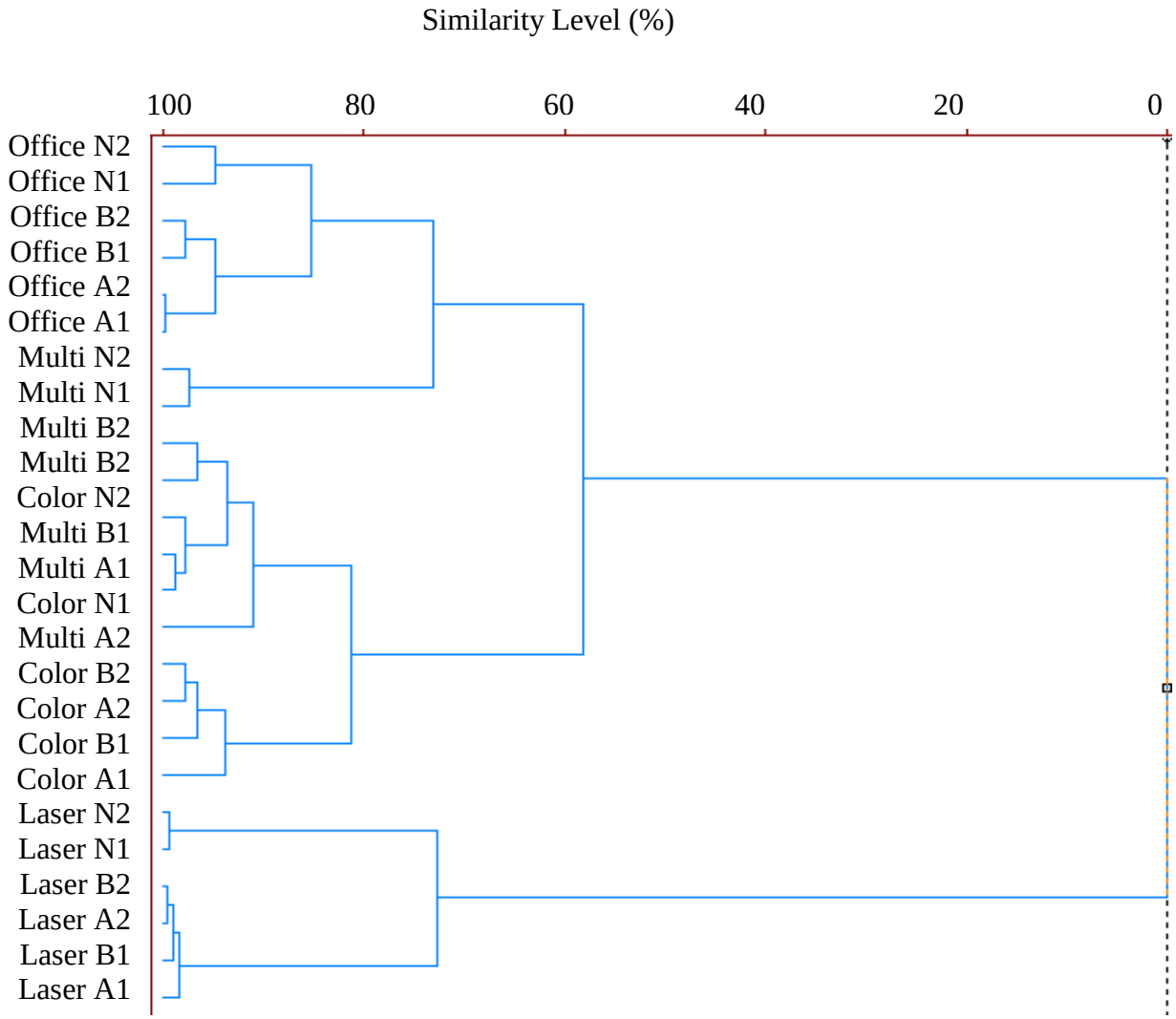

Figure 4.4. Hierarchical cluster analysis dendrogram based on average concentration of five elements for three reams of four different paper types. Euclidean distance and complete linkage were used for clustering. The letter after the paper type refers for the ream and the number refers to the sheet.

reams A and B were clustered together at 94.9% similarity due to similar concentration of all elements (Table 4.5). The sheets of office paper had a higher concentration of Fe and Mg (77.8 and 73.6 µg/g for Fe and 925 and 896 µg/g for Mg) compared to the sheets in ream N (91.5 µg/g Fe and 1023 µg/g Mg). All sheets of this paper type were clustered to at 85.3% similarity.

For multipurpose paper, the sheets in reams A and B were clustered together with 91.0% similarity; however this cluster also contained the two sheets in ream N of color inkjet paper. This was due to a similar concentration of Al in these sheets which only varied by 66.5µg/g. The sheets in ream N of multipurpose paper were clustered with office paper (73.0% similarity) before being clustered with reams A and B of the same paper type. The concentration of Al and Mg in ream N of multipurpose paper was higher than in reams A and B and more similar to the concentrations in office paper than in multipurpose paper (Table 4.4 and Table 4.5).

The sheets in reams A and B of color inkjet paper were clustered with 93.9% similarity. These sheets had similar concentrations of Al and Mg which were lower than the concentrations in the sheets of ream N of this paper type (Table 4.2). The sheets in reams A and B of color inkjet paper were clustered with the sheets in ream N of color inkjet paper and sheets in reams A and B of multipurpose paper at a 81.4% similarity.

Reams A and B of laserjet paper were clustered at a 98.3% similarity level. This indicated that the concentration of all elements within this paper type were similar. The two sheets of ream N were clustered together at 99.4% similarity and ream N was clustered with reams A and B with 72.7% similarity. The concentrations of Al and Mg were higher in ream N than in reams A and B while the other elements were present in similar concentrations (Table 4.3).

All sheets of office, multipurpose, and color inkjet paper were clustered together before being clustered with laserjet paper. Laserjet paper had lower concentrations of Al and Mg and higher concentrations of Fe than the other three paper types. This was also observed in ANOVA in that Al, Ba, Fe, and Mg could be used to differentiate laserjet paper from the other paper types.

4.6. Comparison of PCA and HCA Results

Similar patterns were observed in the differentiation achieved using PCA and HCA. For both procedures, sheets of laserjet and office paper could be differentiated from each other and from the other two paper types. Differentiation between color inkjet and multipurpose paper was not possible. The sheets in ream N were either positioned closely using PCA or clustered together before being clustered to a different paper type for HCA except for color inkjet paper. This is similar to the conclusion from ANOVA that ream N was statistically different than reams A and B.

For this research, the scores plot was generated using PC1 and PC2 and it appeared that the similarity level in HCA was related to the positioning of the sheets of PC1, which accounted for 91.83% of the variance among the data set. The positioning of sheets in ream N of multipurpose paper on PC1 was more similar to the reams of office paper than the other sheets of multipurpose paper. On the dendrogram, the sheets of ream N of multipurpose paper had a higher similarity level to office paper than to multipurpose paper. Ream N of multipurpose paper was differentiated from office paper based on its score on PC2.

Differentiation between color inkjet and multipurpose was not possible using either PCA or HCA. On the scores plot, the sheets of these two paper types were positioned similarly on PC1 and PC2. The sheets in ream N of color inkjet paper were more positive on PC1 than the sheets in reams A and B and were positioned closer to sheets of reams A and B of multipurpose paper. This was also observed in HCA in that the sheets of ream N of color inkjet paper were clustered with the sheets of multipurpose paper before being clustered with other sheets of color inkjet paper. All sheets of laserjet paper were negative on PC1 and were clustered together before being clustered to another paper type. This was also true for office paper where all sheets were most positive on PC1.

The clustering of ream N of multipurpose paper to office paper in HCA indicated that PCA may be more useful for associating an unknown paper sample to the correct paper type than HCA. One advantage of PCA over HCA was that a loadings plot is generated so the positioning on the scores plot could be explained. Another advantage of PCA was differences between paper types could be observed in more than one dimension. Paper types that had similar positioning on PC1 for example, could still be differentiated from each other using PC2. An advantage of HCA over PCA is that a numerical value can be assigned to the level of similarity between a sample and a paper type which may be beneficial in a forensic laboratory. This would be useful when testifying in court because it would assign a numerical value to the similarity level while PCA may be seen as subjective because it is based on visual assessment of the scores plot. A disadvantage of HCA is that there are different combinations of distance and linkage that can be used which would change the level of similarity between samples. PCA would be more useful when determining differences among a data set; however, HCA would be more useful when classifying an unknown sample to predetermined groups.

APPENDIX

APPENDIX A

Figures of merit for ICP-OES for each paper types using the standards analyzed directly before and after the paper samples

Table A.1. Figures of merit for multipurpose paper analyzed by ICP-OES on 052812

	Al	Ba	Fe	Mg	Mn
r^2	0.9977	0.9966	0.9992	0.9997	0.9992
Limit of Detection (µg/L)	-34.81	-0.0962	-8.98	2.274	-0.109
Limit of Quantitation (µg/L)	-33.51	0.570	-8.55	3.60	-0.0232
Highest RSD of normalized signal*	2.34	10.42	1.91	1.77	36.39
Working Range** (µg/L)	0-2000	0.570-25	0-2000	3.60-2000	0-25

* The RSD was calculated at each concentration for each calibration used. The highest RSD among all concentrations was chosen to emphasize the precision of the instrument.

** Working range based only on the concentrations investigated. 2000 µg/L was the highest concentration used for Al, Fe, and Mg and 25 µg/L was the highest for Ba and Mn.

Table A. 2. Figures of merit for color inkjet paper analyzed by ICP-OES on 060612

	Al	Ba	Fe	Mg	Mn
r^2	0.9994	0.999	0.9993	0.9984	0.9998
Limit of Detection (µg/L)	-11.70	-0.0238	-3.764	18.34	0.1828
Limit of Quantitation (µg/L)	-1.051	0.0654	-1.191	19.18	0.5571
Highest RSD of normalized signal*	2.30	5.42	4.07	2.00	2.00
Working Range** (µg/L)	0-2000	0.0654-25	0-2000	19.18-2000	0.5571-25

* The RSD was calculated at each concentration for each calibration used. The highest RSD among all concentrations was chosen to emphasize the precision of the instrument.

** Working range based only on the concentrations investigated. 2000 µg/L was the highest concentration used for Al, Fe, and Mg and 25 µg/L was the highest for Ba and Mn.

Table A.3. Figures of merit for office paper analyzed by ICP-OES on 062312

	Al	Ba	Fe	Mg	Mn
r^2	0.9991	0.9973	0.9999	0.999	0.9991
Limit of Detection (µg/L)	-25.05	0.0790	3.767	13.93	0.0686
Limit of Quantitation (µg/L)	-22.74	0.5948	12.278	14.57	0.3085
Highest RSD of normalized signal*	1.49	3.74	0.404	2.26	1.86
Working Range** (µg/L)	0-2000	0.5948-25	12.278-2000	14.57-2000	0.3085-25

* The RSD was calculated at each concentration for each calibration used. The highest RSD among all concentrations was chosen to emphasize the precision of the instrument.

** Working range based only on the concentrations investigated. 2000 µg/L was the highest concentration used for Al, Fe, and Mg and 25 µg/L was the highest for Ba and Mn.

Table A.4. Figures of merit for laserjet paper analyzed by ICP-OES on 062312

	Al	Ba	Fe	Mg	Mn
r^2	0.999	0.9966	0.9992	0.9991	0.9986
Limit of Detection (µg/L)	-21.17	-0.159	5.982	15.56	0.0787
Limit of Quantitation (µg/L)	-13.46	-0.141	15.56	15.98	0.2431
Highest RSD of normalized signal*	2.20	9.10	1.73	1.34	2.94
Working Range** (µg/L)	0-2000	0-25	15.56-2000	15.98-2000	0.2431-25

* The RSD was calculated at each concentration for each calibration used. The highest RSD among all concentrations was chosen to emphasize the precision of the instrument.

** Working range based only on the concentrations investigated. 2000 µg/L was the highest concentration used for Al, Fe, and Mg and 25 µg/L was the highest for Ba and Mn.

REFERENCES

REFERENCES

1. Skoog DA, Holler FJ, Crouch SR. Principles of instrumental analysis. 6th ed. Belmont, CA: Thomson, 2007.

2. Mocak J, Bond AM, Mitchell S, and Scollary G. A Statistical overview of standard (IUPAC and ACS) and new procedures for determining the limits of detection and quantification; Application to voltammetric and stripping techniques. *Pure Appl Chem.* 69, 297-325 1997.

3. Miller JN, Miller JC. Statistics and chemometrics for analytical chemistry. 4th ed. Harlow, England: Pearson Education Limited, 2000.

4. Zar JH. Biostatistical Analysis 4th ed. Upper Saddle River, NJ: Prentice Hill, 1999.

5. Holik, H. Ed. Handbook of Paper and Board. 2006. Wiley-VCH Verlag GmbH & Co. Weinheim, Germany.

6. Saltman, D. Paper Basics: Forestry, Manufacture, Selection, Mathematics, and Metrics, Recycling. Litton Educational Publishing, Inc 1978 New York, NY

Chapter 5: Discrimination of Paper Type Based on Element Profiles Obtained Using Inductively Coupled Plasma-Mass Spectrometry

In this chapter, the ability to differentiate paper types based on element profiles generated using inductively coupled plasma-mass spectrometry (ICP-MS) is discussed. First, the analytical figures of merit for the instrument were determined. Next, samples of four different paper types all produced by the same manufacturer were analyzed using ICP-MS and the concentrations of different elements in the samples were calculated. The paper samples used for analysis were the same as those analyzed by inductively coupled plasma-optical emission spectroscopy (ICP-OES) discussed in Chapter 4. Finally, principal components analysis (PCA) and hierarchical cluster analysis (HCA) were used to determine if there was association among samples of the same paper type, with differentiation of different paper types, based on the element concentrations determined using ICP-MS.

5.1 Inductively Coupled Plasma-Mass Spectrometry Analytical Figures of Merit

The 14 elements used for ICP-MS analysis were aluminum (Al), barium (Ba), cadmium (Cd), cobalt (Co), chromium (Cr), copper (Cu), iron (Fe), nickel (Ni), magnesium (Mg), manganese (Mn), lead (Pb), antimony (Sb), vanadium (V), and zinc (Zn) which were the same as for the ICP-OES analysis; however, a different range of concentrations was used due to an additional dilution in the preparation of the standards and samples. Calibration curves were generated for each element for each paper type, using the ratio of the element of interest to the appropriate internal standard, to determine the figures of merit for the ICP-MS instrument.

Ideally, Sc should have been used to normalize Mg, Al, V, Cr, Mn, and Fe, however; there was variation in the intensity of Sc and therefore Ge used for normalization of these elements.

For each element, the coefficient of determination, r^2, was used to assess the linearity of the curve. An r^2 value of 0.999 is considered analytically acceptable. However, as the samples were analyzed over several hours and the concentrations used were low, r^2 values of 0.98 were considered acceptable. The elements that showed poor linearity ($r^2 < 0.98$), and were therefore discounted from additional analysis, were Cd, Cr, Cu, Ni, Pb, and Zn. For the remaining elements, the limit of detection (LOD), the limit of quantitation (LOQ), and the relative standard deviation (RSD) of the normalized signal at each concentration was calculated for concentrations greater than the LOQ. Calibration curves were made separately for each paper type and the average values for r^2, LOD, and LOQ are shown in Table 5.1 along with the highest RSD observed for all days. The figures of merit for each paper type can be found in Appendix B.

When these values were calculated for the instrument, the LODs were negative for Co and V. This is because the y-intercept from the calibration curve was used opposed to the average signal of the calibration blanks to convert the signal to concentration[2]. When the signal of the nitric acid blank was compared to the signal of the samples, the nitric acid signal was less than the signal in the samples for both elements and therefore these elements could be used for the element profiles. The low values for LOD and LOQ highlight the ability of ICP-MS to detect trace concentration in paper samples.

Table 5.1 Summary of the average analytical figures of merit for selected elements for ICP-MS analysis

	Al	Ba	Co	Fe	Mg	Mn	Sb	V
r^2	0.999	0.998	0.996	0.999	0.994	0.999	0.998	0.991
Limit of Detection (µg/L)	1.54	0.0590	-0.000610	0.790	0.481	0.0060	0.00408	-0.00172
Limit of Quantitation (µg/L)	4.58	0.0745	0.000410	2.35	1.08	0.0332	0.00662	0.00203
Highest RSD of normalized signal*	14.3	26.4	17.3	4.05	12.3	5.31	7.85	14.1
Working Range** (µg/L)	4.58-76.9	0.0745-0.962	0.000410-0.192	2.35-76.9	1.08-76.9	0.0332-0.962	0.00662-0.962	0.00203-0.192

* The RSD was calculated at each concentration for each calibration used. The highest RSD among the days of analysis was chosen to emphasize the precision of the instrument.

** Working range based only on the concentrations investigated. 76.92 µg/L was the highest concentration used for Al, Fe, and Mg, 0.962 µg/L was the highest for Ba and Mn, and 0.192 µg/L was the highest for Co and V.

Next, the RSD at each concentration was calculated. The highest RSD for each element among the four paper types was reported to show the precision of the instrument. For elements where the RSD was greater than 10%, it was found in the lowest standard. Since the concentration of this standard was close to the LOQ, the variation in the signal is expected. All other concentration for these elements had RSDs less than 10%. All of the elements that were acceptable for ICP-OES, as well as Co, Sb, and V, could be used to generate an element profile for the four paper types.

5.2. Variation in Element Concentration Within Paper Type

The variation of element concentration within a paper type was determined for all elements by calculating the RSD of the ten samples analyzed within a ream (*i.e.*, five samples from two sheets in the ream). For any ream that had an RSD greater than 25%, the Grubbs' test was used to determine if there were outliers within the ream. Since an extra dilution was used in the sample preparation resulting in lower concentrations, an RSD of 25% was used as opposed to the 15% used for ICP-OES analysis. If there was a statistical outlier, the sample was removed and the mean, standard deviation, and RSD were recalculated. This was repeated if the RSD was still greater than 25%. Analysis of variance (ANOVA) was then performed at the 95% confidence level to determine if there was a statistical difference in the concentration of each element among the three reams of each paper type. If there was a statistical difference among reams A, B, and N, Tukey's honestly significant difference (HSD) test was performed, also at a 95% confidence level, to determine which ream was statistically different.

When the calibration curve was used to calculate the concentration of Sb in the samples, the concentrations were negative numbers, which indicated that the sample concentrations were below the LOD for the instrument. Concentrations of Co in the samples were calculated using the calibration curve but when the RSDs were calculated within a ream, the values ranged from 8% in multipurpose paper to 77% in laserjet paper, with most RSDs greater than 30%. There were no statistical outliers determined by the Grubbs' test which indicated that there was too much variation in Co concentration for this element to be considered for the element profile. Therefore, neither Sb nor Co were included for additional statistical analysis. Thus, the comparison of element concentrations was performed using Al, Ba, Fe, Mg, Mn, and V.

For color inkjet paper, the RSDs of all elements were less than 25%. The RSD for most elements was around 15% which indicated that there was little variation in element concentration within a ream (Table 5.2). ANOVA was performed at the 95% confidence level and it was determined that there was a statistically significant difference in concentration among the three reams for Al, Ba, Mn, and V. Tukey's HSD test was performed, also at the 95% confidence level, and it was determined that the concentration of Al, Ba, and V in ream N was significantly higher than in reams A and B. For Mn, the concentration in ream A was statistically lower from the concentration in reams B and N.

For laserjet paper, the RSDs for all elements in all three reams were less than 25%, with RSDs for all samples in reams A and N being less than 20% (Table 5.3). When ANOVA was performed, there was a significant difference in concentration for all elements among the three reams at the 95% confidence level. It was determined from Tukey's HSD test, also at the 95% confidence level, that element concentrations in ream N were statistically higher for Al, Ba, Mg,

Table 5.2. Average element concentration (µg/g) and relative standard deviation (%) for color inkjet paper

Color Inkjet	Ream A		Ream B		Ream N		Significant difference at 95% confidence	Statistically different ream
	Avg. Conc. n=10 (µg/g)	RSD (%)	Avg. Conc. n=10 (µg/g)	RSD (%)	Avg. Conc. n=10 (µg/g)	RSD (%)		
Al	392	16	416	14	483	11	Yes	Ream N
Ba	7.17	16	7.76	15	14.7	16	Yes	Ream N
Fe	54.1	16	59.7	16	56.2	16	No	None
Mg	618	15	644	14	636	17	No	None
Mn	3.03	16	3.72	24	3.74	17	Yes	Ream A
V	0.367	15	0.416	12	0.534	17	Yes	Ream N

Table 5.3. Average element concentration (µg/g) and relative standard deviation (%) for laserjet paper

Laser-jet	Ream A		Ream B		Ream N		Significant difference at 95% confidence	Statistically different ream
	Avg. Conc. n=10 (µg/g)	RSD (%)	Avg. Conc. n=10 (µg/g)	RSD (%)	Avg. Conc. n=10 (µg/g)	RSD (%)		
Al	42.0	19	40.2	19	182	15	Yes	Ream N
Ba	0.856	13	0.708	25	2.43	15	Yes	Ream N
Fe	114	13	98.5	24	90.4	15	Yes	Ream N*
Mg	365	15	312	22	521	15	Yes	Ream N
Mn	4.99	14	4.32	24	5.66	16	Yes	Ream N^{+}
V	0.470	13	0.400	20	0.359	17	Yes	Ream N*

* indicated a significant difference between reams A and N only
+ indicated a significant difference between reams B and N only

and Mg from concentrations in the other two reams. The concentrations in ream N were statistically lower for Fe and V compared to reams A and B. For Fe and V, the difference was between reams A and N and for Mn, the difference was between B and N. There was not a difference in concentration between reams A and B for any element.

For multipurpose paper, the RSDs for all elements in reams B and N were less than 15% indicating that there was little variation within the reams (Table 5.4). For ream A, the RSDs for Fe, Mg and V in ream A were approximately 20% except for Mg where the RSD was 32%. The concentrations of Mg ranged from 405.78 to 1209.30 µg/g and the average concentration was 698.67 µg/g. When the Grubbs' test was performed on the Mg concentrations, none of the samples were determined to be statistical outliers and therefore all samples were included. The Grubbs' test takes into account the standard deviation of the samples and since the range of concentrations was wide, none of the samples were determined to be outliers at the 95% confidence level. When ANOVA was performed at the 95% confidence level, it was determined that there was a significant difference in concentrations of Al, Mn, and V. Tukey's HSD test, also at the 95% confidence level, determined that ream N had statistically higher Al concentration and statistically lower concentration of Mn and V than reams A and B.

For office paper, the RSDs of all elements in reams B and N were 20% or less (Table 5.5). For ream A, the RSD of V was greater than 25%. When the Grubb's test was performed on the V concentrations in ream A, no statistical outliers were identified so all samples were used for ANOVA. The RSD of V was high because the concentration of V in the samples was closest to the limits of detection. This explained why there was variation in the concentration and therefore V was still included for comparison. When ANOVA was performed at the 95%

Table 5.4. Average element concentration (µg/g) and relative standard deviation (%) for multipurpose paper

Multi-purpose	Ream A		Ream B		Ream N		Significant difference at 95% confidence	Statistically different ream
	Avg. Conc. n=10 (µg/g)	RSD (%)	Avg. Conc. n=10 (µg/g)	RSD (%)	Avg. Conc. n=10 (µg/g)	RSD (%)		
Al	479	19	499	9	662	11	Yes	Ream N
Ba	12.2	20	12.0	10	12.7	11	No	None
Fe	60.6	21	60.6	9	63.5	11	No	None
Mg	699	32	668	8	809	11	No	None
Mn	4.67	19	4.80	10	4.14	10	Yes	Ream N
V	0.601	21	0.638	14	0.482	14	Yes	Ream N

Table 5.5. Average element concentration (µg/g) and relative standard deviation (%) for office paper

Office	Ream A		Ream B		Ream N		Significant difference at 95% confidence	Statistically different ream
	Avg. Conc. n=9 (µg/g)	RSD (%)	Avg. Conc. n=10 (µg/g)	RSD (%)	Avg. Conc. n=10 (µg/g)	RSD (%)		
Al	881	19	915	14	866	19	No	None
Ba	10.4	20	11.0	15	9.62	18	No	None
Fe	58.0	20	60.7	14	70.9	18	No	None
Mg	808	24	852	14	937	19	No	None
Mn	4.66	20	4.80	14	4.54	18	No	None
V	0.477	27	0.517	14	0.394	20	Yes	Ream N

confidence level, there was only a statistical difference in concentration among the three reams for V. Tukey's HSD test, also at the 95% confidence level, determined that the concentration of V in ream N was statistically lower than reams A and B for this element. While the concentrations of Ba, Fe, and Mg appear to be different in ream N compared to reams A and B there was not a difference determined by ANOVA. This is because ANOVA takes into account the variance within and among the samples and the variance within the samples is high for this ream.

The concentration of these elements in the samples were similar to the concentrations reported in literature, however; direct comparisons between the concentrations could not be made because difference paper types and different manufacturers were used [3,4]. Since there was not a statistical difference in the concentrations of the six elements between reams A and B for almost all paper types, the average concentration of each element in reams A and B was used for further statistical analysis of each paper type.

5.3. Variation in Element Concentration Among Paper Types

To investigate the variation of element concentration among the four paper types, ANOVA was performed per element at the 95% confidence level using the average element concentration of reams A and B for each paper type. For any elements in which ANOVA determined there was a statistical difference in concentration among the paper types, Tukey's HSD test was performed, also at the 95% confidence level, to determine between which paper types the difference occurred. The results are summarized in Table 5.6.

Table 5.6. Average element concentration in each paper type

	Average Element Concentration (µg/g)					
	Al	Ba	Fe	Mg	Mn	V
LaserJet	40.6	0.804	109	344	4.76	0.442
Color Inkjet	404	7.46	56.9	631	3.38	0.391
Multi-purpose	489	12.1	60.6	684	4.73	0.620
Office	898	10.7	59.3	830	4.73	0.497
Statistical difference at 95% confidence level	Yes	Yes	Yes	Yes	Yes	Yes
Paper type which is statistically different from the others	LaserJet Office	Color Inkjet Laserjet	Laserjet	Laserjet	Color inkjet	Multipurpose

Aluminum could be used to differentiate laserjet and office paper from each other and from the other two paper types. Office and multipurpose paper could be differentiated from both laserjet and office paper; however, they could not be differentiated from each other since the difference in average concentration was 84.7 µg/g. Laserjet paper had the lowest average concentration of Al (40.6 µg/g) in reams A and B, while office paper had the highest average concentration of Al (898 µg/g). Aluminum can be added at many stages of the paper-making process. It is added in the form of kaolin hydrous, calcinated clay, and aluminum trihydrate as a filler to ensure smoothness on the paper surface[5]. Aluminum is also added as a coating to paper in the form of kaolin clay and alumina trihydrate to increase the brightness of the paper.

Barium could be used to differentiate color inkjet jet and laserjet paper from each other and from the other paper types. Office and multipurpose paper could be differentiated from the other paper types but could not be differentiated from each other. The concentration of Ba ranged from less than 1 µg/g in laserjet paper to 12.1 µg/g in multipurpose paper. Barium sulfate is also used as a filler during the paper-making process[5,6].

Iron could be used to differentiate laserjet paper from the other three paper types. Iron oxide is found in bauxite, a precursor used to make aluminum trihydrate[5]. Iron and other transition metals are also present in the pulp material used for paper making[5]. Color inkjet, multipurpose, and office paper had similar concentrations of Fe (approximately 59 µg/g) among all three reams. In contrast, the Fe concentration in laserjet paper was twice as high (109 µg/g). Laserjet paper is made specifically for a laserjet printer which uses heat to fuse toner onto the paper. The other three paper types can be used in inkjet printers where ink is absorbed onto the paper. The higher Fe concentration may be beneficial for this type of printing.

The average concentration of Mg in laserjet paper was approximately half the concentration in the other three paper types and hence, this element could be used to differentiate laserjet from the other three paper types. Additionally, office paper could be differentiated from both color inkjet and laserjet paper based on Mg concentration, but could not be differentiated from multipurpose paper. Even though the concentration of Mg in office paper was about 150 µg/g higher than multipurpose paper, which had the second highest concentration, ANOVA takes into account the variance. While the average concentration in the paper types appeared different, there was high variance among the reams, as indicated by the high RSDs, and therefore the concentrations could not be differentiated between the paper types. Magnesium is added as both a filler, as talc, and as a coating pigment, as ground calcium carbonate and talcum[5].

Color inkjet paper could be differentiated from the other three paper types based on Mn concentration. The concentration of Mn only varied by approximately 1.5 µg/g among all four paper types; however, laserjet, multipurpose, and office paper only varied by 0.03 µg/g. Vanadium could be used to differentiate multipurpose paper from the three other paper types. The concentration of V among the paper types only varied by approximately 0.2 µg/g. A difference of this magnitude is insignificant for the other elements because the concentrations are much higher; however, a difference of 0.2 µg/g results in double the V concentration. Since the concentration of V is so low, slight differences in concentration among paper types results in greater variance. While neither of these elements are typically added in the paper-making process, Mn and V may be present in the raw materials used[5]. While these elements can be used for differentiation, the differences may be exaggerated due to the low concentration when compared to other elements.

In summary, Al could be used to differentiate laserjet and office paper from the other paper types while Ba could be used to differentiate color inkjet and laserjet from the other paper types. Fe and Mg could be used to differentiate laserjet paper, Mn could be used to differentiate color inkjet paper, and V could be used to differentiate multipurpose paper from the other three types. None of these elements could be used to differentiate all paper types from each other due to the large amount of variance within a ream as indicated by the high RSDs. While these results show that differentiation of the paper types was possible, ANOVA can only be used to compare one element at a time. This process is time consuming and does not accurately describe the entire elemental composition of the paper. Therefore, additional multivariate statistical procedures, in which all six elements are considered simultaneously, were investigated.

5.4. Differentiation of Paper Types Using Principal Components Analysis

Since ANOVA could only be used to compare one element at a time, principal components analysis (PCA) was used to simultaneously compare the average concentration of the six elements in reams A and B of all four paper types.

The resulting PCA scores plot is shown in Figure 5.1 with principal component 1 (PC1) and principal component 2 (PC2) accounting for 99.87% of the total variance. The four sheets (two from each ream) from each paper type were positioned similarly on PC1, with the exception of office paper for which spread was observed on PC1. For all paper types, spread was observed among the sheets on PC2. Despite the spread, laserjet and office paper could be differentiated from each other and from the other paper types while differentiation of color inkjet and multipurpose paper was not possible. Laserjet paper was positioned negatively on both PC1 and

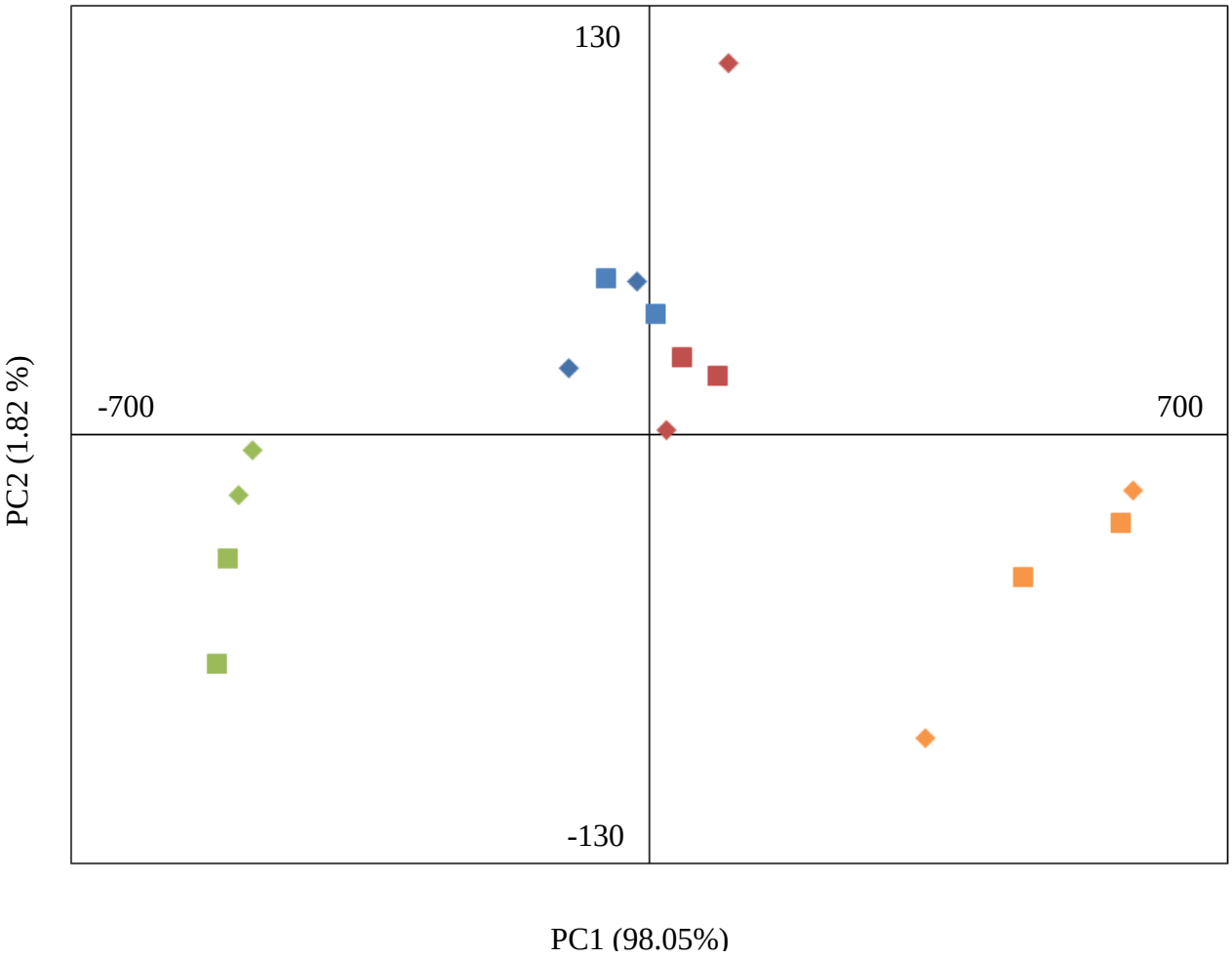

Figure 5.1. Scores plot of PC1 and PC2 based on element concentrations in Reams A (◆) and B (■) of four different paper types. Paper types are as follows: Laserjet (▲), Color Inkjet (▲), Multipurpose (▲), and Office Paper (▲)

PC2. Color inkjet paper was positioned negatively on PC1 and positively on PC2, except for sheet 1 from ream B which was slightly positive on PC1. Multipurpose paper was positioned positively on both PC1 and PC2. Office paper was positively positioned on PC1 and negatively positioned on PC2.

The positioning of the samples on the scores plot could be explained by the positioning of the elements on the loadings plot (Figure 5.2). Iron was weighted negatively on both PC1 and PC2. Magnesium was weighted positively on both PC1 and PC2. Aluminum was weighted most positively on PC1 and most negatively on PC2. Barium, Mn, and V were weighted close to zero on both PC1 and PC2. Both Mn and V were present in concentrations less than 5 µg/g and there was little variation in concentration among the paper types. While the concentration of Ba was higher than Mn and V, the difference in Ba concentration among the paper types was only 10 µg/g compared to a difference of 857 µg/g for Al. Due to the low concentrations and lack of variation among the paper types, Ba, Mn, and V did not contribute substantially to the positioning of the samples on the scores plot. Therefore, positioning of paper samples in the scores plot was mainly based on the concentrations of Al, Mg, and to a lesser extent, Fe.

The positioning of each paper types on the scores plot could be explained using the weighting of the elements on the loadings plot and the mean-centered concentrations of the elements in each paper type. This procedure was explained in Chapter 4.

Laserjet paper was positioned negatively on both PC1 and PC2 on the scores plot because it had the highest concentration of Fe and lowest concentration of Al and Mg among all paper types. The mean-centered data for Fe was positive while the mean-centered data for Al and Mg were negative for this paper type. Iron was weighted negatively on both PC1 and PC2 on the loadings plot, and when the negative weighting was multiplied by the positive mean-centered

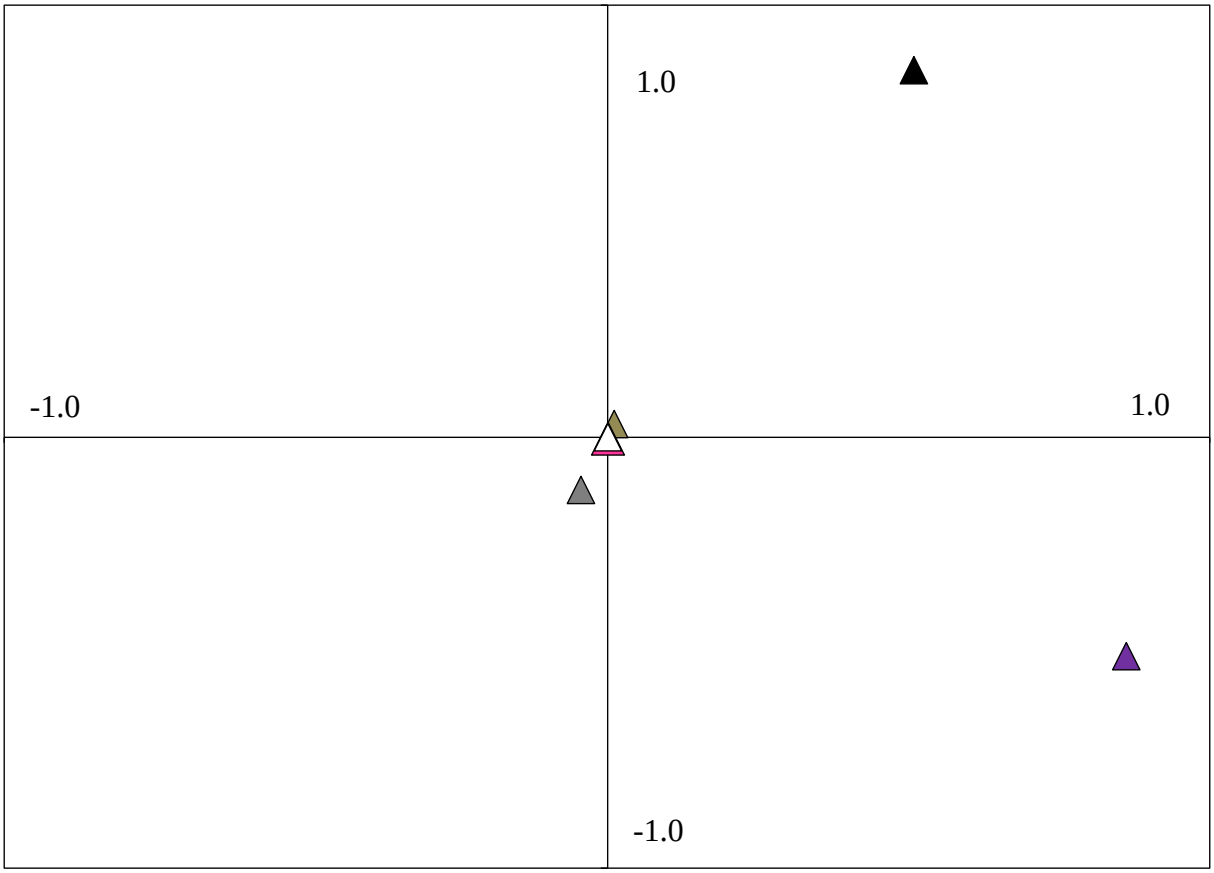

Figure 5.2. Loadings plot of PC1 and PC2 based on element concentrations in two reams of four different paper types. Elements are as follows: Al (▲), Ba (▲), Fe (▲), Mg (▲), Mn (▲), and V (△)

data, the contribution from Fe on the scores was negative. Both Al and Mg were weighted positively on PC1 on the loadings plot. When the positive weightings were multiplied by the negative mean-centered data, the resulting contribution of both Al and Mg on PC1 was negative. The weightings of all elements on PC1 were summed and the resulting score on PC1 was negative. For this paper type, the contribution of Al to PC2 was positive but this was outweighed by the negative contribution from both Fe and Mg resulting in a negative score on PC2.

Office paper was positioned positively on PC1 and negatively on PC2 on the scores plot. The positive weighting on PC1 was due to the positive mean-centered data for both Al and Mg which were weighted positively on PC1. The contribution of Al to PC2 was negative while the contribution of Mg to PC2 was positive. The concentration of Al was greater than the concentration of Mg and therefore the sheets of office paper were positioned negatively on PC2.

Multipurpose paper was positioned positively on both PC1 and PC2 in the scores plot. For this paper, both Al and Mg were positive in the mean-centered data. Both elements had positive contributions on PC1 so that when the mean-centered data were multiplied by the eigenvector for PC1, the resulting scores were positive on this PC. Magnesium, which was weighted positively on PC2, was present in the highest concentration among all elements for this paper type and therefore the sheets were positive on PC2. Three sheets were clustered close together while sheet 2 of ream A was positioned more positively on PC2. This sheet was more positive on PC2 because the Mg concentration was 100 µg/g higher than the other sheets of this paper type.

Color inkjet paper was positioned slightly negatively on PC1 and positively on PC2. For this paper type, Al was negative in the mean-centered data while Mg was positive. When the negative Al concentrations were multiplied by the positive weighting of Al on PC1, it resulted in

negative scores for the sheets on PC1. The exception was sheet 1 of ream B which was positioned slightly positive on PC1 because it had the highest concentration of Al among the four sheets. This sheet also had the highest concentration of Mg. The positive contribution of the eigenvector of Mg was greater than the negative contribution of Al and resulted in the overall positive positioning on PC1 for this sheet. The mean-centered data for Mg was positive for most sheets and, when multiplied by the positive weighting on PC2, resulted in positive scores for the sheets on PC2. The exception to this was sheet 2 of ream A for which Mg had a negative contribution in the mean-centered data. When multiplied by the positive weighting on PC2, there was a negative contribution to the score for this sheet. As a result, this sheet was positioned more negatively on PC2 than the other sheets of color inkjet paper.

It should be noted that, based on the first two PCs, it is not possible to differentiate multipurpose and color inkjet papers. Although color inkjet paper is positioned negatively on PC1 and multipurpose paper is positioned positively, there is spread among sheets of the same paper type, making differentiation difficult. Additionally, the concentrations of Al, Fe, and Mg were similar between the two paper types such that differentiation on PC2 was also not possible.

The scores for sheets in ream N of each paper type were calculated and projected onto the scores plot generated previously (Figure 5.3). In general, the sheets of ream N could not be easily associated to sheets A and B of the corresponding paper type.

The two sheets of ream N of laserjet paper were the most closely positioned to each other on both PC1 and PC2 compared to the sheets of ream N for other paper types. This was because these two sheets contained similar concentrations of all elements. These sheets of ream N were positioned more positively on both PC1 and PC2 than reams A and B of the same paper type, mainly due to differences in the concentrations of Al and Mg. The concentration of Al in ream N

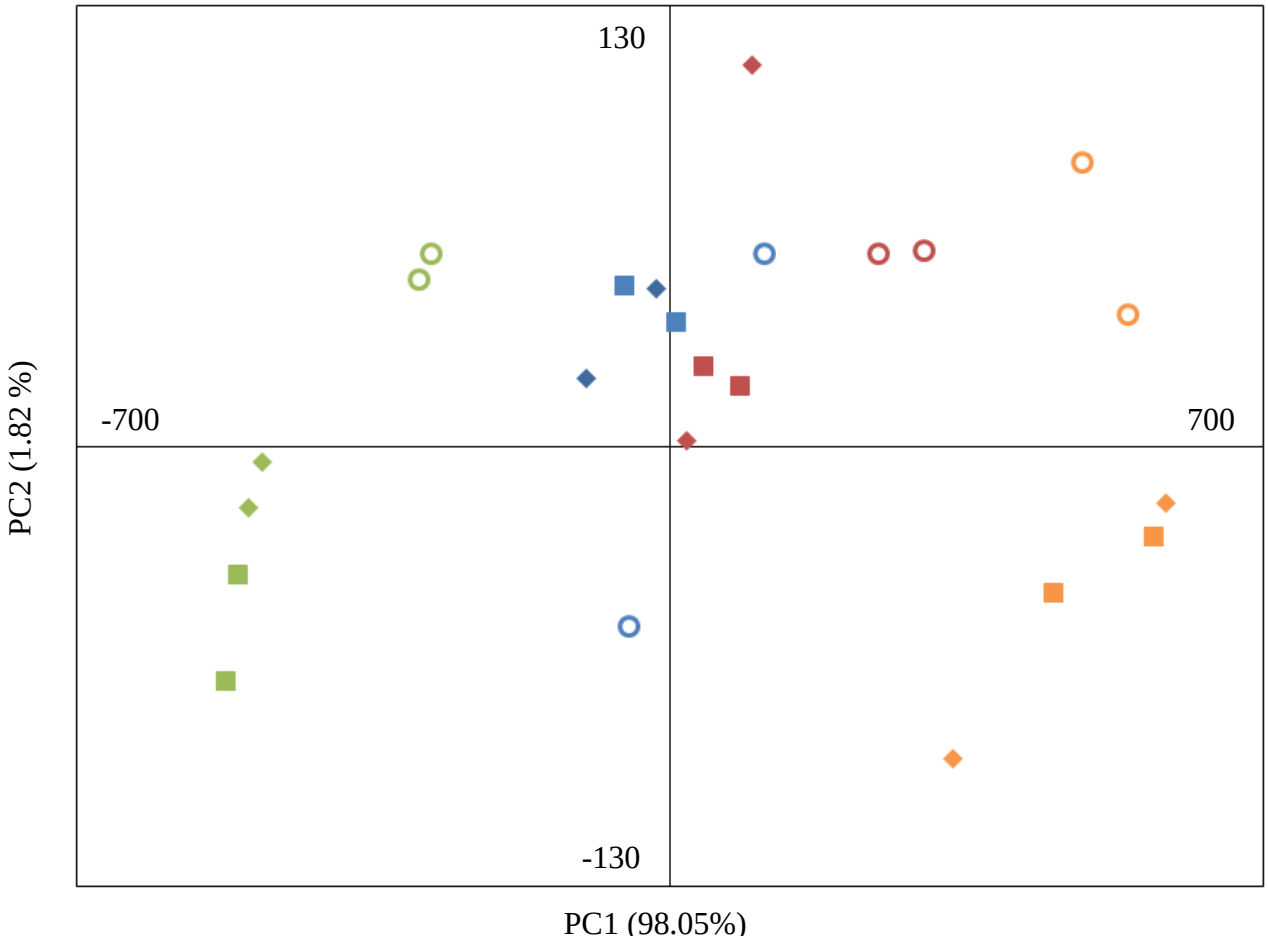

Figure 5.3. Scores Plot Showing the Scores for the New Reams (○) Projected onto the Scores Plot for the Reams A (◆) and B (■) of Laserjet (▲), Color Inkjet (▲), Multipurpose (▲), and Office Paper (▲)

of laserjet paper was approximately five times greater than the concentration in reams A and B, which resulted in the more positive positioning on PC1. The concentration of Mg in ream N was approximately 100 µg/g greater than the Mg concentration in reams A and B, which resulted in the more positive positioning on PC2.

The two sheets of ream N of office paper had similar positioning to each other on PC1, although there was spread in positioning on PC2. The difference in concentration of Al for these sheets was 69.7 µg/g while the difference in Mg concentration was only 11.1 µg/g. The spread on PC2 was mainly due to the differences in Al concentration between the two sheets (901 µg/g and 832 µg/g respectively). The sheets in ream N were similar in positioning to the sheets of reams A and B on PC1; however, they were positioned positively on PC2 while the sheets in reams A and B were negative on PC2. The concentration of sheets 1 and 2 in ream N were within the Al concentration range of sheets of reams A and B (792 µg/g to 969 µg/g) and therefore had similar scores on PC1. However, the sheets of ream N had higher concentrations of Mg than reams A and B, which resulted in more positive positioning of ream N on PC2.

The two sheets of ream N of multipurpose paper were also positioned relatively closely on PC1 and PC2; however, the concentrations of Al and Mg in one sheet were approximately 50 µg/g higher than the concentrations in the other, resulting in some spread, particularly in PC1. The sheets from ream N were positioned slightly more positively on PC1 than sheets from reams A and B due to higher concentrations of Al in ream N. The sheets in ream N were also positioned more positively on PC2 than the three sheets of reams A and B due to the higher concentration of Mg in ream N. As previously noted, sheet 2 in ream A was positioned most positively on PC2 due to the high Mg concentration (767 µg/g), which was still higher than the Mg concentrations in ream N.

The two sheets from ream N of color inkjet paper showed the most spread of all the ream N sheets. Sheet 1 was positioned negatively on both PC1 and PC2 whereas, sheet 2 was positioned positively on both PC1 and PC2. Again, the positioning was mainly due to the Al and Mg concentrations. The difference in Al concentration between the two sheets was 80.4 µg/g and the difference in Mg concentration was 179 µg/g. For sheet 1, the mean-centered data were negative for both Al and Mg. When these concentrations were multiplied by the positive weightings of Al and Mg in the loadings plot, the resulting positioning was negative on both PC1 and PC2. For sheet 2, the mean-centered data for both Al and Mg were positive. When these concentrations were multiplied by the positive weightings of Al and Mg in the loadings plot, the positioning was positive on both PC1 and PC2.

Sheet 1 from ream N of color inkjet paper was positioned similarly on PC1 as the sheets in reams A and B because the concentration of Al was similar. This sheet was positioned negatively on PC2 because the concentration of Mg was approximately100 µg/g lower than the Mg concentration in reams A and B. Sheet 2 from ream N had the highest concentration of Al and Mg among all sheets of color inkjet paper, which resulted in the most positive positioning on PC1. The positive positioning on PC2 was dominated by the high concentration of Mg in this sheet. The concentrations of both Al and Mg were more similar to the concentrations in multipurpose paper than reams A and B of color inkjet paper, which was observed in the scores plot by the close positioning of these sheets of the two paper types. The concentration of Al in the sheets in reams A and B was less than 445 µg/g and the concentration of Mg was less than 660 µg/g. In the sheets of multipurpose paper, the concentration of Al in multipurpose paper was greater than 470 µg/g and the concentration of Mg was greater than 630 µg/g.

It is interesting to note that the sheets of ream N for all paper types had similar positioning on PC2. While the positioning on PC2 was mainly influenced by Mg, the concentration of this element in ream N ranged from 521 μg/g for laserjet paper to 937 μg/g for office paper. However, PC2 only accounted for 1.8% of the total variance in the data set and hence, all sheets from ream N of all paper types were positioned similarly on this PC despite the range in Mg concentration.

5.5. Clustering of Paper Types Using Hierarchical Cluster Analysis

Hierarchical cluster analysis (HCA) was performed using Euclidean distance and complete linkage on the average element concentration per sheet using the sheets in all three reams for each paper type. Sheets 1 and 2 of ream N were clustered together at least a 93.7% similarity level or higher for all paper types except color inkjet paper (Figure 5.4). In this case, sheet 1 from ream N was clustered to other sheets of color inkjet paper and sheet 2 from ream N was clustered to multipurpose paper. All sheets of laserjet paper were clustered together before being clustered to another paper type. This was the only paper type where the sheets were clustered together before being clustered to another paper type.

Sheets 1 in reams A and B and both sheets in ream N of office paper were clustered together at an 87.2% similarity level because they had the highest concentration of Mg among all paper types and similar concentrations of Al (Tables 5.5). Sheet 2 of ream A and B of office paper and the sheets in ream N of multipurpose paper were clustered together at 77.8% because

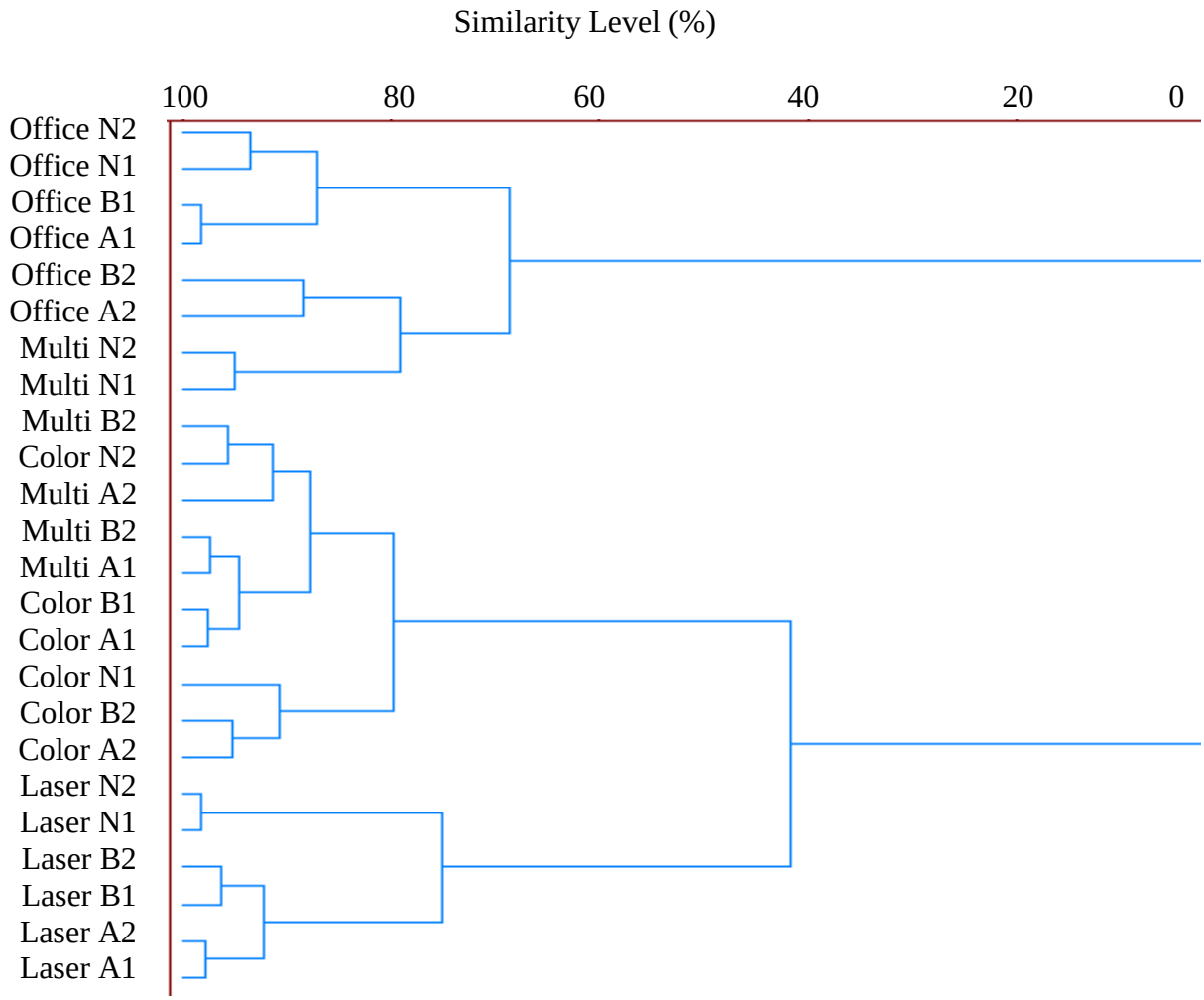

Figure 5.4. Hierarchical cluster analysis dendrogram based on average concentration of five elements for three reams of four different paper types. Euclidean distance and complete linkage were used for clustering. The letter after the paper type refers for the ream and the number refers to the sheet.

they had similar concentrations of Al, which were the second highest among paper types, and similar concentrations of Mg. All sheets of office paper and the sheets in ream N of multipurpose paper were clustered together at 68.7% similarity because they had the highest concentration of Al and Mg among all paper types.

The sheets in reams A and B of multipurpose paper and all sheets of color inkjet paper were clustered together at a 79.9% similarity level. These sheets had similar concentrations of Al, Mg, and Fe (Tables 5.2 and 5.3). Sheet 2 of ream N of color inkjet paper was clustered with multipurpose paper before it was clustered with the other sheets of color inkjet paper. This sheet had concentrations of Al and Mg that were higher than the other sheets of color inkjet paper and were more similar to multipurpose paper. Sheet 1 of ream N of color inkjet paper was clustered with sheets in reams A and B of color inkjet paper due to similar concentrations of Al and Mg.

The four sheets in reams A and B of laserjet paper were clustered at a 92.3% similarity level. These sheets had similar had similar concentrations of Al and Mg, which were lower than that of other paper types and similar concentrations of Fe, which were higher than the other paper types (Table 5.4). All sheets of laserjet paper were clustered at a 75.2% similar level because they had the most similar concentrations of Al and Mg, which were lower than the other paper types. The concentration of Fe only ranged between 87.7 µg/g and 118 µg/g among all sheets of this paper type which was the highest of all paper types.

5.6 Comparison of PCA and HCA Results

When the results of PCA and HCA were compared, there was similar grouping of the paper types into three groups by both procedures. Laserjet and office paper were differentiated

each other and the other two types of paper, while it was more difficult to differentiate the sheets of color inkjet and multipurpose paper.

The calculations used to cluster samples by HCA are not related to the grouping of samples by PCA. However, the positioning of the papers on PC1 can be used to explain the clustering observed in HCA for these data because PC1 accounted for 98.05% of the variance. PCA uses two dimensions to display the data while HCA is limited to one dimension and therefore there were some cases where the positioning on PC2 influenced the clustering on the scores plot. For example, sheet 1 of ream B of color inkjet paper had a PC1 score closer to sheet 1 of ream A of multipurpose paper; however, it was clustered to sheet 1 of ream A of color inkjet paper. This was because the score on PC2 was more similar between these two sheets of color inkjet paper.

The sheets of all reams of laserjet paper had similar positioning on PC1 and these sheets were clustered at a 75.2% similarity level using HCA. The sheets of ream N of multipurpose paper and all sheets of office paper were positioned most positively on PC1 (PC1 scores between 244 and 584), due to high concentration of Al and Mg, and these sheets were clustered together at 68.7% similarity level. The sheets of color inkjet and multipurpose paper could not be differentiated from each other on PC1. A similar trend was apparent with HCA because sheets of color inkjet paper were clustered to sheets of multipurpose paper before being clustered to other sheets of color inkjet paper. All sheets of color inkjet and sheets in reams A and B of multipurpose paper were clustered at a 79.9% similarity level.

In PCA, the loadings plot can be used to explain the differentiation and the scores plot allows for a visual differentiation of the sheet in two dimensions. However, interpretation of the association and discrimination of samples in the scores plot can be subjective. HCA generates a

similarity level associated with the clustering which would be more useful in a forensic laboratory because it would be beneficial when testifying in court. Both methods allowed for the differentiation of laserjet and office paper while neither method allow for the differentiation of color inkjet and multipurpose paper based on element concentrations determined using ICP-MS.

APPENDIX

APPENDIX B

Figures of merit for ICP-MS for each paper types using the standards analyzed directly before and after the paper samples

Table B.1. Figures of merit for color inkjet paper analyzed by ICP-MS on 053112

	Al	Ba	Co	Fe	Mg	Mn	Sb	V
r^2	0.9972	0.9984	0.9935	0.9989	0.9911	0.9987	0.9992	0.9929
Limit of Detection (µg/L)	0.6700	0.00141	-0.00059	0.2994	0.6618	-0.00082	-0.00445	0.0019
Limit of Quantitation (µg/L)	1.564	0.0244	0.00015	0.3304	0.8460	0.01732	-0.00112	0.00762
Highest RSD of normalized signal*	14.32	6.82	8.88	3.40	8.49	5.30	4.93	9.48
Working Range** (µg/L)	1.564-76.92	0.0244-0.962	0.00015-0.192	0.3304-76.92	0.8460-76.92	0.01732-0.962	0-0.962	0.00762-0.192

* The RSD was calculated at each concentration for each calibration used. The highest RSD among all concentrations was chosen to emphasize the precision of the instrument.

** Working range based only on the concentrations investigated. 76.92 µg/L was the highest concentration used for Al, Fe, and Mg, 0.962 µg/L was the highest for Ba and Mn, and 0.192 µg/L was the highest for Co and V.

Table B.2. Figures of merit for multipurpose paper analyzed by ICP-MS on 053112

	Al	Ba	Co	Fe	Mg	Mn	Sb	V
r^2	0.9987	0.9974	0.9927	0.9992	0.992	0.9988	0.9992	0.9917
Limit of Detection (µg/L)	2.957	-0.00976	-0.000453	0.2072	1.007	-0.00689	-0.00759	-0.000159
Limit of Quantitation (µg/L)	8.241	0.00214	0.000224	0.2646	1.500	-0.00413	-0.00691	0.000725
Highest RSD of normalized signal*	1.54	26.38	9.14	3.14	6.94	4.81	4.72	9.99
Working Range** (µg/L)	8.241-76.92	0.00214-0.962	0.000224-0.192	0.2646-76.92	1.500-76.92	0-0.962	0-0.962	0.000727-0.192

* The RSD was calculated at each concentration for each calibration used. The highest RSD among all concentrations was chosen to emphasize the precision of the instrument.

** Working range based only on the concentrations investigated. 76.92 µg/L was the highest concentration used for Al, Fe, and Mg, 0.962 µg/L was the highest for Ba and Mn, and 0.192 µg/L was the highest for Co and V.

Table B.3. Figures of merit for office paper analyzed by ICP-MS on 061912

	Al	Ba	Co	Fe	Mg	Mn	Sb	V
r^2	0.9998	0.9988	0.9970	0.9992	0.9957	0.9994	0.9986	0.9878
Limit of Detection (µg/L)	0.1226	0.1160	-0.00117	-0.03717	-0.0439	0.00839	0.0132	-0.00393
Limit of Quantitation (µg/L)	0.4042	0.1173	-0.00014	0.09090	0.6054	0.0347	0.0152	0.000682
Highest RSD of normalized signal*	3.83	2.41	7.74	2.43	10.23	3.52	2.31	6.56
Working Range** (µg/L)	0.0402-76.92	0.1173-0.962	0-0.192	0.0909-76.92	0.6054-76.92	0.0347-0.962	0.01518-0.962	0.000682-0.192

* The RSD was calculated at each concentration for each calibration used. The highest RSD among all concentrations was chosen to emphasize the precision of the instrument.

** Working range based only on the concentrations investigated. 76.92 µg/L was the highest concentration used for Al, Fe, and Mg, 0.962 µg/L was the highest for Ba and Mn, and 0.192 µg/L was the highest for Co and V.

Table B.4. Figures of merit for laserjet paper analyzed by ICP-MS on 061912

	Al	Ba	Co	Fe	Mg	Mn	Sb	V
r^2	0.9996	0.9973	0.9991	0.9991	0.9986	0.9991	0.9956	0.9914
Limit of Detection (µg/L)	2.422	0.1283	-0.00024	2.690	0.2985	0.02325	0.01522	-0.00468
Limit of Quantitation (µg/L)	8.106	0.1542	0.0014	8.733	1.373	0.0811	0.01932	-0.0009
Highest RSD of normalized signal*	5.78	4.43	17.33	4.05	12.28	5.31	7.85	14.13
Working Range** (µg/L)	8.106-76.92	0.1542-0.962	0.0014-0.192	8.733-76.92	1.373-76.92	0.0811-0.962	0.01932-0.962	0-0.192

* The RSD was calculated at each concentration for each calibration used. The highest RSD among all concentrations was chosen to emphasize the precision of the instrument.

** Working range based only on the concentrations investigated. 76.92 µg/L was the highest concentration used for Al, Fe, and Mg, 0.962 µg/L was the highest for Ba and Mn, and 0.192 µg/L was the highest for Co and V.

REFERENCES

REFERENCES

1. Skoog DA, Holler FJ, Crouch SR. Principles of instrumental analysis. 6th ed. Belmont, CA: Thomson, 2007.

2. Mocak J, Bond AM, Mitchell S, and Scollary G. A Statistical overview of standard (IUPAC and ACS) and new procedures for determining the limits of detection and quantification; Application to voltammetric and stripping techniques. *Pure Appl Chem.* 1997; 69: 297-325

3. Spence LD, Baker AT, Byrne JP. Characterization of document paper using elemental compositions determined by inductively coupled plasma mass spectrometry. *J. Anal. At. Spectrom* 2000; 15: 813-819.

4. McGaw EA, Symanski DW, Smith RW. Determination of trace elemental concentrations in document papers for forensic comparison using inductively coupled plasma-mass spectrometry. *J. Forensic Sci* 2009; 54: 1163-1170.

5. Holik H. Ed. Handbook of Paper and Board. 2006. Wiley-VCH Verlag GmbH & Co. Weinheim, Germany.

6. Saltman D. Paper Basics: Forestry, Manufacture, Selection, Mathematics, and Metrics, Recycling. Litton Educational Publishing, Inc 1978 New York, NY

Chapter 6 Conclusions

6.1 Summary of Research

6.1.1 Research Objectives and Goals

The objective of this research was to determine if inductively coupled plasma-optical emission spectroscopy (ICP-OES) was sufficiently sensitive to create element profiles that could be used to differentiate paper samples using statistical procedures. Differentiation of paper types based on element profiles generated using inductively coupled plasma-mass spectrometry (ICP-MS) had previously been successful; however, the use of ICP-OES for this purpose had not been investigated[1-3]. The statistical procedures investigated for differentiation of the paper samples in this project were analysis of variance (ANOVA), principal components analysis (PCA), and hierarchical cluster analysis (HCA).

In order to achieve this objective, several goals had to be met. The first was to create element profiles for different types of paper (*i.e.*, color inkjet, laserjet, multipurpose, and office paper) that were all manufactured by Hewlett Packard. Two reams of each paper type were purchased at the same time and a third ream was purchased approximately one year later. The element profiles were first compared within a ream to determine if there were differences in element concentration within a single ream. The profiles were then compared among the three reams using ANOVA to determine if there was a difference in element concentrations based on time of production. Next, these profiles were compared using multivariate statistical procedures to assess the association among sheets of the same paper type and the differentiation among the

different paper types. Finally, the results of association and differentiation achieved by statistical procedures after analysis by ICP-OES and ICP-MS were compared.

6.1.2 ICP-OES Summary

The elements that were above the limit of detection and were reproducible over the time of analysis for ICP-OES were Al, Ba, Fe, Mg, and Mn. The element concentrations were then compared within a ream to determine if there was a statistical difference within a ream because this would be very useful in a forensic laboratory. When a sample is submitted to a forensic laboratory, it is most likely to be a sheet or part of a sheet that needs to be identified by paper type and manufacturer. Therefore, it is important that there are not statistical differences within a ream so that a sample could be correctly associated to the ream of the corresponding paper type. It was found that there were not significant differences in the element concentration among the samples within a ream.

Next, using ANOVA and Tukey's honestly significant difference (HSD) test, the average element concentration for each of the three reams for a paper type were compared. It was determined that if there was a statistical difference in concentration, it was ream N that was statistically different for all paper types. This is important in a forensic laboratory to determine the time at which a document was created. If a company used color inkjet paper from Hewlett Packard to print all documents but in a multipage document, a single sheet was found to have different concentrations than other sheets, it could be possible that this sheet was not printed at the same time as the others. These differences could be due to the difference rolls used to compose the ream; however, in this research, the within ream differences were minimal compared to differences in reams purchased at different times.

In PCA, the sheets in reams A and B were clustered closely together for each paper type and differentiation of office and laserjet paper was possible. Differentiation between color inkjet and multipurpose paper was not possible. When the sheets in ream N were projected onto the scores plot, the two sheets in ream N were positioned closely together for all paper types. Association of the sheets in ream N to the sheets in reams A and B was possible only for office paper. The sheets in ream N of color inkjet were more closely associated with the sheets in reams A and B of multipurpose paper than the corresponding sheets of color inkjet paper. In HCA, the sheets in reams A and B were clustered together first and then the two sheets in ream N were clustered at at least a 72% similarity level for office and laserjet paper. The sheets in ream N of multipurpose paper were clustered to office paper at a 73.0% similarity. The remaining sheets of multipurpose paper and all sheets of color inkjet paper were clustered together at an 81.4% similarity level.

This project showed that ICP-OES was sufficiently sensitive for the analysis of paper samples. Element profiles using Al, Ba, Fe, Mg, and Mn were generated for each of the four paper types. Using PCA and HCA, differentiation of two of the paper types was possible. It was also possible to differentiate production time because the sheets in ream N were not closely associated to sheets in reams A and B of the corresponding paper type.

A limitation of ICP-OES analysis was that only a few elements could be used for analysis due to the detection limits of the instrument. For many elements, the detection limits of the instrument were higher than the concentrations present in the paper samples and could not be used for the element profile. The samples could not be made more concentrated because the digestion procedure was limited by the mass of the paper that could be completely digested and the requirement of 2% nitric acid for the ICP-OES. This technique was successful for the

analysis of paper samples used for this project and showed potential for use in a forensic laboratory; however, more paper types would need to be investigated before ICP-OES analysis of paper could be implemented in a forensic laboratory.

6.1.3 ICP-MS Summary

It had previously been shown that ICP-MS was successful at generating element profiles for paper samples and that differentiation of these paper types was possible. The purpose of analyzing the samples by ICP-MS for this project was to allow for comparison of the differentiation achieved by statistical procedures after analysis by ICP-MS and ICP-OES. The elements that could be used for the element profile for ICP-MS were Al, Ba, Fe, Mg, Mn, and V. This included an additional element, V, which could not be measured by ICP-OES because it was below the detection limits for the instrument. Using ANOVA and Tukey's HSD test, it was again determined that there was not a difference in element concentration within a ream and if there was a difference in concentration among the three reams of a paper type, it was ream N that was statistically different.

When PCA was performed, there was spread among the sheets of laserjet and office paper for reams A and B. This spread was because of the extra dilution used in the sample preparation which resulted in concentrations close to the limit of detection of the ICP-MS instrument. Differentiation between color inkjet and multipurpose paper was not possible due to similar positioning on both PC1 and PC2 in the scores plot, as was seen in the scores plot for ICP-OES as well. When the sheets in ream N were projected onto the scores plot, they were all similar in positioning on PC2 and therefore could be not be associated back to reams A and B for any paper type. However, these results were misleading because PC2 accounted for less than 2%

of the variance of the data set. When HCA was performed, only the sheets in reams A, B, and N of laserjet paper were clustered together at a 75% similarity level. For the other paper types, sheets were clustered with different paper types rather than all sheets of one paper type being clustered together, as was previously observed for the ICP-OES data.

6.1.4. Comparison of Association and Discrimination Using ICP-OES and ICP-MS Data

When the results of the multivariate statistical procedures were compared, the same patterns were observed by both ICP-OES and ICP-MS. However, there was more spread in the samples of office and multipurpose paper when analyzed by ICP-MS which was a result of the dilution used and was not reflective of the capabilities of the instrument. If the dilution was the same as for ICP-OES analysis, it is likely that more elements could be used for the element profile because the detection limits of ICP-MS are in the ng/L range while detection limits for ICP-OES are in the µg/L range. If higher concentrations were analyzed by ICP-MS, there would be less variation in the measurements of the samples which would result in better association on the scores plot.

Even though the dilution used for the two techniques was different, similar concentrations were observed after analysis of the samples. The concentrations measured by ICP-OES were slightly higher than those observed by ICP-MS; however, the positioning of the samples on the scores plots was similar. For both techniques, only laserjet and office paper could be differentiated from each other and from the other paper types. Differentiation between color inkjet and multipurpose paper was not possible. The loadings plot explains which elements contribute most to the variance in the data set. For both techniques, the elements that contributed to positioning were Al, Fe, and Mg and the positioning of these elements on the loadings plot

was very similar for the two techniques. The similar positioning of the samples indicated that the contribution of each element to the positioning of the samples on the scores plots was similar regardless of the technique used.

When HCA was performed on the data, similar clustering was achieved in both ICP-OES and ICP-MS. For both techniques, all sheets in ream N were clustered together before being clustered to sheets in reams A or B for all paper types except for color inkjet paper. This was also seen by ANOVA in that if there was a difference in element concentration among the three reams, it was ream N that was statistically different for all paper types For both techniques, the sheets in reams ream N of color inkjet paper were clustered to multipurpose paper before being clustered to color inkjet paper. All sheets in reams A and B of multipurpose paper and all sheets of color inkjet paper were clustered together.

All sheets of laserjet paper were clustered together before being clustered to another paper type. All sheets of office paper and the sheets in ream N of multipurpose paper were also clustered together. For ICP-OES, all sheets of office paper were first clustered together before being clustered to multipurpose paper ream N; however, for ICP-MS, sheet 2 in both reams A and B were clustered with sheets in ream N of multipurpose paper being clustered to other sheets of office paper. The results of HCA were similar to the results of PCA in that only laserjet and office paper could be differentiated.

6.2 Future Work

The purpose of this project was to determine if ICP-OES could be used to generate element profiles for paper samples. These profiles were then subjected to statistical procedures to determine if differentiation of papers types was possible. Finally, the differentiation of the paper

types by ICP-OES analysis was compared to differentiation following ICP-MS analysis. The comparison of the two techniques was limited due to the extra dilution that was used during the sample preparation for ICP-MS analysis of the samples. This study should first be repeated so that samples were diluted in the same way prior to analysis by ICP-MS and ICP-OES. All samples were diluted to 2% nitric acid first to ensure the acid concentration would not be too high for either instrument as was previously done in our laboratory. The samples for ICP-MS analysis were further diluted using the internal standard provided by the laboratory where the analysis was performed. To ensure that the same dilution of the digest was analyzed by both instruments, the concentration and volume of internal standard added to the diluted digest would have to be the same for both techniques. This would allow for the resulting element concentrations in the samples to be directly compared between the two instruments. Due to time and financial limitations, the samples could not be re-prepared and analyzed for this project.

Another improvement that could be made to this project would be to increase the size of the data set. This could be done in many different ways. The first would be to use the same paper types as used in this project but collect samples over a longer period of time and from different locations (*e.g.*, online, from different stores, from different states, in consecutive months, over 2-3 year periods). This would allow for observations to be made as to how the element concentrations within a paper type changed based on production time and production location. A second way for this study to be improved would be to collect more paper types from the same manufacturer produced at the same time. This would improve the PCA and HCA by increasing the size of the data set. With a small data set, slight differences in element concentration resulted in differences in positioning on the scores plot and clustering on the dendrogram. When a larger data set is used, the underlying patterns in the data become more apparent. If there are more

comparisons made, the discrimination among paper types would be greater due to differences in element concentration and the association among sheets of the same type would be stronger due to similar concentrations.

A final way to expand the data set used for this project would be to include the same paper types from different manufacturers. This would show if there were trends among similar paper types (*e.g.*, all office paper had high Al concentrations) or if there was a trend among different paper types from the same manufacturer (*e.g.*, all Hewlett Packard paper had similar Mn concentrations). These types of characterizations would be useful in a forensic laboratory to make general observations about the identity of an unknown sample. Once either the paper type or manufacturer was determined, individual element concentrations could be useful for determining the actual identity of the sample.

Finally, only two multivariate statistical procedures were applied to this data set. In literature, supervised statistical procedures, such as discriminant analysis and soft independent modeling of class analogy have been applied to discrete data. This is different than the unsupervised procedures used in this research which did not make assumptions about the data before statistical analysis. In supervised procedures, the data are divided into a training set and a test set. The training set is used to develop a model based on the known classification of the samples (which for these data would be paper type). Samples in the test set are then classified using the model. These methods would improve this project by assigning a confidence level to the classification made. The reams purchased at a later time or from a different manufacturer would be classified using the model to see if appropriate classification at a given confidence level was possible.

The purpose of this project was to determine if ICP-OES was sufficiently sensitive for the analysis of paper and if this technique was an acceptable alternative to ICP-MS analysis. Differentiation of the four paper types was possible using the profiles generated from ICP-OES analysis; however, association of reams purchased at a different time was not possible. Overall, this project was successful in showing ICP-OES could be used for the elemental analysis of paper. ICP-OES was determined to be a viable alternative to ICP-MS for elemental analysis of paper. This is beneficial for forensic science because ICP-OES is less expensive and more widely available than ICP-MS. If physical differentiation of paper types is not possible by microscopic examination, differentiation of paper types is possible using ICP-OES.

REFERENCES

REFERENCES

1. Trejos T, Flores A, Almirall JR. Micro-spectrochemical analysis of document paper and gel inks by laser ablation inductively coupled plasma mass spectrometry and laser induced breakdown spectroscopy. *Spectrochimica Acta Part B* 2010; 65: 884-895.

2. Spence LD, Baker AT, Byrne JP. Characterization of document paper using elemental compositions determined by inductively coupled plasma mass spectrometry. *J. Anal. At. Spectrom* 2000; 15: 813-819.

3. McGaw EA, Symanski DW, Smith RW. Determination of trace elemental concentrations in document papers for forensic comparison using inductively coupled plasma-mass spectrometry. *J. Forensic Sci* 2009; 54: 1163-1170.